



**Development of O-ring from the NR/EPDM Filled Silica/CB Hybrid Filler for
Use in the Solid Oxide Fuel Cell Testing System**

Chea Sophos

**A Thesis Submitted in Fulfillment of the Requirements for the
Degree of Master of Science in Sustainable Energy Management**

Prince of Songkla University

2019

Copyright of Prince of Songkla University



**Development of O-ring from the NR/EPDM Filled Silica/CB Hybrid Filler for
Use in the Solid Oxide Fuel Cell Testing System**

Chea Sophos

**A Thesis Submitted in Fulfillment of the Requirements for the
Degree of Master of Science in Sustainable Energy Management**

Prince of Songkla University

2019

Copyright of Prince of Songkla University

Thesis Title Development of O-ring from the NR/EPDM Filled Silica/CB Hybrid Filler for Use in the Solid Oxide Fuel Cell Testing System

Author Mr. Chea Sophos

Major Program Sustainable Energy Management

Major Advisor

.....
 (Asst. Prof. Dr. Warangkana Jutidamrongphan)

Examining Committee:

.....Chairperson
 (Dr. Khamphe Phoungthong)

Co-advisor

.....
 (Dr. Montri Luengchavanon)

.....Committee
 (Asst. Prof. Dr. Warangkana Jutidamrongphan)

.....
 (Asst. Prof. Dr. Kua-anan Techato)

.....Committee
 (Dr. Montri Luengchavanon)

.....
 (Asst. Prof. Dr. Kua-anan Techato)

.....Committee
 (Assoc. Prof. Dr. Suchada Chantrapromma)

.....Committee
 (Dr. Jiraporn Chomane)

The Graduate School, Prince of Songkla University, has approved this thesis as fulfillment of the requirements for the Master of Science Degree in Sustainable Energy Management

.....
 (Prof. Dr. Damrongsak Faroongsarng)
 Dean of Graduate School

This is to certify that the work here submitted is the result of the candidate's own investigations. Due acknowledgement has been made of any assistance received.

.....Signature
(Asst. Prof. Dr. Warangkana Jutidamrongphan)
Major Advisor

.....Signature
(Dr. Montri Luengchavanon)
Co-advisor

.....Signature
(Asst. Prof. Dr. Kua-anan Techato)
Co-advisor

.....Signature
(Mr. Chea Sophos)
Candidate

I hereby certify that this work has not been accepted in substance for any degree and is not being currently submitted in candidature for any degree.

.....Signature

(Mr. Chea Sophos)

Candidate

ชื่อวิทยานิพนธ์	การพัฒนาโอริงจากสารเติมแต่งซิลิกา / CB ไฮบริด NR / EPDM สำหรับใช้ในระบบทดสอบเซลล์เชื้อเพลิงออกไซด์ของแข็ง
ผู้เขียน	Mr. Chea Sophos
สาขาวิชา	การจัดการพลังงานอย่างยั่งยืน
ปีการศึกษา	2562

บทคัดย่อ

งานวิจัยนี้นำเสนอผลของก๊าซออกซิเจนและอุณหภูมิโดยรอบต่อโอริงที่ขึ้นรูปด้วยระบบวัลคาไนซ์แบบกึ่งประสิทธิภาพ (Semi EV) ที่สัมผัสกับทางเข้า (27 ถึง 31 °C) และการไหลออก (53 ถึง 58 °C) ท่อของการกระจายก๊าซออกซิเจนในเซลล์เชื้อเพลิงออกไซด์ของแข็ง (SOFC) โอริงยางธรรมชาติ / เอทิลีนโพรพิลีนไดอีนโมโนเมอร์ (NR / EPDM) ถูกเตรียมด้วยอัตราส่วน silica/CB ไฮบริดที่อัตราส่วนระหว่าง 00/60, 10/50, 20/40, 30/30, 40/20, 50/10 และ 60/00 โอริงที่เตรียมขึ้นสอดคล้องกับผลิตภัณฑ์อุตสาหกรรมมาตรฐานสำหรับโอริง (มอก. 2728-2559) ที่มีความแข็งขั้นต่ำ 65-75 Shore A และความต้านทานแรงดึง 7 MPa ทำการศึกษาสมบัติเชิงกลของโอริงก่อนและหลังการบ่มและทำการศึกษาสันฐานพื้นผิวและหน้าตัดของ O-ring NR / EPDM และเปรียบเทียบกับ O-ring มาตรฐานหลังจากการทดสอบเป็นเวลา 1 ชั่วโมง 6 ชั่วโมง 12 ชั่วโมงและ 24 ชั่วโมงในระบบทดสอบ SOFC เป็นผลให้สารประกอบที่มีอัตราส่วนของซิลิกา / CB 40:20 มีคุณสมบัติเชิงกลที่ดีที่สุดและผ่านมาตรฐานโอริง (มอก. 2728-2559) (ค่า P-value มาตรฐานพร้อมโอริงที่เตรียมไว้: 60 / 00 = 0.273, 50/10 = 0.273, 40/20 = 0.144, 30/30 = 0.465, 20/40 = 0.465, 10/50 = 1.000 และ 00/60 = 0.273 > ระดับนัยสำคัญ 0.05) และราคาของโอริงที่เตรียมไว้ - แหวนถูกกว่ามาตรฐานโอริงเนื่องจากราคาของพาราที่ใช้ในการกำหนดโอริงที่เตรียมไว้ต่ำมาก หลังจากการทดสอบใน SOFC ยังคงสามารถใช้โอริงมาตรฐานและทดสอบใน SOFC ได้แม้ว่าจะมีรอยแตกภายในหลังจาก 1 ชั่วโมงและ 6 ชั่วโมงการแตกหักเล็กน้อยหลังจาก 12 ชั่วโมงและการสำรวจจลิกและตื้นภายในโอริงหลัง ทดสอบตลอด 24 ชั่วโมง

คำหลัก: คาร์บอนแบล็ค, EPDM, โอริง, ยางธรรมชาติ, ซิลิกา, เซลล์เชื้อเพลิงออกไซด์ของแข็ง

Thesis Title	Development of O-ring from the NR/EPDM Filled Silica/CB Hybrid Filler for Use in the Solid Oxide Fuel Cell Testing System
Author	Mr. Chea Sophos
Major Program	Sustainable Energy Management
Academic Year	2019

ABSTRACT

This research presents the effects of oxygen gas and ambient temperatures on the O-rings molded from a semi-EV exposed to the inlet (27 to 31°C) and outflow (53 to 58°C) pipe of oxygen gas diffusion in SOFC testing system. Mixing of NR/EPDM were prepared with the proportion of silica/CB hybrid filler of 00/60, 10/50, 20/40, 30/30, 40/20, 50/10 and 60/00 phr. The fabricated O-ring complies with the industrial product standard for O-ring (TIS 2728-2559) with the minimum hardness of 65-75 Shore A and the tensile strength of 7 MPa. The mechanical properties of the NR/EPDM filled silica/CB compound before and after aging were carried out and the best compound were chosen to make the O-rings and test in the SOFC testing system. The surface and cross-section morphology of the NR/EPDM filled silica/CB O-rings were also investigated and compared with the standard O-ring after testing in SOFC testing system. As a result, the compound with the ratio of the silica/CB of 40:20 provides the best mechanical properties and pass the standard O-ring (TIS 2728-2559) (P -value of standard with prepared O-rings: 60/00 = 0.273, 50/10 = 0.273, 40/20 = 0.144, 30/30 = 0.465, 20/40 = 0.465, 10/50 = 1.000 and 00/60 = 0.273 > significant level 0.05) and the price of prepared O-ring is cheaper than the standard O-ring due to the very low price of NR used in the formulation of prepared O-ring. After testing in SOFC, still the prepared and standard O-rings can be used to test in SOFC although there are some inner cracks after 1 hour and 6 hours, slight fracture after 12 hours and shallow and deep traverse inside the O-ring after 24 hours testing.

Keyword: Carbon black, EPDM, O-ring, natural rubber, silica, solid oxide fuel cell

ACKNOWLEDGEMENT

First of all, I would like to express my deepest heartfelt gratitude to my co-advisor, Dr. Montri Luengchavanon who willingly helps me to do and finish this research and master's degree journey, also thoroughly explains and guides both research work and academic study; particularly, the way to do laboratory experiment, kindly supports all the materials to do my experimental test and sample test, courageously motivates me to finish master's degree. My deepest sincere appreciation to Dr. Ekasit Anancharoenwong for his kindness for providing me the materials and allowing me to do the laboratory work in the Heavy Industries Laboratory at Prince of Songkla University (PSU), Surat Thani Campus and his guidance and explanation about rubber application. I would like to offer my crucial thanks to my advisor, Asst. Prof. Dr. Warangkana Jutidamrongphan who accepts me as advisee and relentlessly motivates and encourages me to go on my master's degree and always assists me whenever I need her help. I would particularly like to demonstrate my greatest gratitude to my co-advisor, Asst. Prof. Dr. Kua-anan Techato, Dean of Faculty of Environmental Management who firstly accepts me to study in the Sustainable Energy Management program and exactly has a great management and study plan for my short time research work to graduate as soon as possible and help me to pay for my last sample test at Science Equipment Center.

Secondly, I would like to say great thanks to my thesis chairperson, Dr. Khamphe Phoungthong, internal committee, Assoc. Prof. Dr. Suchada Chantrapromma and external committee, Dr. Jiraporn Chomanee for spending your valuable time to come and join my thesis defense and literally revise my thesis book.

Additionally, I am particularly grateful for the laboratory assistance given by Ms. Mintra Trongtorkarn, Mr. Priwan Pongwan, Mr. Suppachai Jina, Ms. Chatcha Phetthong, Ms. Piyawadee Luangchuang, Mr. Chayanin Khongkhot, and Mr. Passakorn Thongthung who take their time to assist to some parts of my experimental work, share experience and opinions during my research study in Sustainable Energy Management program and assist my laboratory work at PSU, Surat Thani campus.

Moreover, I would also like to show my gratitude to all lecturers and staffs in the Faculty of Environmental Management in PSU Hat Yai campus and in the Science and Industrial Technology in PSU Surat Thani campus for giving me all lectures and for their administrative and generous assisting in my staying, studying, and laboratory working in Thailand. I appreciate the valuable support, encouragement, suggestions, comments, and idea offered by my colleagues, seniors, juniors, and all friends in both PSU, Hat Yai campus and Surat Thani campus.

Furthermore, I owe a very significant debt to the Thailand Education Hub for Asian Countries (THE-AC) through the Master's degree program (Contract no. 098), for providing fully financial support for thesis research at Department of Sustainable Energy Management, Faculty of Environmental Management, PSU for the academic year 2017 to 2019.

Finally, whole hearted thanks to my beloved families for relentlessly support and encouragement in every decision, problem, and circumstance that I met.

Chea Sophos

TABLE OF CONTENTS

TITLE PAGE	i
APPROVAL PAGE	ii
CERTIFY	iii
ABSTRACT IN THAI	v
ABSTRACT IN ENGLISH	vi
ACKNOWLEDGEMENTS	vii
TABLE OF CONTENTS	ix
LIST OF TABLES	xiii
LIST OF FIGURES	xiv
THE LIST OF ABBREVIATIONS	xviii
CHAPTER I: INTRODUCTION	1
1.1 Research background	1
1.2 Research objectives	3
1.3 Research questions	3
1.4 Scope of study	3
CHAPTER II: REVIEW OF LETERATURE	4
2.1 O-ring	4
2.1.1 History and general description	4
2.1.2 O-ring cross-section	5
2.1.2.1 Advantages of smaller cross-section	5
2.1.2.2 Advantages of larger cross-section	5
2.1.3 O-ring applications	6
2.1.4 Advantages of O-rings	6
2.1.5 O-ring compounds and their applications	6
2.1.5.1 Polyacrylate (ACM)	6
2.1.5.2 Polychloroprene rubber (CR)	7
2.1.5.3 Nitrile butadiene rubber (NBR)	7
2.1.5.4 Hydrogenated nitrile butadiene rubber (HNBR)	7
2.1.5.5 Ethylene propylene rubber (EPDM)	7
2.1.5.6 Silicone rubber (VMQ)	7

	x
2.1.5.7 Fluorosilicone (FVMQ)	8
2.1.5.8 Liquid silicone rubber (LSR)	8
2.1.5.9 Fluorocarbon (FKM)	8
2.1.5.10 HiFluor (FKM)	8
2.1.5.11 Parofluor (FFKM)	8
2.2 Deformation force	9
2.3 Static axial seals	12
2.4 Dynamic sealing applications	12
2.5 Reciprocating dynamic seals	12
2.6 Rotary seals	13
2.7 Installations and design recommendations	13
2.7.1 General recommendations	14
2.7.2 Manual installation	15
2.7.3 Automatic installation	15
2.8 O-ring properties	15
2.8.1 Physical properties	15
2.8.2 Chemical properties	30
2.8.3 Thermal properties	32
2.9 Effects of temperature on rubber O-ring	35
2.10 Effects of hydrogen gas on rubber O-ring	40
2.11 O-ring operation and design	41
2.11.1 Back-up ring	41
2.11.2 Advantages	42
2.12 Category of rubbers used in the rubber blending	42
2.12.1 Acrylonitrile-butadiene rubber (NBR)	42
2.12.2 Hydrogenated nitrile rubber (HNBR)	44
2.12.3 Carboxylated nitrile rubber (XNBR)	45
2.12.4 Hydrogenated carboxylated nitrile rubber (HXNBR)	46
2.12.5 Styrene-butadiene rubber (SBR)	48
2.12.6 Chloroprene rubber (CR)	48
2.12.7 Polyvinyl chloride (PVC)	49
2.13 Natural rubber (NR)	49

	xi
2.14 Ethylene-propylene-diene rubber-based nanoblends	50
2.15 Carbon black (CB)	55
2.16 Vulcanization chemicals	57
2.17 Vulcanization accelerators	57
2.18 Classification of organic accelerators	58
2.19 Accelerator activators	60
2.20 Typical properties and types of fillers	60
2.20.1 Action of fillers	60
2.21 Sulfur vulcanization	61
2.21.1 Vulcanization reagents	61
2.21.2 Accelerated vulcanization	62
2.22 Peroxide crosslinking	64
2.22.1 General features of peroxide crosslinking	64
2.23 Previous studies of fillers	65
2.24 Previous study of O-ring seal testing	67
2.25 Fuel cell	71
2.25.1 Solid oxide fuel cell (SOFC)	72
CHAPTER III: MATERIALS AND METHODS	74
3.1 Materials	74
3.2 Compound preparation	74
3.3 Cure characteristics	77
3.4 Vulcanization and measurement of mechanical properties	77
3.5 Thermo-oxidative aging	79
3.6 O-ring molding	79
3.7 O-rings used in SOFC testing system	80
3.8 Observations of crack morphology and fracture surface	82
3.9 Data analysis	83
CHAPTER IV: RESULTS AND DISCUSSIONS	84
4.1 Cure characteristics	84
4.1.1 Scorch time (min)	84
4.1.2 Cure time (min)	84
4.1.3 Minimum torque (N.m)	85

	xii
4.2 Mechanical properties	86
4.2.1 Tensile strength (MPa)	87
4.2.2 Modulus	87
4.2.3 Elongation	88
4.2.4 Hardness	89
4.3 Comparison of mechanical properties between the prepared O-ring and standard O-ring based on Thai Industry Standard	90
4.4 Price of prepared O-ring and standard O-ring	91
4.5 Appearances of standard O-ring and NR/EPDM filled silica/CB O-ring	92
4.6 Crack initiation and growth behavior in O-rings	93
CHAPTER V: CONCLUSIONS	99
SUGGESTIONS	99
REFERENCES	100
VITAE	111

LIST OF TABLES

Table 2.1	Guide to Durometer scale selection Quality of bedding materials depth	18
Table 2.2	Conversion for durometer hardness scales	18
Table 2.3	Short summary of the low-temperature leak test data	38
Table 2.4	The basic properties of diene rubber components in the EPDM rubber The major components of rice husks	52
Table 2.5	Types of carbon black used in tires	56
Table 2.6	The most important accelerators groups	58
Table 2.7	Typical sulfur cross-linking systems for carbon black filled rubbers	59
Table 2.8	Classification of accelerator groups and their relative curing speeds	61
Table 2.9	Compositions of conventional, semi-EV and EV vulcanization systems	62
Table 2.10	Vulcanizate structure and properties of three different sulfur-curing systems	63
Table 2.11	Peroxides for curing of elastomers	65
Table 2.12	Advantages and disadvantages of peroxide crosslinking	65
Table 2.13	Kind of electrolytes and their efficiency, temperature, and output	72
Table 3.14	Blend formulations	75
Table 4.15	Mechanical properties of vulcanized blended rubber before aging	86
Table 4.16	Mechanical properties of vulcanized blended rubber after aging	86
Table 4.17	Mechanical properties of standard O-ring based on Thai Industry Standard	86
Table 4.18	Wilcoxon Signed Ranks Test Statistics	90
Table 4.19	Mechanical properties of standard and prepared O-ring	91
Table 4.20	Price of prepared O-ring in Thai baht	91
Table 4.21	Price of standard O-ring in Thai baht	91

LIST OF FIGURES

Figure 2.1	The characteristics of O-rings, D is the outer diameter, d_1 is inner diameter, and d_2 is the cross-section's diameter	5
Figure 2.2	Relationship between hardness, compression, deformation force, and cross-section of 1.78 mm	9
Figure 2.3	Relationship between hardness, compression, deformation force, and cross-section of 2.62 mm	9
Figure 2.4	Relationship between hardness, compression, deformation force, and cross-section of 3.53 mm	10
Figure 2.5	Relationship between hardness, compression, deformation force, and cross-section of 5.33 mm	10
Figure 2.6	Relationship between hardness, compression, deformation force, and cross-section of 6.99 mm	11
Figure 2.7	Grooves design for static seals	11
Figure 2.8	Grooves design for reciprocating seals	
Figure 2.9	Groove design for rotary seals	12
Figure 2.10	O-ring installation over transverse bores	13
Figure 2.11	Piston installation with O-ring	14
Figure 2.12	Rod installation with O-ring	14
Figure 2.13	Shore durometer	14
Figure 2.14	IRHD Hardness tester	16
Figure 2.15	Shore A hardness tester	20
Figure 2.16	Molded dumbbell	21
Figure 2.17	Tensile tester	21
Figure 2.18	Unnicked 90° angle	24
Figure 2.19	Slit (Trouser) specimen	24
Figure 2.20	Rotating drum	25
Figure 2.21	Rotating platform	26
Figure 2.22	Rotating samples	26
Figure 2.23	Effects of compression set on an O-ring's cross-section	27
Figure 2.24	Compression set test method A	28

Figure 2.25	Compression set test method B	28
Figure 2.26	Bashore resilience testing	29
Figure 2.27	Compression set in increasing temperatures	29
Figure 2.28	O-ring swell	31
Figure 2.29	Shrinkage due to plasticizer extraction	32
Figure 2.30	Material performance in high temperatures	33
Figure 2.31	Temperature retraction, or "Tr-10"	34
Figure 2.32	Gough-Joule effect	35
Figure 2.33	Relation between stiffness and temperature	35
Figure 2.34	Influence of temperature on tensile strength of rubbers	37
Figure 2.35	O-ring installation with and without back-up ring	41
Figure 2.36	Effect of pressure with and without back-up ring	42
Figure 2.37	Polymerization and compositional structure of NBR	43
Figure 2.38	Catalytic hydrogenation of NBR to prepare HNBR and the polymer microstructure of HNBR	44
Figure 2.39	HNBR versus NBR property comparison	44
Figure 2.40	Polymer microstructure of HXNBR	46
Figure 2.41	HXNBR versus HNBR properties comparison	47
Figure 2.42	Hevea Brasiliensis, the rubber tree	49
Figure 2.43	The structure of EPDM rubber macromolecules	51
Figure 2.44	The structure of NBR rubber macromolecules	53
Figure 2.45	Dimension of carbon black primary particle size and dimension of aggregate and agglomerate which have been made in cross-linking reaction of elastomer and filler (a) and basic properties of carbon black (b)	54
Figure 2.46	Types of silanol group in the surface particle of silica	54
Figure 2.47	The role ZnO, fatty acid and activator in accelerated sulfur vulcanization. X- accelerator residue, L – ligand (basic nitrogen or zinc carboxylate)	64
Figure 2.48	Schematic of a solid oxide fuel cell (SOFC)	73
Figure 3.49	Internal mixer	76
Figure 3.50	Two-roll mill machine	76

Figure 3.51	Moving Die Rheometer, MDR 2000	77
Figure 3.52	Tensile Testing Machine, Zwick Roell Germany (Z010)	78
Figure 3.53	Shore Instruments Durometer set, Instron model	78
Figure 3.54	(a) Top view of mold housing, (b) Cross-section view of Mold housing, (c) O-rings mold with four housing	79
Figure 3.55	Compression machine, PR1D-W280L300 PM	80
Figure 3.56	Schematic of solid oxide fuel cell testing system	81
Figure 3.57	Solid oxide fuel cell testing system; (1) inlet of hydrogen gas, (2) outflow of hydrogen gas	81
Figure 3.58	Installation of O-rings in the mating surface pipes/valves in Solid oxide fuel cell testing system	82
Figure 3.59	Scanning Electron Microscope	82
Figure 4.60	Scorch time	84
Figure 4.61	Cure time	85
Figure 4.62	Minimum torque	85
Figure 4.63	Tensile strength at different blend ration of un-aged and aged carbon black filled NR/EPDM	87
Figure 4.64	The 100% modulus at different blend ration of un-aged and aged carbon black filled NR/EPDM	88
Figure 4.65	Elongation at break at different blend ration of un-aged and aged carbon black filled NR/EPDM	89
Figure 4.66	Hardness properties at different blend ration of un-aged and aged carbon black filled NR/EPDM	90
Figure 4.67	The surfaces' characteristics and cross-sections of the standard O-rings	92
Figure 4.68	The surfaces' characteristics and cross-sections of the NR/EPDM O-rings with silica and CB ratio of 40/20	92
Figure 4.69	The O-ring rubber production with inside diameter of 8 mm and cross-section diameter of 2.3 mm	92
Figure 4.70	The surfaces' characteristics and cross-section of the NR/EPDM filled silica/CB O-rings exposed to 1 hour, 6 hours, 12 hours, and 24 hours of oxygen gas in SOFC testing system at the inlet gas	

- flow rate of 0.5 L/mn and temperature of 27 to 31°C 93
- Figure 4.71** The surfaces' characteristics and cross-section of the NR/EPDM filled silica/CB O-rings exposed to 1 hour, 6 hours, 12 hours, and 24 hours of oxygen gas in SOFC testing system at the outlet gas flow rate of 0.5 L/mn and temperature of 53 to 58°C 95
- Figure 4.72** The surfaces' characteristics and cross-section of the commercial/standard O-rings exposed to 1 hour, 6 hours, 12 hours, and 24 hours of oxygen gas in SOFC testing system at inlet flow rate of 0.5 L/mn and temperature of 53 to 58°C 96
- Figure 4.73** The surfaces' characteristics and cross-section of the commercial/standard O-rings exposed to 1 hour, 6 hours, 12 hours, and 24 hours of oxygen gas in SOFC testing system at the outlet gas flow rate of 0.5 L/mn and temperature of 53 to 58°C 97

LIST OF ABBREVIATIONS

A	: Accelerator
ACM	: Polyacrylate
AFCs	: Alkaline fuel cells
ASTM	: American Standard Test Method
B	: Boron
C	: Carbon
CaO	: Calcium oxide
Ca(OH) ₂	: Calcium hydroxide
CB	: Carbon black
CBS	: <i>N</i> -Cyclohexyl-2-benzothiazolesulfenamide
cm ³	: Cubic centimeter
CO	: Cobalt
CO ₂	: Carbon dioxide
CR	: Polychloroprene rubber or Chloroprene rubber
CTAB	: Cetyl trimethylammonium bromide
CTP	: <i>N</i> -(Cyclohexylthio)phthalimide
CV	: Conventional vulcanization
D	: Outer diameter
DCBS	: <i>N,N</i> -dicyclo-2-benzothiazylsulfenamide
DCPD	: Dicyclopentadiene
DETU	: Diethylenethiourea
DOTG	: <i>N,N'</i> -di- <i>o</i> -tolylguanidine
DPG	: <i>N,N'</i> -diphenylguanidine
DPTT	: Dipentamethylenethiuram tetrasulfide
DPTU	: <i>N,N'</i> -diphenylthiourea
DTDM	: 4,4'-dithiobismorpholine
d ₁	: Inner diameter
d ₂	: Cross-section's diameter
ENB	: 5-ethylidene-2-norbornene
EPR	: Ethylene-propylene rubber

ETU	: Ethylthiourea
EV	: Efficient vulcanization
EPDM	: Ethylene propylene diene monomer
etc.	: Et cetera – and so forth
e.g.	: Exempli gratia - for exemple
ENB	: Ethylidene norbornene
EPC	: Easy processing channel
E-SBR	: Emulsion polymerization
EVA	: Ethylene-vinyl acetate
e ⁻	: Electron
F	: Fluorine
FEF	: Fast extruding furnace
FFKM	: Parofluor
FKM	: Fluorocarbon or HiFluor
FT	: Fine thermal
FVMQ	: Fluorosilicone
g/cm ³	: Grams per cubic centimetre
h	: Hour
HAF	: High abrasion furnace
HD	: 1,4-hexadiene
HDPE	: High-density polyethylene
HMF	: High modulus furnace
HNBR	: Hydrogenated nitrile butadiene rubber
HP	: Brand name of standard O-ring-Lezyne HP O-ring Kit
HXNBR	: Hydrogenated carboxylated nitrile rubber
Hz	: Hertz
H ₂	: Hydrogen
H ₂ O	: Water
H ₂ O ₂	: Hydrogen peroxide
ID	: Inside diameter
i.e.	: Id est – that is

IR	: Synthetic counterpart
IRHD	: International Rubber Hardness Degrees
IIR	: Butyl rubber
ISAF	: Intermediate SAF
ISO	: International Organization for Standardization
Kg/cm ²	: Kilogram per square centimeter
kJmol ⁻¹	: Kilojoule per mole
kN/m	: Kilonewtons per meter
kW	: Kilowatts
lbf/in	: Pound force per inch
LDPE	: Low-density polyethylene
LSR	: Liquid silicone rubber
L/mn	: Litre per minute
mm	: Millimeters
mm/min	: Millimeter per minute
m	: Meter
MBS	: 2-morpholinothiobenzothiazole
MCFCs	: Molten carbonate fuel cells
MDR	: Moving Die Rheometer
MgO	: Magnesium oxide
MnO	: Manganese (II) oxide
MPa	: Mega Pascale
MT	: Medium thermal
MTB	: 2-mercaptobenzothiazole
MTBS	: Dibenzothiazyl disulfide
MU	: Moonie Unit
M100	: Modulus 100, 100% elongation
m ² /g	: Square meter per gram
N	: Nitrogen
NBR	: Nitrile butadiene rubber or acrylonitrile-butadiene rubber
NBS	: National Bureau of Standards

nm	: Nanometer
N.m	: Newton meter
NMR	: Nuclear magnetic resonance
NR	: Natural rubber
NRN	: Natural rubber nanocomposite
N/cm	: Newton per centimeter
OD	: Outside diameter
ORR	: Oxygen reduction reaction
OTBG	: O-tolylbiguanide
OTOS	: Oxydiethylenesulfenamide
O ²	: Oxygen
P	: Phosphorus
PAFCs	: Phosphoric acid fuel cells
PbO	: Piperonyl butoxide
Pb ₃ O ₄	: Triplumbic tetroxide
PEMFCs	: Proton exchange membrane fuel cells
phr	: Parts per hundred rubber
PP	: Polypropylene
psi	: Pounds per square inch
pt	: Platimum
PVC	: Polyvinyl chloride
Q	: Silica content
rpm	: Round per minute
RR	: Recycled rubber
S	: Sulfur
S'	: Torque
SA	: Steric acid
SAF	: Superabrasion furnace
SBR	: Styrene-butadiene rubber
Sb ₂ S ₃	: Antimony sulphide
SEM	: Scanning Electron Microscope

SiOH	: Silanol sorts
SOFC	: Solid oxide fuel cell
SRF	: Semi-reinforcing furnace
S-SBR	: Solution anionic polymerization
STR 5L	: Standard Thai Rubber 5L Grade
TBBS	: <i>N-tert-butyl-2-benzothiazylsulfenamide</i>
TBzTD	: Tetrabenzylthiuram disulfide
$t_{c,90}$: Optimum vulcanization time
TESPT	: Bis(triethoxysilylpropyl) tetrasulfide
TETD	: Tetraethylthiuram disulfide
T_{fail}	: The measured leakage temperature
T_g	: Glass transition temperature
TMTD	: Tetramethylthiuram disulfide
TMTM	: Tetramethylthiuram monosulfide
TPE	: Thermoplastic elastomer
TPV	: Thermoplastic Vulcanisate
tr	: Temperature retraction
t_{s2}	: Scorch time
t_{s90}	: Cure time
US	: United states
USA	: United States of American
UV	: Ultraviolet
VMQ	: Silicone rubber
wt%	: Weight percentage
WWII	: World war II
XNBR	: Carboxylated nitrile rubber
ZBEC	: Zinc dibenzylthiocarbamate
ZDBC	: Zinc dibutylthiocarbamate
ZDEC	: Zinc diethylthiocarbamate
ZDMC	: Zinc dimethylthiocarbamate
ZEPC	: Zinc ethylphenylthiocarbamate

ZMBT	: Zinc 2-mercaptobenzothiazole
ZnO	: Zinc oxide
Z5MC	: Zinc pentamethylene dithiocarbamate
°C	: Celsius degree
°F	: Fahrenheit
ΔT	: The difference between T_{fail} and T_g
%	: Percentage
μ	: Micro

CHAPTER 1

INTRODUCTION

1.1 Research background

Fuel cells are the device which produce electricity electrochemically and continuously as a gaseous fuel is burnt and applied in a continuous manner. Fuel cells depict a later era and highly efficient-power-alteration tool in the future's conveyance and immobile power productions that are still being studied, researched, and developed particularly in Europe, America, and Japan. It is a direct power alteration tool which consists the power sources including natural gas, hydrogen, ethanol, methanol, formic acid, or phosphoric acid and an oxidant such as air or oxygen. In addition, the use of fuel cells also provides very low emission of pollution and very little pollution by forming a harmless byproduct, namely water and many size-scale use (Mumtaz et al., 2017).

Solid Oxide Fuel Cell, SOFC is one among them which has the efficiency of energy generation is more than 50% and it can be increased to 85% if the waste heat is reused or recycled (Garcia-Garcia et al., 2017; Xu et al., 2017). This type of fuel cell operates at high temperature approximately 1000 °C. At the recent time, it can be adjusted to the lower heat of 600 °C to 850 °C (J. H. Kim et al., 2017). In this fuel cell, due to the system operates at the high temperature therefore, it does not require to use the expensive catalysts such as platinum to make this fuel cell cheaper (Ratso et al., 2017; Song et al., 2017). SOFC is the fuel cell that uses hard-ceramic materials as an electrolyte such as Zirconium Oxide, Yttrium Oxide (Hou et al., 2017). The utilization of solid electrolytes makes it easy to operate without problems with water management and corrosion of materials. And it uses a number of fuels such as hydrogen, hydrocarbons, syngas, ammonia, oxygen and solid carbon to supply to the systems (Zhang et al., 2017).

It is not only SOFC type that needs to enter the fuel gas into it but also all types of fuel cell do. Therefore, the fuel cell system must have a fuel gas storage unit. Generally, hydrogen and oxygen are the appropriate fuel for electricity generation from the fuel cell. On the other hand, the significant issues of inaccuracy in

cell experiment is owing to the gas leak, both of the air from the external into the anode section and from air traversing from the cathode over cracks or holes (Sinha, S. C. and Kendall, 2003; Williams, 2009). For this issue, researchers are working and developing methods for storing gas for use in the fuel cell in order to make the electricity production system from fuel cell reliable and widely uses. Their research designed the system of electricity production of SOFC by simulating gas input into the system and using the O-ring tires to test for leakage to prevent liquid or gas fluid leakage that contain steel or solid components because in the high pressure of gases diffusion and high temperature, the metal and solid parts cannot prevent the gas or liquid leakage. Although many researchers have reported the effects of high-pressure hydrogen, nitrogen, carbon dioxide, and argon on the sweltering crack of the rubber elements (Atkinson, 2002; Briscoe & Liatsis, 1992; Briscoe et al., 1994; Embury, 2004; Ender, 1986; Epstein & Plesset, 1950; Gent & Lindley, 1961; Gent & Tompkins, 1969; Stevenson & Morgan, 1995; Yamabe et al., 2013) yet still it has no research which addresses the induction of this phenomenon by high flow rate and oxygen pressure at ambient temperature.

In this study, the O-rings were molded from a sulfur semi efficient vulcanization (semi-EV) system and exposed to oxygen gas diffusion at the flow rate of 0.5 L/mn and the temperature ranging from 27 to 31 °C and 53 to 58 °C in the SOFC testing system. The O-rings were produced by using the ethylene-propylene-diene-monomer (EPDM) rubber which has good weather resistant properties and natural rubber (NR) that has an excellent mechanical property as the major composites. Blends of the NR and EPDM were prepared in the internal mixture and on a two-roll mill with the various proportion of silica/carbon black (silica/CB) hybrid filler of 00/60, 10/50, 20/40, 30/30, 40/20, 50/10, and 60/00 parts per hundred rubbers (phr). The mechanical properties of the NR/EPDM filled silica/CB compound before and after aging were carried out and the best compound were chosen to make the O-rings and test in the SOFC testing system. The surface and cross-section morphology of the NR/EPDM filled silica/CB O-rings were also investigated and compared with the HP standard O-ring after testing for 1 hour, 6 hours, 12 hours, and 24 hours in SOFC testing system.

1.2 Research objectives

1.2.1 To test mechanical properties of NR and EPDM rubber filled silica and CB hybrid filler compounds.

1.2.2 To produce O-rings from NR and EPDM rubber filled silica and CB hybrid filler compounds and test O-rings in SOFC testing system.

1.3 Research questions

1.3.1 Which proportion of Silica and CB hybrid filler in the NR and EPDM rubber filled silica and CB hybrid filler compounds has the best mechanical properties?

1.3.2 How are mechanism and degradation of the prepared O-rings produced from the NR and EPDM rubber filled silica and CB hybrid filler compounds when exposing to the SOFC environment?

1.4 Scope of study

- This study was focused on the various formula of the NR and EPDM rubber filled silica and CB hybrid filler compounds to make the O-rings
- The mechanical properties including tensile strength, modulus, elongation at break and hardness before ageing and after thermal ageing were tested and complied the standard O-rings

CHAPTER 2

REVIEW OF LITERATURE

2.1 O-ring

2.1.1 History and general description

O-ring rubber seal is an artificial seal which is considered and developed into practical utilization by the Danish emigrant namely Niels Christensen in USA. In 1937, Niels Christensen filed an O-ring patent in US as he developed his research on street car brake systems yet in 1896, J. O. Lundberg acknowledged the exist of O-ring in Swedish patent. From 1882, a spherical-shape rubber ring is represented in the neck of the glass bulb in the Edison's light bulb patent. The O-ring seal was taken as the aircraft industry's own and a normal and robust seal for hydraulic systems in the period of WWII and it was broadly adopted by all general industry and car manufactures.

The O-ring seal is one among the most beneficial designs today and an extensively used and significant machine item. The O-ring is illustrated in Figure 2.1. Countless products have never been brought on the market if the O-rings do not exist to seal liquids and gases. The form of O-ring is simple and flexible. It requires little space, can use in many purposes, and is easy to mount. Back of the description above lies a considerable technology in compounding the synthetic rubbers and in quality controlling of production to specific purposes and in order to obtain the essential precision and a reliable seal (Plc, 2007).

An O-ring is a round-donut-shape ring or a torus Figure 2.1. O-rings can be fabricated from many composites such as plastic materials, or even metal, and elastomeric or rubber. It is formed in order to avoid the leakage of a fluid or gas. O-ring works and acts jointly with the gland in which the O-ring is set up. The gland is usually removed from the metallic hardware. It has many different kinds and characteristics of glands. Both gland and O-ring process all at once to seal and are created in a must as a group to reach the excellent performance.

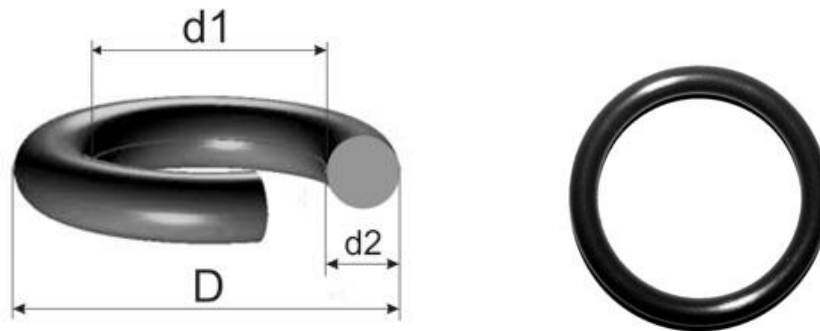


Figure 2.1 The characteristics of O-rings, D is the outer diameter, d_1 is inner diameter, and d_2 is the cross-section's diameter

2.1.2 O-ring cross-section

O-ring cross-section refers to the clearance gap space between the mating surfaces. On the other hand, there are two other diameters such as ID and OD of an O-ring gland. Generally, these two diameters are influenced by diameter of the mating surface of the rod, piston, and bore. The O-ring's cross-section is seen as fairly whimsical yet the bigger or smaller cross-section of O-ring have some different advantages. The advantages of these two cross-sections is described below.

2.1.2.1 Advantages of Smaller Cross-Section

The small O-ring's cross-section is light and has more compact. It is cheaper particularly for Fluorocarbon (FKM) or fluorosilicone (FVMQ) which has the high cost. For machined grooves, it needed less machines because the small size of grooves. It has more resistant to explosive decompression.

2.1.2.2 Advantages of Larger Cross-Section

One of advantages of the larger cross-section of O-ring is less prone to compression set. Large cross-section forms smaller-volume swells in liquid on a percentage basis than the small one. Moreover, it has larger tolerance during the maintaining acceptable compression squeeze and compression ratio over full stack-up range. Lastly, it creates little prone to leakage in view of contamination; dirt, lint, scratches, etc. (*O-Ring Design Guide*, 1990).

2.1.3 O-ring applications

O-rings are used principally in numerous fields of application. They can be used as activating or sealing elements in the hydraulic slipper seals and wipers. The O-ring is used for fixing or maintenance to assure the quality application in all industries' fields such as general engineering, aerospace, and automotive.

The O-ring is consumed primarily in static sealing applications such as radial and axial static seals. For radial static seal, it is used for bushing, pipes, cylinders, and covers and for axial static seal, it is used for caps, flanges, and plates. Whereas in the dynamic applications, the O-rings are recommended for average-service conditions only. The limitation of them are the pressure and speed which they face to seal for below function sealing of reciprocating plungers, pistons, rods, etc. and against to enclosing of rotating movements, moderately pivoting, spiral, or on rotary transmissions, spindles, shafts, lead through, etc. (Solutions, 2016).

2.1.4 Advantages of O-rings

O-ring has a number of advantages comparing with other sealing items. First, it is simple, requires less hardware and has low-cost with one-piece groove design. Second, it allows smaller hardware for compaction and has less risk with fool proof installation. Third, it is suitable to a large categories of sealing problems such as static, dynamic, single, or double acting and has wide-compound options for closeness with nearly all liquid. Lastly, its opening of plenty of sizes of ex stock global for accessible maintenance and restoration (Solutions, 2016).

2.1.5 O-ring compounds and their applications

O-rings are being able to mould into many compounds and can be moulded in harnesses from 40 to 90 Shore A.

2.1.5.1 Polyacrylate (ACM)

ACM acrylic rubber consists of great chemical resistance to the substances such as mineral oil, oxygen, and ozone. Their water compatibility and cold

adaptability of ACM are poor remarkably comparing with Nitrile butadiene rubber (NBR).

2.1.5.2 Polychloroprene rubber (CR)

Polychloroprene rubber (CR), Neoprene (tradename) was the earliest in order of synthetic rubber. It presents great ozone, aging, and chemical resistance and has great mechanical properties in terms of large scale of temperature.

2.1.5.3 Nitrile butadiene rubber (NBR)

NBR is the ordinary word for acrylonitrile-butadiene terpolymer. The acrylonitrile exists of nitrile enclosed compositions variously from 0.18 to 0.50 markedly. Polymers which have greater CAN load/size present a little swell in gasoline and aromatic solvents. Other lessened CAN polymers show better compression set and has the elasticity in temperature range. Polymer is appointed to Buna-N too.

2.1.5.4 Hydrogenated nitrile butadiene rubber (HNBR)

Hydrogenated NBR, air-resistant was grown as alternative of nitrile rubber. HNBR has the bonds of double C-C in the predominant polymer chain. It is saturated with hydrogen atoms which increases the material's oxidation resistance and thermal stability called "hydrogenation" process.

2.1.5.5 Ethylene propylene rubber (EPDM)

EPDM is a polymer synthesized from three different monomers such as ethylene, propylene, and a diene third monomer which utilized in cross-linking.

2.1.5.6 Silicone rubber (VMQ)

Silicone elastomer, VMQ has great insulating properties and likely to be physiologically neutral with comparatively poor tensile strength, low tear and wear resistance.

2.1.5.7 Fluorosilicone (FVMQ)

Fluorosilicone, a silicone polymer structure with fluorinated side-chains, a side-chains which is used for developed fuel and oil resistance. They have a similarity to those silicones in term of the mechanical and physical properties.

2.1.5.8 Liquid silicone rubber (LSR)

Liquid silicone rubber has a tremendous benefit that can efficiently produce great amount silicone parts. Flash less manufacturing provides favorable circumstances for severe molded forms for instance for automotive applications and very careful pharmaceutical.

2.1.5.9 Fluorocarbon (FKM)

Fluorocarbon (FKM) has an excellent resistance. It can handle in high temperatures and be able to resist to a wide range of chemicals. Their permeability and compression set are also exceptional.

2.1.5.10 HiFluor (FKM)

HiFluor (FKM) is a high-performance fluoroelastomer that provides chemical in almost all media comparing to perfluoro elastomers (FFKM); particularly, HiFluor presents dominant benefit over conventional FKM polymers in polar solvents. In all industrial parts, HiFluor provides a broadly application solutions. From typical O-ring in standard dimension both imperial and metric through to diaphragms and molded engineering sectors owing to clients' drawing, the combination is able to process in rubber-metal composites too.

2.1.5.11 Parofluor (FFKM)

The parofluor series exist of leading perflyorinated elastomers (FFKM) under the trade names called Paroflyor and Paroflyour Quantum. Paroflyour compositions provide excellent retained resiliency comparing to other perflyourinated elastomers since they have been improved particularly for intensely challenging sealing utilization (ParkerHannifinCorporation, 2018).

2.2 Deformation force

Deformation force is the essential force that deform a cross-section of O-ring by a provided-percentage number based on the compound modulus. Deformation force is provided by distinctive cross-section of O-ring since it is analogous to seal geometry. The relationship of hardness, compression, and cross-section is illustrated in the following graphs. The information refers to all elastomers, that cause the deformation forces are contributed for individual hardness rank. The forces required to deform elastomers during assembly of flanges, for instance, be able to achieve from the graphs in Figure 2.2, Figure 2.3, Figure 2.4, Figure 2.5, and Figure 2.6, and forces which affect seals on less resilient plastic parts can also be approximately calculated (ParkerHannifinCorporation, 2018).

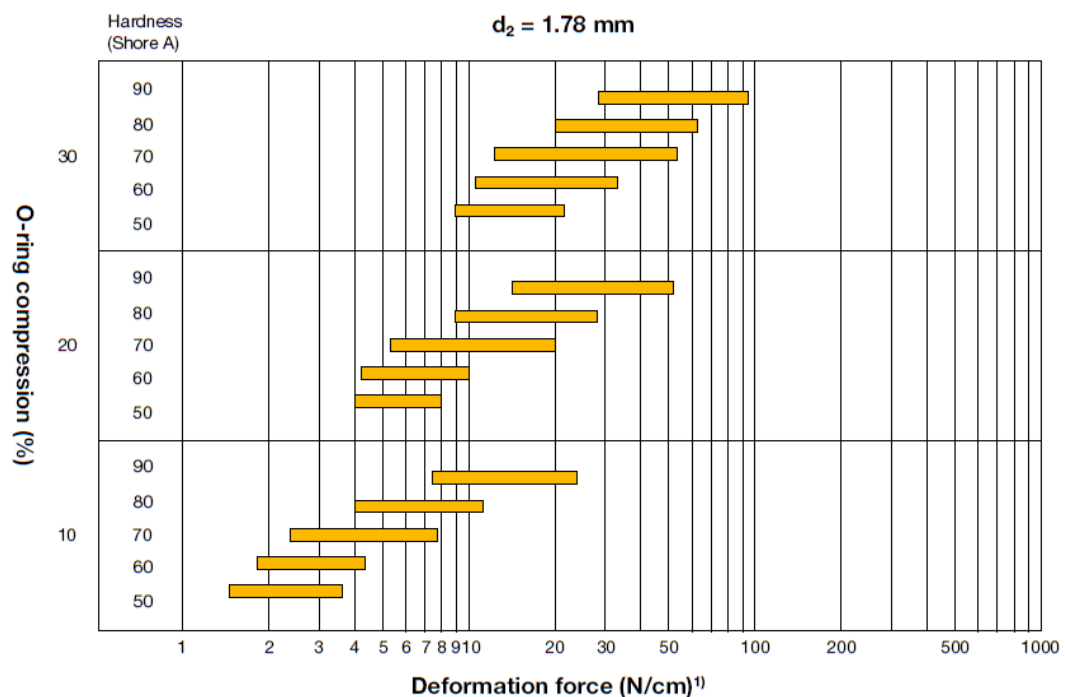


Figure 2.2 Relationship between hardness, compression, deformation force, and cross-section of 1.78 mm

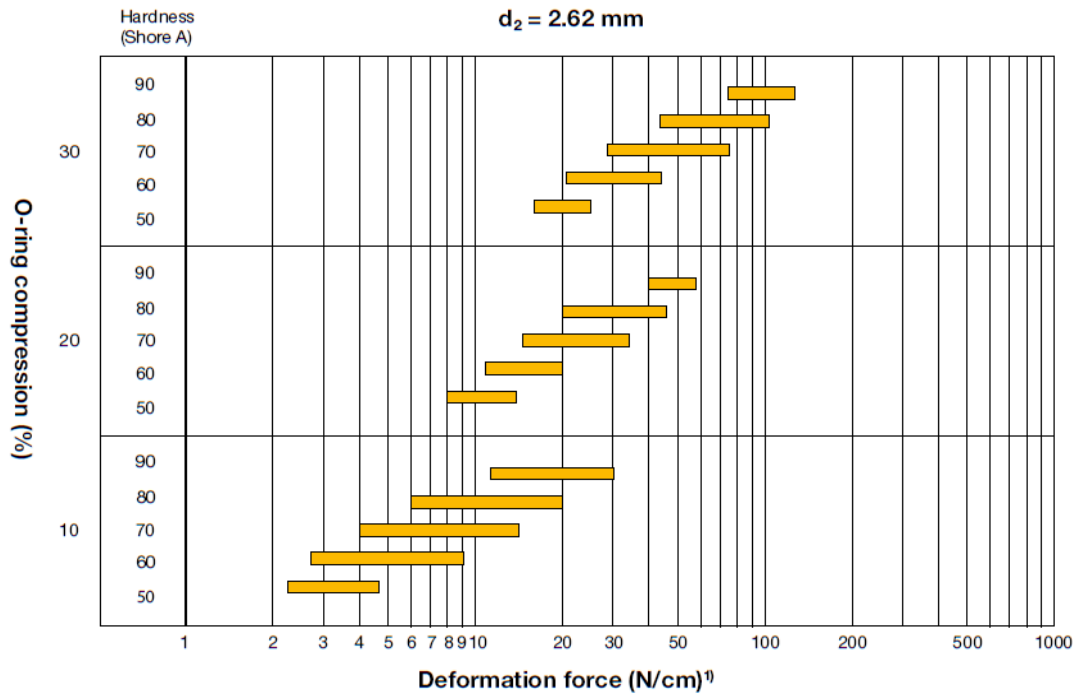


Figure 2.3 Relationship between hardness, compression, deformation force, and cross-section of 2.62 mm

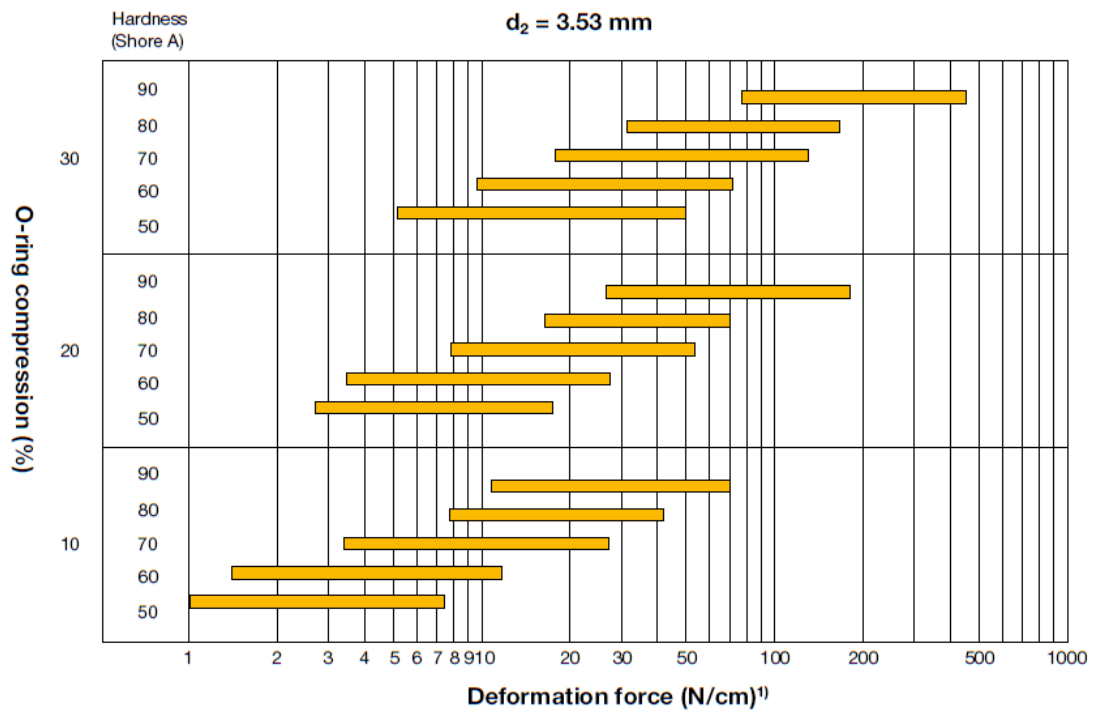


Figure 2.4 Relationship between hardness, compression, deformation force, and cross-section of 3.53 mm

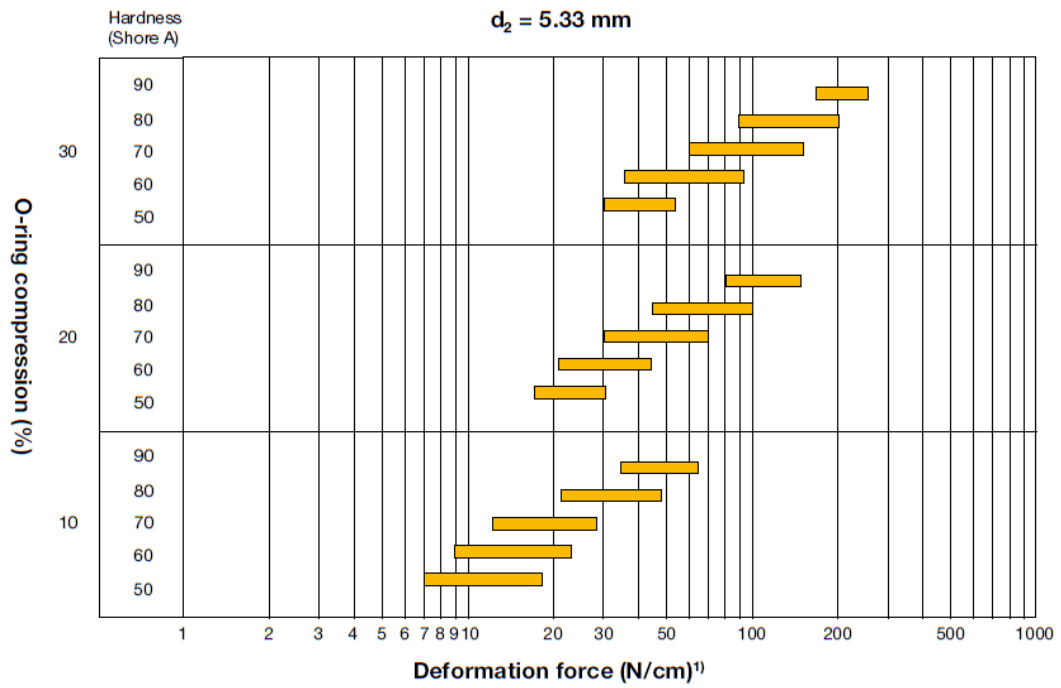


Figure 2.5 Relationship between hardness, compression, deformation force, and cross-section of 5.33 mm

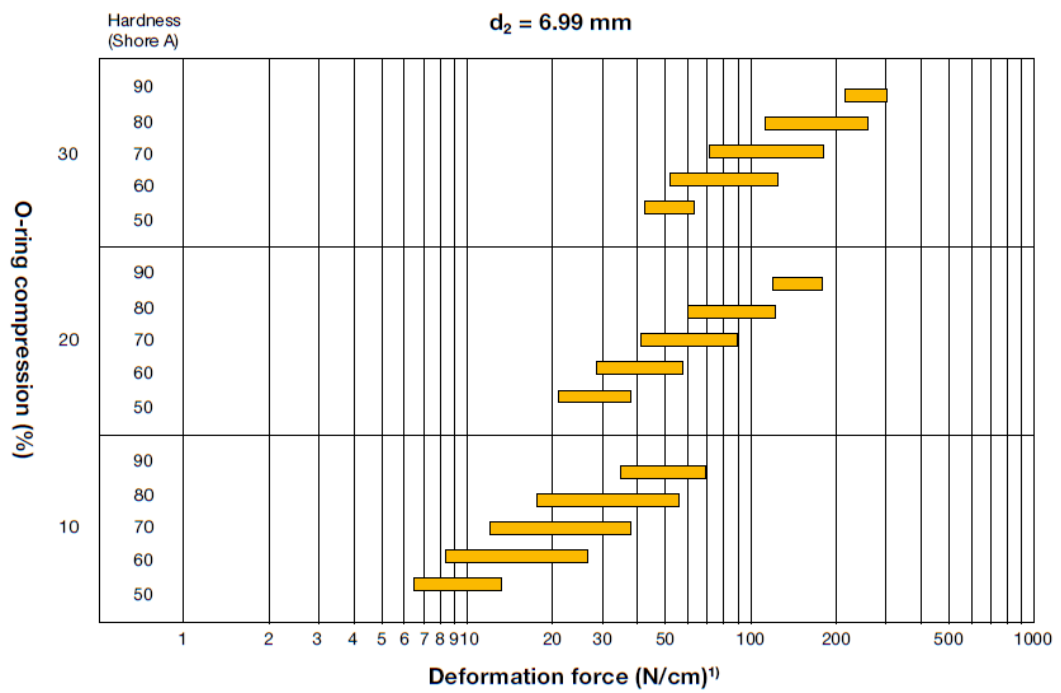


Figure 2.6 Relationship between hardness, compression, deformation force, and cross-section of 6.99 mm

2.3 Static axial seals

The pressure comes from outward or inward is the first attention while forming grooves for static axial seals. During the outward pressure the groove's OD is primary and the width of groove is the first attention for the ID. When the pressure is inward, the ID is primary Figure 2.7. This guarantees that the O-ring requires to relocate the least distance to seal the extrusion gap. The measurement of groove appendix contains two charts for static axial seals. One is for fluid and another is for vacuums and gases. The fluid functions of grooves are greater to permit an increased swell. On the other hand, the smaller groove measurement is being able to utilized if it has no anticipated swelling problems.

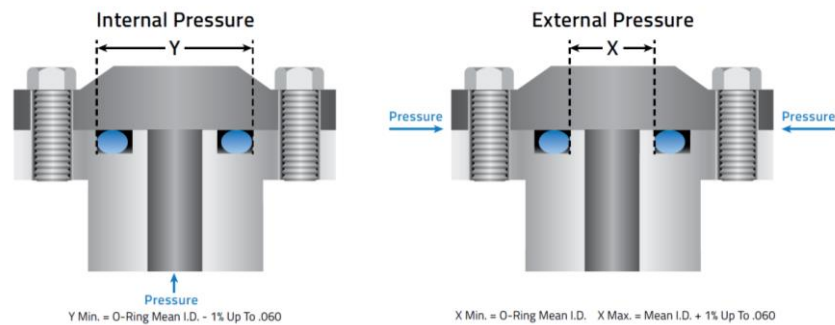


Figure 2.7 Grooves design for static seals

2.4 Dynamic sealing applications

2.5 Reciprocating dynamic seals

In dynamic reciprocating applications, usually O-ring is utilized within hydraulic, rod seals, or pneumatic piston Figure 2.8. There two stroke applications: the short stroke, smaller diameter O-rings have a strong performance and the longer stroke which demands thicker diameter of cross-sectional O-ring. Dynamic sealing applications have numerous failure modes increasing which are not troubles for static O-rings. Further specific aspect is detailed in the section of failure mode. For the surface finished of tools, they are critical to enlarge seal existence and actions. The conceptual surface of micro-finishing is from 10 to 20 μ -inches. Inherent lubrication of the surface wipes away by the end of the stroke when surface of micro-finish is under 5 micro-inches.

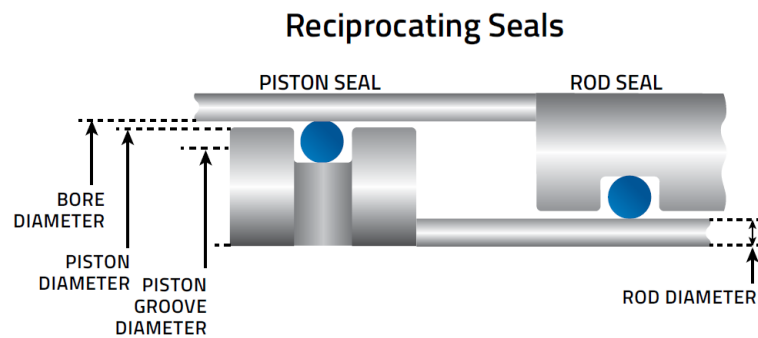


Figure 2.8 Grooves design for reciprocating seals

2.6 Rotary seals

Rotary seals are reliable seal beneath the proper conditions and confirmed by O-rings. Rotary seals are demonstrated in Figure 2.9. Three factors which must be matched to the appropriate compound of O-ring as Feet in minute values, Adequate durometer, and hardware configuration. A successful rotary O-ring commonly needs a shaft hardness value (55 Rockwell) (*The Definitive O-Ring Design Guide O-Ring Design Guide Content*, 2019).

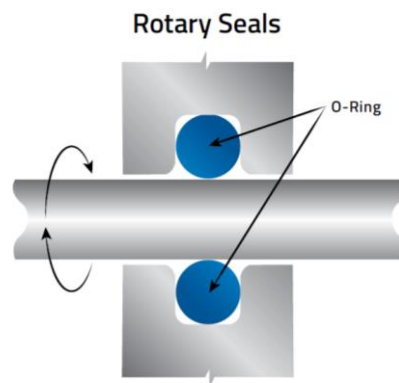


Figure 2.9 Groove design for rotary seals

2.7 Installations and design recommendations

Depending on ISO 3601-2, they recommend the following design but it cannot deploy for the special Isolast materials.

2.7.1 General recommendations

In advance of beginning installment, it needs to inspect the marks such as Lead-in chamfers made according to the drawing, Bores deburred and edges spherical, manufacture leftover part, for instance, chips, impurity and irrelevant pieces, removed, Screw thread tips covered, Seals and components greased or oiled, guarantee broadcast affinity with the elastomeric elements. Trelleborg Sealing Solutions suggests to consume the liquid to be enclosed, and do not consume oils together with solid supplements, for instance, molybdenum disulphide or zinc sulphide. O-ring installment crossing over crosswise bores is shown in Figure 2.10, Piston installment with O-ring is demonstrated in Figure 2.11, and Rod installment with O-ring is illustrated in Figure 2.12.

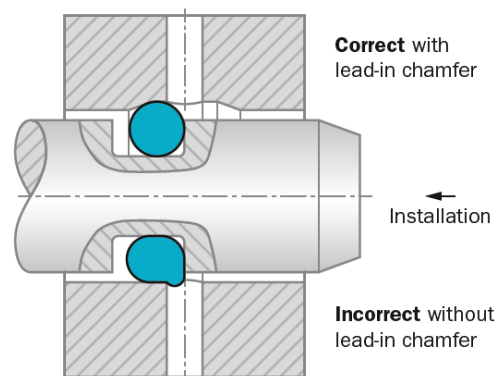


Figure 2.10 O-ring installation over transverse bores

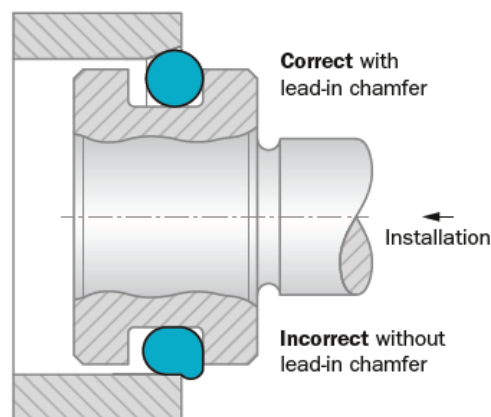


Figure 2.11 Piston installation with O-ring

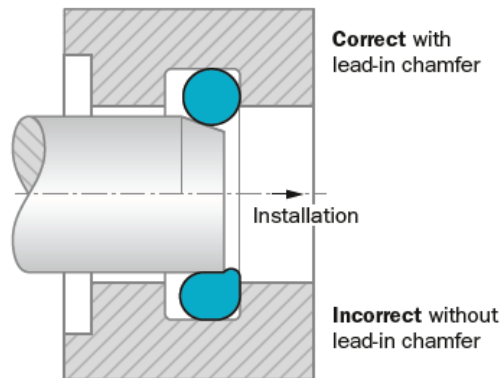


Figure 2.12 Rod installation with O-ring

2.7.2 Manual installation

For manual installation, it is recommended to use devices with the absence of knifelike corner, guarantee that the O-Ring is not crooked by using installation aids to assist correct positioning, use installation aids wherever possible, do not overmuch expanse O-Rings, and do not elongate O-Rings succeed of cord at the juncture.

2.7.3 Automatic installation

Automatic O-Ring installation requires good preparation. The surfaces of the O-Rings are intermittently conducted by various designs. This provides many profits in the time of installment by reducing the installment power and non-adhere impacts, effortless deportation.

The management and installment of dimensionally unsteady elements demand a great deal of experience. Reliable automated installation thus demands extraordinary management and package of the O-Rings (Solutions, 2016).

2.8 O-ring properties

2.8.1 Physical properties

Before choosing an elastomeric compound to use in O-ring application, you should regard a certain way of physical properties including resilience, hardness, abrasion resistance, modulus, compression set resistance, tensile strength, tear

resistance, and elongation. These physical properties are expanded and they are present in a given material. This expansion has a massive effect on the performance of material to hand over an effective seal.

Hardness: usually characterize as the resistance to indentation beneath specific conditions. An elastomer hardness is more precisely thought of as two relevant properties. Those properties are processed and inherent hardness. For inherent hardness, every elastomer has its own one on account of chemical structure. Both vulcanization and compounding can utilize to modify and supplement the inherent hardness. Hardness, processed hardness in molded rubber piece is a component of cross-link density and also the bulk of fillers. In the period of vulcanization, the final molded part will be harder as the cross-linking is given more. Processed hardness is used to judge the potential influence of a molded seal since it is one among the most common benchmark in the industry of rubber. Hardness inappropriately is one among the least consistent concepts too. In that case, there is the limitation only of comparability in the most-used measurement scales. Drawing a clear and smooth equivalence between readings on two distinct scales is frequently beyond the bounds of possibility although when samples are being measured, they are still very similar since the single “universal hardness” unit does not exist. Now a day, in rubber industry sector, there are two influential hardness tests such as Shore durometer Figure 2.13 and International Rubber Hardness Degrees (IRHD) Figure 2.14. In rubber industry, Shore and durometer words evolve into synonym for all practical purposes since Shore Instruments made more progress in the durometer-gauges marketing.

Presently, Durometer scales is offered in a wide-ranging by companies to adjust or conform to the standard ASTM D 2240. Durometer scales are formed to gauge hardness and they are designed in everything ranging from textile windings to plastic to foam. Typically, Rubber Hardness is calculated and represented by a Shore Type A or Type D durometer. You have to distinguish as always to choose which scale is applied in your needed situation for instance, 95 Shore A or 46 Shore D because there is more than one scale. The full category of materials which are guided to the selected Durometer scales is listed in Table 2.2. Durometer, Shore A is a

flexible and easily transported device. It uses not only as a frustum (made shorter) cone indenter mark but also an adjusted steel emerges to measure the resistance of rubber to indentation. The indenter point is forced back into the frame of durometer during the durometer is pressed opposite to a flat rubber specimen. This power is withstander by the emerges. Once unalterable contact of the durometer point touches the specimen, a reading is captured quickly (one second) except that an extended in time interval is wanted. Five-time reading is usually recorded and then the reading provides a mean value as result. The bulk of force that the rubber applied on the indenter point is shown as an arbitrary scale from 0 to 100 on a gauge. Harder element will bring about higher durometer numbers. The value 0 of reading would be exhibitivive of a liquid meanwhile 100 value would signify a hard plane surface such as glass or steel.



Figure 2.13 Shore durometer



Figure 2.14 IRHD Hardness tester

Noticeably, the value of reading which is smaller than 10 or bigger than 90 Shore A is not considered and unreliable. For elements which is stronger or tough than Shore A for instance polyurethanes and plastics are measured more correctly on a Shore Type D durometer that uses a more inflexible spring and a sharp 30° angle indenter point. The most of O-ring tools is in possession of reading from 40 to 90 Shore A. The almost accurate conversion for several of the durometer scales that are utilized the most is listed in Table 2.1.

Table 2.1 Conversion for durometer hardness scales

Type A	Type B	Type C	Type D	Type O	Type OO
100	85	77	58		
95	81	70	46		
90	76	59	39		
85	71	52	33		
80	66	47	29	84	98
75	62	42	25	79	97
70	56	37	22	75	95
65	51	32	19	72	94
60	47	28	16	69	93
55	42	24	14	65	91
50	37	20	1	61	90
45	32	17	10	57	88
40	27	14	8	53	86
35	22	12	7	48	83
30	17	9	6	42	80
25	12			35	76
20	6			28	70
15				21	62
10				14	55
5				8	45

Table 2.2 Guide to Durometer scale selection

Durometer scale	Most commonly used on
Type A	All O-ring compounds
Type B (not commonly used)	Moderately hard rubber
Type C (not commonly used)	Medium hard rubber and plastics
Type D	Hard rubber; polyurethane; thermoplastic elastomers (TPEs)
Type DO	High density textile windings
Type O	Soft rubber; medium density textile windings
Type OO	Sponge rubber and plastics; low density textile windings
Type OOO	Plastic foams
Type T	Medium density textile windings

Even though both 70 and 90 Shore A of O-rings are the most standard, the application will take control the necessary hardness. For low-pressure seals, they just require the softer compounds which offer smaller resistance yet the more extrude resistant tool is needed for the high-pressure seals. Considering and deciding about hardness property frequently entail compromise that one may guarantee the usefulness of the seal for long-term life. As an illustration, a relative hard blend may withstand the high-pressure extrusion yet its application could lead to raise in dynamic seals' frictional build-up. Friction increment causes to have high temperature and this high heat induces the seal degrading and makes the seal's life shorter. Significantly, it is necessary to be aware of the imprecision art of measuring the hardness of a rubber sample (see Figure 2.15). Contingent upon the particular gauge in use and the expertise of its machine's operator, the same sample probably give in two or more distinct readings. There are numerous impact factors to a test result such as utilization of force, rate of the durometer is applied to the specimen, number of times that goes by before recording the reading, and temperature of the sample at the testing time. Therefore, a tolerance of ± 5 points is added in the reading of all durometers yet it is still occasionally not adequate to predict completely all of the variances to be seen in testing. Though sometimes the advance technology has decreased many of the discrepancies, at the cost of the portability and simplicity which firstly made durometer popular. To get the accurate results of sample testing, it is recommended to

test several times and calculate the average number. Regardless of the long-standing close association between two points Shore and durometer, be realize the exist of companies which have high-quality durometers. One of them has a Micro hardness tester that have been developed for utilize on very small or too intermittently shaped specimens to be measure meticulously by standard durometers. The other broadly used tester is International Rubber Hardness. It uses a rounded indenter and a dial gauge calibrated. They are formed to adjust or adapt to the ASTM D 1415 standard.



Figure 2.15 Shore A hardness tester

Tensile strength: the force load needed to crack a sample of rubber is called tensile strength which is measured and represented both in pounds per square, psi or mega pascals, MPa. Conversion rate from MPa to psi is just using the MPa value multiply by 145 and from psi to MPa is dividing the psi figure by 145. For instance, 14 MPa converts to 2030 psi. In order to have the better knowledge about tensile strength, first remembrance that there are van der Waals forces, intermolecular forces assisting to hold lengthy polymer chains in place. Intermolecular forces reach the weakest point during the irregularities of structure which the molecules cannot fit as a group closely and amorphous structure that results in a non-regimented, too organized, or controlled. Nevertheless, some polymers have their component molecules and those component molecules lined up in very regular patterns. The mixture of both van der Waals forces and this regularity may be adequate to fit the

chains inside a rigid or crystalline pattern. Elastomer's ability is significant for tensile strength. Tensile strength predominantly depends on them to partially strain crystallize during the expanse. Larger crystallization approaches the increment of strength and resistance to stress for instance, Natural rubber, an elastomer which has a very consistent chain structure and strain crystallizes has high tensile strength. The temporary nature of strain crystallization definitely permits a natural rubber to get back to its original pattern once the stress is released. Inherently weak tensile strength of elastomer alike styrene butadiene is being able to improved their strength by using highly particulate reinforcing agents such as carbon black and silica (ordinary agents). In dynamic sealing, most of application will need an elastomeric composite at least 1000 psi equaled to 6.9 MPa of tensile strength. In most cases, the molded dumbbell (see Figure 2.16) is used to examine a tensile strength of compound in ASTM D 412. The dumbbell is put in the grips or jaws of a tensile tester (see Figure 2.17). the dumbbell started after the tester is switched on to pull firmly until the sample breaks at 500 mm per minute rate. The force load applied on the specimen at the rupture time is spoken to be the tensile strength of specimen. Lowest tensile strength is frequently utilized as the two qualification criterion during a brand-new element is specified and as a control criterion accompanying a $\pm 15\%$ production tolerance in the period of testing batches of mixed material.

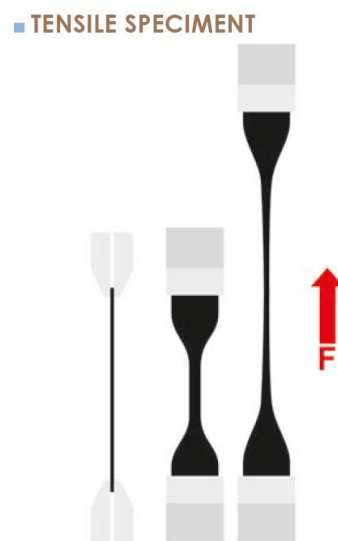


Figure 2.16 Molded dumbbell



Figure 2.17 Tensile tester

Modulus: it is the force or stress (possibly the best single gauge of an overall toughness of compound and extrusion resistance) to form a certain elongation (strain). The modulus stress is illustrated in psi as pounds per square inch. The range of elongation can be 50%, 100%, or even 300%. For comparing aim and experimental test, the most broadly used value is 100%. In industry literature usually use M100 or modulus 100 to represent 100% elongation. The higher modulus of compounds the more resistant to extrusion and resilient. In general, the hard compound has the high modulus. Modulus is recognized as tensile modulus or stress as well since it fundamentally measures the tensile strength at a specific elongation instead of at rupture. Simultaneously, Modulus commonly measures with tensile strength on the same dumbbell sample shown in Figure 2.16 as reported in ASTM D 412. The tester notes the psi (942.5) and an elongation (100%) as the sample is expanded. The value in psi is the sample's modulus at that elongation. Lowest value of modulus is utilized usually as a qualification criterion during a brand-new tool is specified. It could do the work of a control criterion within a production tolerance of $\pm 25\%$ during operating finished sections.

Elongation: elongation is the increasing percentage in original length (strain) of an elastic sample due to the stress or tensile force put into the sample. Elongation is vice versa proportional to modulus, hardness, and tensile strength. When a material has very large strength of tensile, hardness, and modulus, it will have less elongation under stress. For hard tool which has high modulus and tensile strength requires more stress to stretch more than a soft tool that has low modulus and

tensile strength. Ultimate elongation is the elongation when the sample cracks. In accordance with ASTM D 412, ultimate elongation is mostly marked together with modulus and tensile strength in the period of tensile testing. Some elastomeric tools were much more forgiving than others in this field. For natural rubber, it is able to elongate up to 700% before fracturing and Fluorocarbons commonly explode, break, or tear at approximately 300% of elongation. These figures are considered to highlight only analogous failure manner and is not a satisfactory seal installation value. Overstretching is possible to be the certain cause of an O-ring to fail, therefore elongation is a significant installation element; particularly, alike gland and seal measurement decrease. In bigger seal, the increment of small percentage can have a greater expansion in a smaller seal. By the reason of the number of elongations which is given can mean immensely distinct things, elongation is doubtlessly related to an initial size of seal. Yet extension is infrequently a trouble, setting up small diameter, high durometer, and low elongation seals could be problematic in some case or situation.

Tear resistance: it is a resistance to the growth of a small cut (nick) in a surface or an edge in a vulcanized (cured) rubber sample during the tension is applied. It is generally present in kilonewtons per meter (kN/m) or pound force per inch (lbf/in). Tear resistance is a significant consideration either as the finished item is take off from the mold or as it behaves in real service. Tear resistance could be measured by the same ASTM D 412 equipment or systems utilized in the tensile strength, elongation, and modulus testing. Distinct types of sample can be utilized to gauge either the initial tear or the propagate tear. The resistance to the begin of a tear is demonstrated in Figure 2.18 and the resistance to the stretch of a tear is illustrated in Figure 2.19. These both ways, the specimen is put in the grips of tester then apply a homogeneous pulling force (stress) until the break point. Then this stress might be divided by the thickness of sample to reach the tear resistance for that specific sample. Three individual specimens are basically tested and a mean value is computed. All-natural rubber, epichlorohydrin, and polyurethane contain superb tear resistance; however, countless components are not extremely strong in this area. Remarkably, both FVMQ and silicone have weak tear resistance. It is probably logical; however, in

fact, it is a common misunderstanding that hardness is spontaneously equivalent to excellent tear resistance. Compounds which have less tear resistance beneath 100 lbf are extremely in danger for instalment destruction; particularly, in methods featuring non-polished spaces such as with threads, burrs, and slots and/or sharp, non-radius edges. During destruction, the components with low tear resistance will be unsuccessful in utility hurriedly. This is particularly truthful for dynamic seals. Low tear resistance is associated to low abrasion resistance.

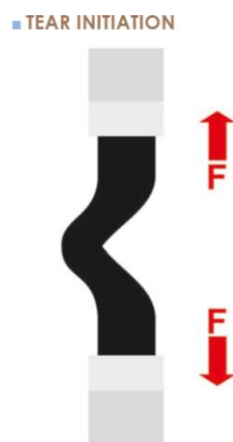


Figure 2.18 Unnicked 90° angle

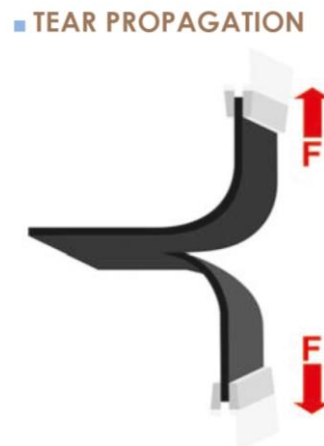


Figure 2.19 Slit (Trouser) specimen

Abrasion resistance: Abrasion resistance refers to the rubber compound's resistance to wearing away by contact with a mobile abrasive surface. Abrasion resistance is gauged as a percentage loss depended on initial weight. When

in fact the nicking (cutting) of a surface seal is an immediate event, scraping (abrasive rubbing) is much more of a developing phenomenon which progresses over time. seals are extremely susceptible to abrasion when they are in motion. Hard composite likely illustrates less abrasive wear than the soft one. The utilization of a harder composite is possible to gain the friction in dynamic seals too. Furthermore, raising friction brings about seal-degrading heat.

Abrasion resistance is difficult to gauge correctly since there are a lot of potential factors such as surface contamination and heat variation. Testing normally includes the uniform application of an abrasive tool (sandpaper) to the specimen's surface. Three distinct abraders are explained in ASTM standards. The first is D 1630 relies on a National Bureau of Standards (NBS) abrader which illustrated in Figure 2.20, the second is D 2228 which utilizes a Pico abrader (see Figure 2.21), and the last one is D 3389 uses a Taber Abrasion to make use of a double-head abrader and a rotary platform as demonstrated in Figure 2.22. Notwithstanding of the particular testing method, the relative number of specimen tool which is extinct as a result of abrasion is a great sign of abrasion resistance. In general, hydrocarbon-based elastomers is likely to provide superior abrasion resistance than fluorocarbon one. The elastomers which have greater abrasion resistance than hydrocarbon-based elastomer is carboxylate nitrile and hydrogenated nitrile and the elastomer that has the excellent abrasion resistance is Polyurethane.

■ NBS ABRADER

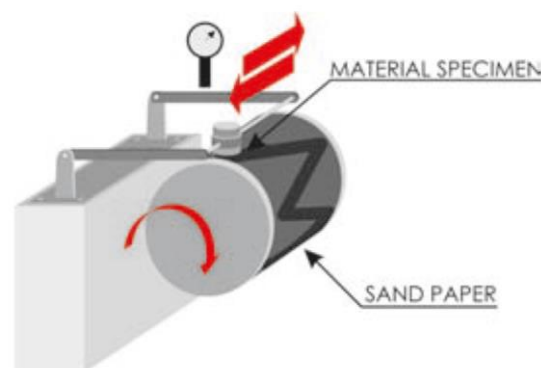


Figure 2.20 Rotating drum

■ PICO ABRADER



Figure 2.21 Rotating platform

■ TABER ABRADER

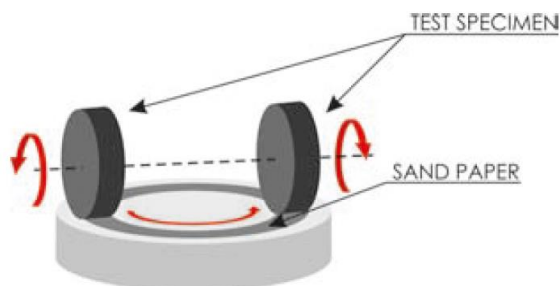


Figure 2.22 Rotating samples

Compression set: by expressing as a percentage, the compression set of elastomers is the result of testing the capability of rubber to rebound to the initial thickness after progressive compressive stresses over a period of time. In the seal's life term, stress relaxation is alike failing while compression set is considered as death. The compression set's impact on the cross-section of an O-ring is illustrated in Figure 2.23. Measuring and getting the accurate amount of stress relaxation is hard; however, compression set is not difficult to gauge. The specific aspect in ASTM D 395 specifies the compression set experiment for rubber that will be compacted in liquid or air media. Those are the method A (for consistent force) and method B (for

consistent deflection). Though they are in different method, their basic methodology is considerably the same. Usually testing utilizes of barrel-shaped disk compression set test buttons with the thickness of 12.45 mm and diameter of 28.96 mm. instead of buttons, die-cut plied or stacked specimen within 1.78 mm thick and the same diameter may be replaced. The plied or button specimens are substituted between steel plates. In method A as illustrated in Figure 2.24, the plates are forced all at once using both a pre-defined outside force or a calibrated spring. Whereas in method B as demonstrated in Figure 2.25, a bolt-tightened instrument and steel spacers are utilized. Referring to a choice between two possibilities, 25% of initial thickness of compression is held for 22 hours' time given at a particular heat 100 °C, these last two variables depended on expected service circumstances. Beyond the removing from the compression instrument with a cooling time of haft hour, the samples are gauged by utilizing a dial micrometre. Compression set can be measured and presented as a percentage of original deflection or sample thickness. The high amount of compression set is to be refrained; however, unintentionally happened fluid swell or the international application of bigger squeeze might compensate. Facing either shrinkage or large compressions set, seals are extremely possible to fail. Seals are most likely to fail when there is both high compressions set and shrinkage. In Figure 2.27, it demonstrates about how various materials behave to increasing temperature.

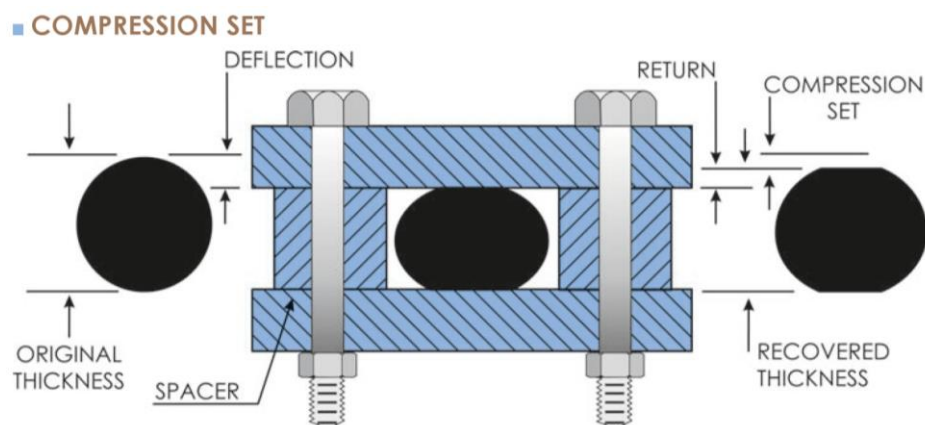


Figure 2.23 Effects of compression set on an O-ring's cross-section

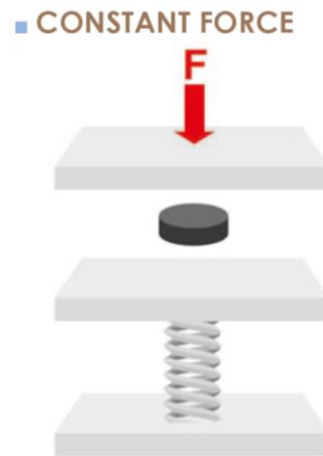


Figure 2.24 Compression set test method A

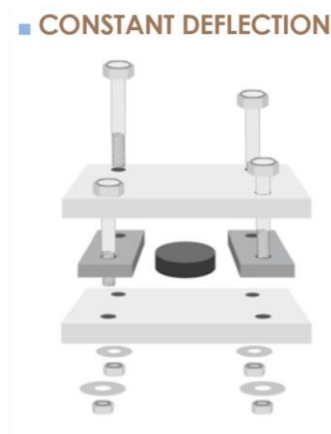


Figure 2.25 Compression set test method B

Resilience: resilience has another name recognized as rebound. In ASTM D 2632 description, resilience mentions about a compound's ability to get back to its initial shape and size beyond temporary deformation. The experiment of rebound is usually falling a small weight onto an experimental sample like a compression set button as illustrated in Figure 2.26. The expansion to which the weight bounces back is marked as the initial drop height's percentage. Material which be able to regain its dimension quickly may cause a rebound amount of 70% is considered as a highly resilience material and the amount from 40 to 50% are mostly for the plurality of elastomers tested. Compounding might develop an elastomer in this field; however, it is also possible to take away from good resilience which is

greatly an inherent property. Rebound is the most critical in the rule of dynamic seals. Although the physical properties are significant in a given material it is not the last episode of the story. Chemical properties are critical as well. Therefore, they are detailed as the following section.

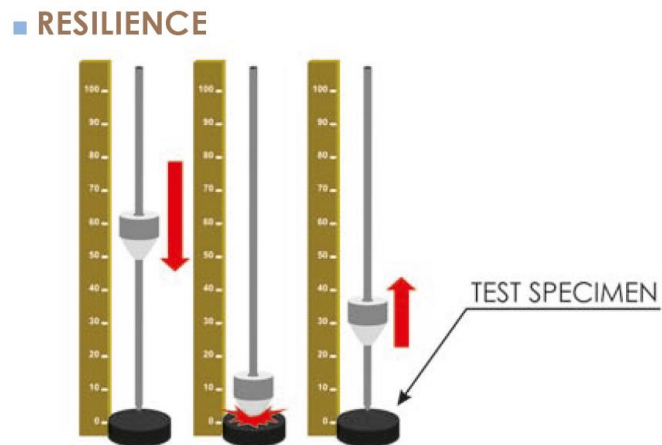


Figure 2.26 Bashore resilience testing

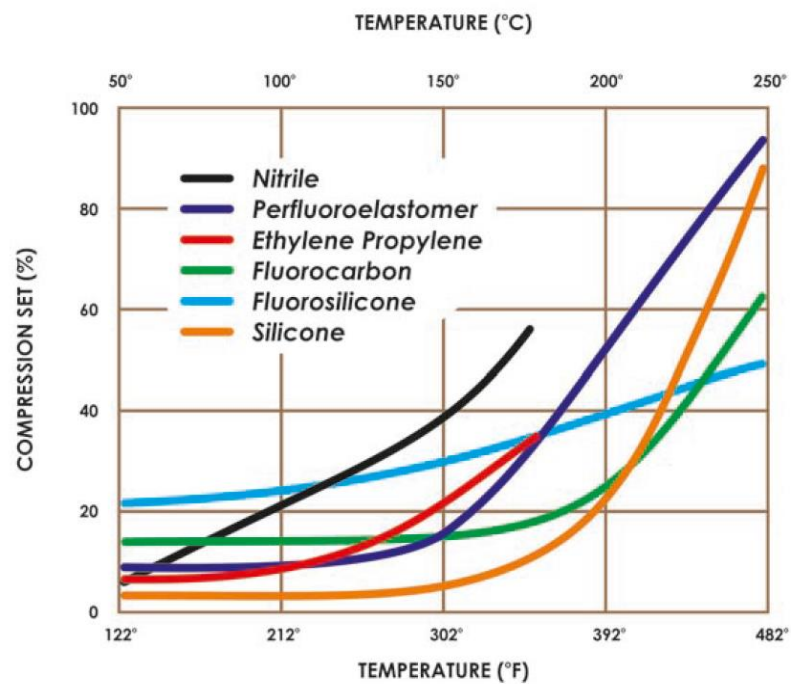


Figure 2.27 Compression set in increasing temperatures

2.8.2 Chemical properties

There are some significant chemical properties to be considered. They are compatibility and volume change.

Compatibility: it indicates to resistance of a seal material to be in possession of its chemical properties degraded both permanently and temporarily by the reason of contact with a gas or liquid. Due to “Likes dissolve likes”, the real glue to compatibility between the fluid and seal being enclosed is divergent chemical network. For instance, oil-derived-material O-ring seal are possible to extremely compromised when put in contact with fuels or oils. The most result tends to have extreme physical growth of the O-ring as result of the seal’s failure. The O-ring swell is shown in Figure 2.28. To be more resistant to the initial system fluid, the seal ought to have the resistance to each and all additives as well that might be happened upon the operation system. For instance, applications of oil field usually use film-forming amine prevention to cover tubular merchandise and assist to avoid metal erosion. Unluckily, amine prevention do as curing agents for some fluorocarbon elastomers which can make the seal to be harden and failed. An O-ring in this function would require to be resistant to the fluids which are sealed and to the added amine inhibitors for giving an effective and durable seal. Whether the fluids do not degrade the elastomeric composition straightforwardly, some of them reduces the surfaces next to the seal together with metal corrosion, hence lowering the effectiveness of the seal itself. You have to retain as well that even though some composites developed from a specific polymer might be all right for utilize in a given fluid, not all composites of those polymer will be suitable for utilize in that liquid. By the reason of a properties of compounds are a next to outcome of its mutual components namely reinforcing agents and plasticizers, each single formulation may be tested under actual service situation to find out exactly its suitability for an operation. To figure out the chemical compatibility, it has no unique ASTM experiment. Instead, compatibility is assumed to be a broad approach incorporating shifts (or the lack of that) in an amount of material properties, individual with their own experiment methods. Physical properties (Elongation, hardness, modulus, and tensile strength) be able to compromised all if a compound is not adaptable with or resistant to a given fluid. The

most seeable proof of chemical incompatibility probably is a shift in the volume of material.

■ EVIDENCE OF INCOMPATIBILITY



Figure 2.28 O-ring swell

Volume change: it indicates both the raising (in Figure 2.28) and declining (in Figure 2.29) in the volume of a sample that has been in contact with a fluid and usually marked as a percentage of the original volume. This contact might categorize from casual Splashing to stable Immersion. Minor result of volume shifts points out a relative compatibility between the sample and fluid, whereas the major change demonstrates an incompatibility. A sample which swells double its original volume is spoken to assist undergone a 100% increase. Swelling makes an elastomeric seal turn into softer and shrinkage causes the seal harden. A little swollen seal is still working. A restricted amount of swell might even compensate for other factors as compression set. Otherwise, shrinkage can make worse an existent compression set issue. Alongside some of its soluble element (like plasticizer) having been drawn out by the fluid system, a seal of O-ring which has undergone shrinkage is more likely to leaks. In the testing method, ASTM D 471, it described the volume shift experiment typically employs ASTM, Industry Reference Material (IRM) oil, ASTM Reference Fuels, Type 4 (IV) Reagent Water, and service liquids. Notwithstanding of the liquid in use, experiment includes immersing a known-properties material specimen in the liquid for a particular duration (for instance 70 hours) at a particular temperature (for example $100^{\circ}\text{C} \pm 2^{\circ}\text{C}$), the two variables depended on the circumstances expected in service. Material degradation is then found out depend on shifts in physical properties which includes volume.

EVIDENCE OF INCOMPATIBILITY



Figure 2.29 Shrinkage due to plasticizer extraction

2.8.3 Thermal properties

High or low temperatures can affect the chemical and physical properties of an elastomeric element involving of volume, hardness, elongation, tensile strength, compression set, and modulus. particularly if the exposure is for an extended time. Due to O-ring frequently face utmost high or cold temperature or either both extremes in some cases, there are significant thermal properties you have to consider such as the effects of low and high heat, thermal expansion's efficiency, and the effect of Gough-Joule.

High temperature effects: except for specially formulated, elastomers will commonly weaken during the early exposure in the high heat. Enlarging expose temperature can make irreversible shifts in elongation and tensile strength and changes in the chemical composition of a seal such that it hardens and breaks. The supplementary oxidation, cross-linking, and/or plasticizer evaporation are the cause of this hardening. Figure 2.30 demonstrates how high heat affects a small quantity of the most used materials. ASTM has four distinct methods to test the effects of high heat. They are designed to measure the quantity of material deterioration that issues from exposure to a temperate environment. The predominant difference of them is the tool utilized to maintain or hold the pressure and temperature on the sample. First device is D 454 which utilizes an air-pressure chamber to imitate the lowering effects of heat and air. Next tool is D 572 that uses a familiar oxygen-pressure chamber to compute degradation by heat and oxygen. Third device is D573 which describes the experiment in an air microwave oven. The last one is D 865 which details heat and air experiment within a test tube enclosure.

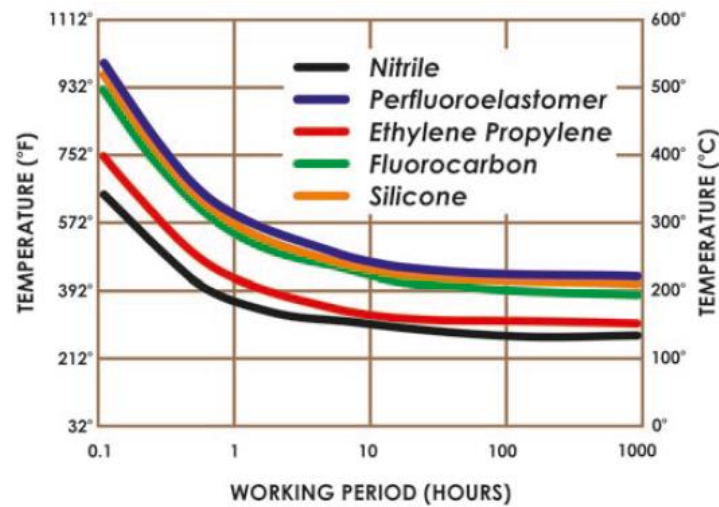


Figure 2.30 Material performance in high temperatures

Low temperature effects: different from the shifts resulting from high heat exposures, shifts given by low heat exposure are usually not permanent and possible to be reversed when the temperature returns. For instance, expanded exposure to low heats will raise the hardness of elastomers, nevertheless, the material will be soft again once the heat increases. The most significant consideration which relate to low heat increases involves seals that must operate in a small-pressure environment as well. Unless the seal compound which is selected adequately soft and bouncy, the mixture of little heat would make both shrinking and solidification of the seal and small service pressure which will not assist hold the seal to face the mating surface could make failure and leakage. ASTM has two principle methods to test the effects of low temperature. First device is Method A, ASTM D 2137 as an idea to gauge the brittleness point, or the smallest heat at which a specimen will not fracture or break when hit occurred one time only. The last one is Method details in ASTM D 1329 (typically recognized as a TR-10). In this test, the heat recantation experiment (as shown in Figure 2.31) is cared about many within the rubber industry to be the most helpful barometer of a little heat operation of material. In the summing-up, the TR-10 gauges' material resilience. Specimens are refrigerated in a stretched state. After that they are warmed steadily up to their 10% loss of stretch (take back by 10%). These test's results are reliable to give a good foundation for assessment the impacts of crystallization and the effects of little heat on visco-elastic properties. The results of TR-10 are usually considered to be regular alongside with the ability to

perform of most dynamic seals. In Static seals, they are possible to function at temperature of 8°C under the temperature of TR-10.

■ LOW TEMPERATURE TESTING

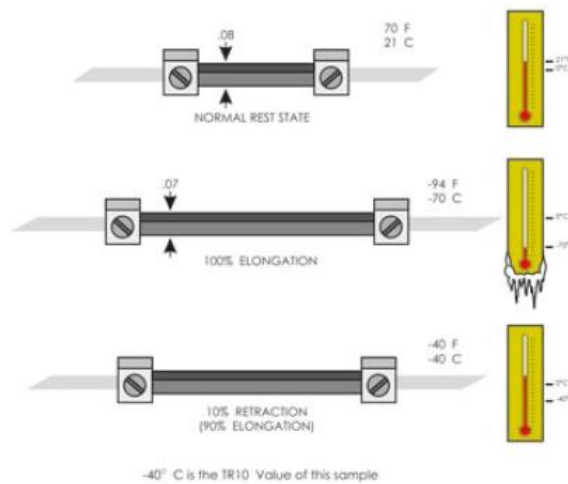


Figure 2.31 Temperature retraction, or "Tr-10"

Coefficient of thermal expansion: Coefficient of thermal expansion is might be presented in both straight and volume amount. For the coefficient of linear thermal expansion, it is the shift in distance per unit of the distance for a 1° increase in heat. Whereas the coefficient of volumetric thermal expansion is the shift in volume which is separated by two by the output of the initial volume and the shift in heat. The coefficient of volumetric expansion in solids state is equalled to three times of the coefficient of linear expansion. On account of the elastomeric compositions contain larger coefficients of expansion than aluminium and steel, thermal expansion might make a tight seal to swell and spill the gland due to the increasing of heat. Glands have been recognized to explode, break, or tear under the force applied by an extending seal. On the contrary, a designing seal that offers the minimum of squeeze only in a low heat setting is not possible to look to thermal impacts for assist in tightening the seal.

Gough-Joule effect: two related phenomena are described in the Gough-Joule effect as illustrated in Figure 2.32. First phenomena, differently from most elements, rubber temperature up once rapidly elongate while the second one, rubber which is held stationary at one end and stretched beneath a provided force (load) will correctly take back if local temperature is exerted. This is concordant with

facts since the rubber's forced macromolecular structures are trying to get back to a less-forceful state. The Gough-Joule effect is probably the most significant in the rotary seal method, that extreme installed elongation beside with system temperature could make an O-ring to take back, dooming the design, and seizing the quickly rotating shaft (Seals, 2019).

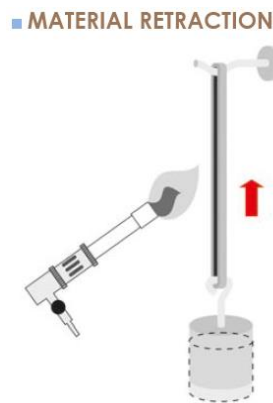


Figure 2.32 Gough-Joule effect

2.9 Effects of temperature on rubber O-ring

(Cui et al., 2013) has done a research to try to simulate polymeric seals/gaskets in actual work and to forecast the sealing force during the change of temperature. Their research was carried out to acknowledge the material stiffness change when difference of the temperature is applied. As result, the stiffness of LSR shows up to change according to temperature experience.

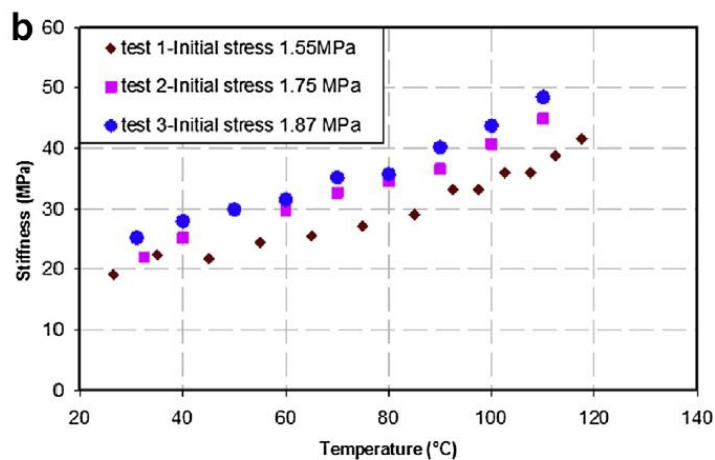


Figure 2.33 Relation between stiffness and temperature

(Kenneth T. Gillen et al., 1996) conducts a study on strain of a butyl-B O-ring for 24 hours at a heat of 80 °C and later decreased the heat to room temperature. It was found that the enclosed power decreased by 40 percent and came to an analogous “equilibrium condition” subsequently the heat went down to room temperature. An comparable aspect was also done with FVMQ O-rings were utilized (K. T. Gillen et al., 2005). The result of their work shows that sealing power went down undoubtedly with the reduction of heat that was as a reason of thermal shortening of the seals. (Derham, 1997) also stated that there is a reduction of 50 percent of sealing force when he operated the heat cycling experiments with fluoroelastomer and altered the heat from 80 °C to 23 °C. The inflexibility of the polymeric element raised after quick sealing force relaxation in the first 2 or 3 hours in his further work. The raised element inflexibility is being able to utilized to give a reason for the great load decrease following the decreasing heat. The test results of either Gillen or Derham demonstrates that it is not only thermal contraction that effects to the great decreasing of sealing force but also have other somethings do.

(Tan et al., 2011) testing a silicone gasket element exposed to Proton-exchange membrane (PEM) fuel cell with the operation temperature of 80 °C and 60 °C to keep the reactant gas and liquid within their respective regions. By using micro indentation testing, they found that the surface hardening occurred and the elastic modulus increased for the aged silicone element. The heat has a declare impact on the solidification. Similarly, (Schulze et al., 2004) stated the deterioration of seals in PEM fuel cells when they were operated.

Another research has investigated on failure behavior of rubber O-ring beneath the ambient heats of 30 °C to 100 °C. They found that their break deterioration became more severe with an increment in the ambient temperature. The severe fracture deterioration below great heat is considered as reason of reduction of mechanical properties with increment of ambient heat (Yamabe et al., 2013).

(Xuming Chen et al., 2016) has checked into thoroughly the glass transition temperature (T_g) and great-pressure compression force relaxation characteristics of numerous elastomers at low heat, and present their impact on low heat sealing performance below operating condition of static as well as cycling

pressure/heat. As the results, the O-ring did not show any cracks when tested under low temperature, and only showed cracks under low and high temperature cycling and the combination of high temperature and high external pressure is the leading factor to induce such cracks in PR2 testing. At low temperature, elastomers were normally strong enough to stand the high internal compressive/tensile stresses/strain, and did not show cracks, at high temperature, however, elastomers became weak and could not withstand such high internal compressive/stresses/strain, and generated cracks through internal tears in the initial squeeze direction (radial direction).

(Akulichev et al., 2018) were conducted the test in numerous face seal fixtures to evaluate the ability of Viton V747-75 O-rings to seal for a range of temperature. The result showed that the test temperature had a much greater impact on the sealing performance of the O-rings than did the gland surface finish or initial O-ring position. At 30 °F and below, satisfactory seals were not achieved because the O-rings did not track the seal test gap opening as a result of insufficient resiliency of Viton elastomer. The high heat abrasion patterns produced were minor, but the low-heat abrasion patterns were more declared and were seen as fracture close by the edge of the O-ring (Lach, 1993).

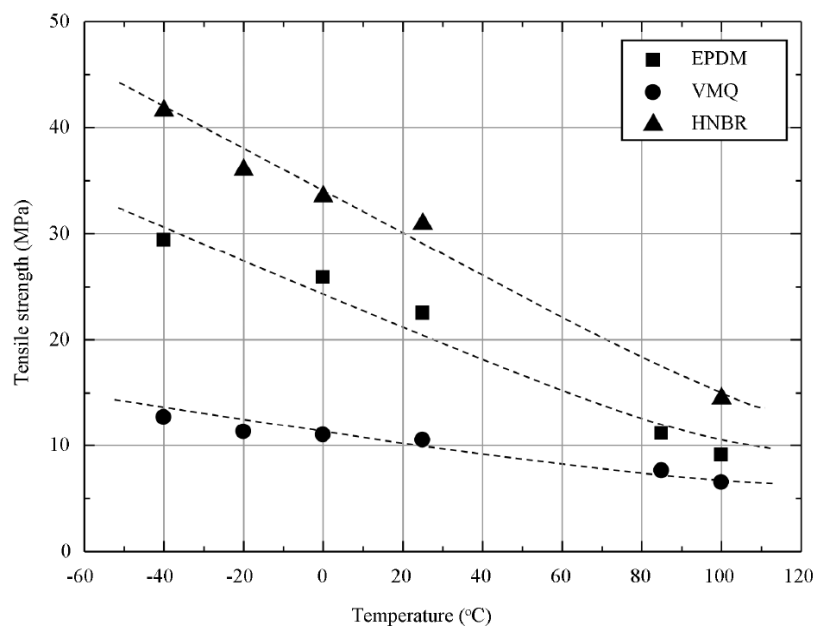


Figure 2.34 Influence of temperature on tensile strength of rubbers

There are two factors that make the rubber seals got gas leak: the gas passage over the elements and gas passage from the surface leak. The gas passage over elastomers is recognized to reduce when the heat is decrease. The contender catastrophe triggered scientists and engineers from a variety of commerce to learn the low-heat characteristics of elastomer seals to be utilized in gas include scheme. By cause of their struggling, some publishing came into view. A short main points of the testing details and findings of the existing literature is demonstrated in Table 2.3.

The compression force and tested distinctness gas pressure were provided in parentheses. Other way applied to check the More explanation is the glass transition (T_g) was provided in parentheses too. For more explanation, the bookworm is assigned to the registered publishing reports. ΔT illustrates the distinctness of the determined leak heat T_{fail} and the glass transition. Particular experimental terms are detailed in notes. Most seal failure is at temperature about 10 to 35 °C under T_g relying on their applied pressure distinctness and compression rank.

For plenty of high-tech use, it is vital for the compactness of this sort of schemes can withstand a great heat rank. The compactness of elastomer O-ring seals at small heats is often observed as well by checking the leak gas amount and the sealing power at the same time as particular thermal cycles.

For this situation, the leak is able to take place at small heat by the causes of the contact pressure reduces because of the thermal shortening and a loss of stretchiness happens in the time of freeze stage.

Great heat effect to the breakdown of the element that leads to gas leak. Small heat effects the performance of the seal since the rubber- T_g contributes in more vital parametric shift. The stiffness of the elastomer increases as the temperature decreases. Although a leakage can occur at low temperatures, all the performances of the seal be able to get back if a adequate great heat is recovered (Troufflard et al., 2018).

Table 2.3. Short summary of the low-temperature leak test data.

Elastomer type	T _g , °C	TR-10, °C	Typical conditions		Special conditions		Notes
			T _{fail} , °C	ΔT, °C	T _{fail} , °C	ΔT, °C	
Taylor (15% compression/345 bar)							
Nitrile	-37 (DTMA)		-56	-19			
Arctic Nitrile	-35 (DTMA)	-49	-62	-27			
Camlast 1049	-18 (DTMA)	-19	-40	-22			
Aflas	7 (DTMA)		-23	-30			
Viton	3 (DTMA)		-34	-37			
Burnay and Nelson (1 bar)							
FKM E60C	-18		-30	-12			
Stevens et al. (10/20% compression/14 bar)							
FKM E60C	-18		-31	-13			Results are for 10% compression
FKM B70	-21		-33	-12			
FKM B600	-13		-26	-13			
FKM GLT	-29	-31	-44	-15			
FKM GLFT	-23	-24	-36	-13			
Weise et al. (25% compression/1 bar)							
Viton1	-7		-35	-28			
Viton2	1		-20	-21			
Viton3	-6		-31	-25			
Viton5	-23		-44	-21			
EPDM	-30		-61	-31			
Silicone	-31		-63	-32			
Warren (16.6–18.5% compression/100 (175) bar)							
HNBR LT	-32	-36	-54	-22	-41	-9	Pressurized after the cooling step
FKM LT	-19	-31	-55	-36	-32 (-21)		
FKM ULT	-27	-40	-56	-29	-42 (-45)	-15 (-18)	
Jaunich (13–38% compression/1 bar)							
FKM	-18		-29	-11			13% compression
			-33	-15			25% compression
			-53	-35			38% compression
Omnés and Heuillet (24% compression/5 bar)							
HNBR	-18				-30	-12	Pressurized after the cooling step
Grelle et al. (25% compression/1 bar)							
FKM	-17		-38	-21	-10	7	Partial release of compression

2.10 Effects of hydrogen gas on rubber O-ring

(Yamabe et al., 2013) investigate on breakdown characteristics of rubber O-ring under cyclic exposure to high-pressure hydrogen gas. The rubber O-ring were tested under the hydrogen pressures ranging from 10 to 70 MPa. They found that the cyclic hydrogen exposure caused cracks in the O-rings, and their crack fracture turns into more severe with the increment in the hydrogen constrain.

(Ono et al., 2018) conducts a study of unfilled NBR compounds by applying it into the great pressure hydrogen. Their objective is to understand the chemical reduction of this elastomer element during expose to great pressure hydrogen. Their results show that the great pressure hydrogen exposure did not take place any chemical form shifts in NBR by Nuclear magnetic resonance (NMR) determination. Subjecting to danger the elastomer elements to the great pressure hydrogen, the hydrogen gas disappears into the elastomer elements and releases from them in the state of dispersion after quick gas reduction in air pressure of the ambient great pressure hydrogen. The disappearance of hydrogen gas into the elastomer compounds of an O-ring issued from the great pressure hydrogen exposure makes some sort of cracks including overflow, fracturing and bending. Yamabe and Nishimura revealed the foam expansion characteristics utilizing an ocular microscope between 5.5 and 7.0 min after the decompression with transparent unfilled EPDM exposed to hydrogen gas pressure of 10 MPa and heat of 30 °C.

(Koga et al., 2011) did a research on the influencing factors on blister fracture of rubber O-rings under high-pressure hydrogen environment. They have found that the sensitive factors influencing on the crack damage of rubber O-rings were the material, decompression time (rate), O-ring filling ratio, and temperature. The tensile strength of the rubber O-rings goes down with an increase in temperature and the crack damage of the rubber O-rings became more serious with an increase in the temperature.

Frequently, the O-ring seals were utilized in great-pressure hydrogen storage systems for avoidance gas leaking. Nevertheless, the seal element that exposed next to great pressure hydrogen gas is failed as the results of the swelling caused by disappeared hydrogen. It is significant to form the elastomer seals to utilize

in the great pressure hydrogen gas in order to make clear the impact of swelling on the sealing characteristics of the elastomer O-ring. Although the little number of publication on the swelling characteristics of elastomer elements exposed to great pressure hydrogen gas is accessible and nearly all of those publishing reports are organized by Yamabe team in Japan. Yamabe team made a durability inspector tool that be able to expose elastomer O-rings to great pressure hydrogen many times. By utilizing this tool, the fracture crack, swelling and hydrogen passage of elastomer O-ring are observed. Their results illustrated that the raised volume caused by swelling is impacted from hydrogen pressure, heat, amount of hydrogen and the sort of fillers namely silica and CB (Zhou et al., 2017).

2.11 O-ring operation and design

2.11.1 Back-up ring

Back-up Rings are the items use to protect and support the O-ring. They are fabricated from extrusion-resistant element and usually have a rectangular cross-section. Back-up rings are set up in a groove alongside with an elastomeric sealing item, preference with a matching O-ring in static applications. They prohibit the extrusion of the elastomeric sealing item which receives pressure into the sealing gap. The O-ring installation with and without back-up ring is demonstrated in Figure 2.35 and the effect of pressure to O-ring with and without back-up ring is demonstrated in Figure 2.36.

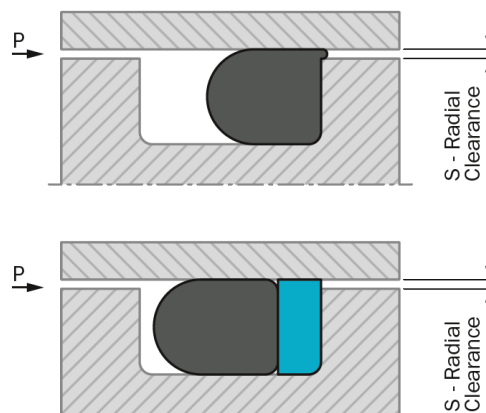


Figure 2.35 O-ring installation with and without back-up ring

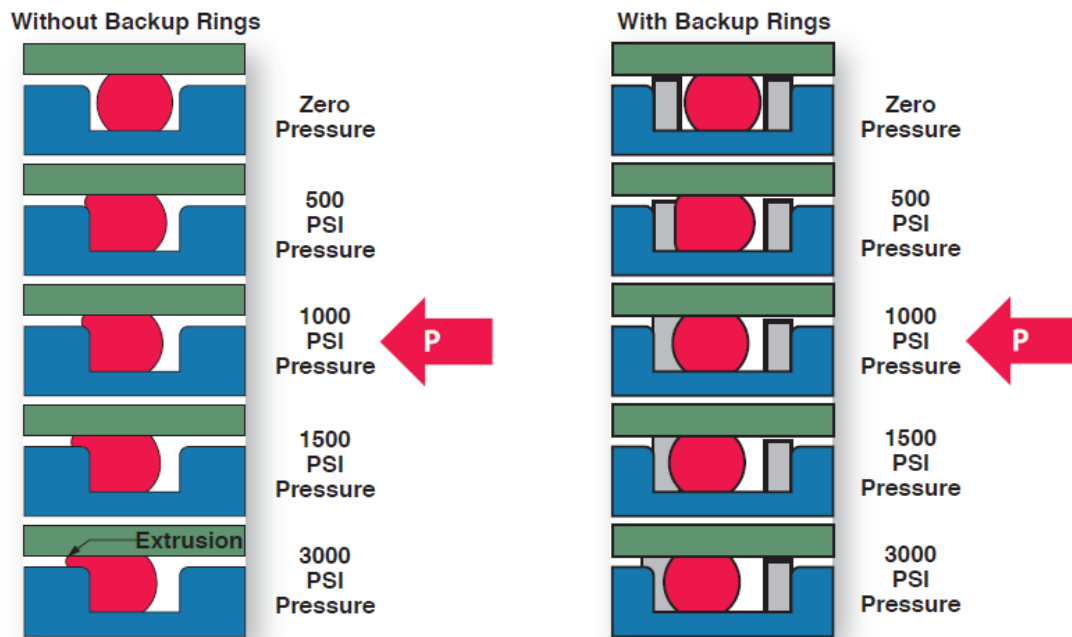


Figure 2.36 Effect of pressure with and without back-up ring

2.11.2 Advantages

O-ring has many advantages in any uses as the following. It can use in high pressure applications with a low hardness and static and dynamic application, and use for internal and external sealing applications. In the other hand, it is compensated for large temperature fluctuations and of radial sealing gaps and it is possible to use in both reciprocating and rotating movements (Solutions, 2016).

2.12 Category of rubbers used in the rubber blending

2.12.1 Acrylonitrile-butadiene rubber (NBR)

NBR is a complicated group of not impregnate copolymers of butadiene and acrylonitrile. It is created by emulsion polymerization as illustrated in Figure 2.37. A little number of a third monomer in some brands of NBR is added to improve the adhesiveness or properties of elastomer. NBR is significant rubber. NBR's property is resistance to the substance whose molecules do not have opposite positive and negative poles chemicals, solvents, oils motor fuel, and fats.

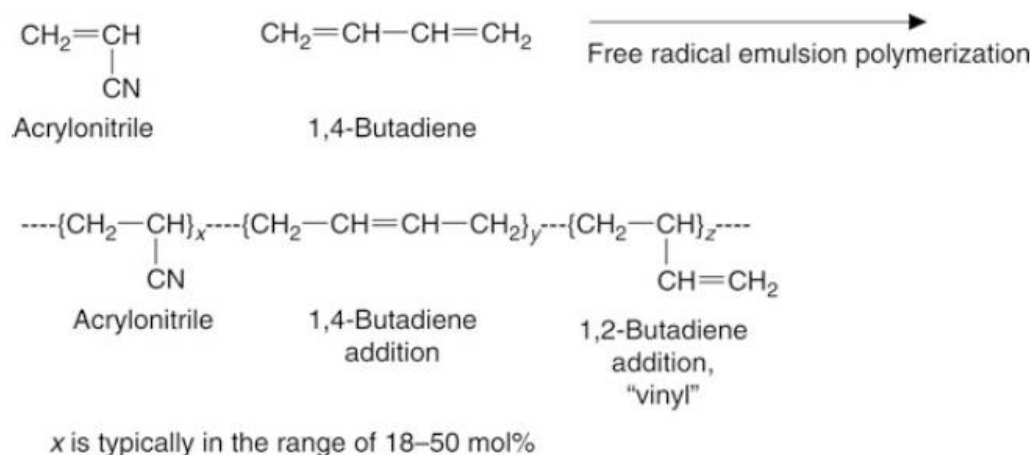


Figure 2.37 Polymerization and compositional structure of NBR

NBR, type of statistical copolymer including either nitrile or butadiene systems, offers space to govern the measurements of the constitutional units in balance with the properties for miscellaneous end-use applications. NBR consists of outstanding abrasion resistance, compression set, and excellent tear resistance compared to other commonly utilized rubbers. A larger amount of acrylonitrile builds up greater strength, bigger resistance to swelling by hydrocarbon oils, and interior permeability that comes at the price of inferior adaptability at smaller heat. 18 to 50 % number of acrylonitrile are added in the final copolymer to improve the specific qualities of rubber; especially, a greater acrylonitrile's percentage would be utilized to get a great-power rubber. Whereas the smaller acrylonitrile's percentage would be utilized to get a more flexible rubber at the smaller temperatures.

The predominant inconvenience in NBR is low weather resistance and poor ozone. This disadvantage causes it inappropriate for applications where these features would be needed. NBR is able to endure most of the extreme application due to its tolerance to wide-range (-30 to $+100$ °C) of operating heat. NBR is a priceless material in latex blend processing due to its great oil resistance and sturdiness over time (durability) of nitrile rubber (Markovic, G. Visakh, 2017).

2.12.2 Hydrogenated nitrile rubber (HNBR)

NBR is able to modify by hydrogenation reactions that improve the desired advantageous mechanical characteristics and temperature resistance properties. The subsequent structure of the hydrogenated nitrile rubber is usually depicted as HNBR (Figure 2.38), that is recognized for the removal of the initial inadequacy in nitrile rubber.

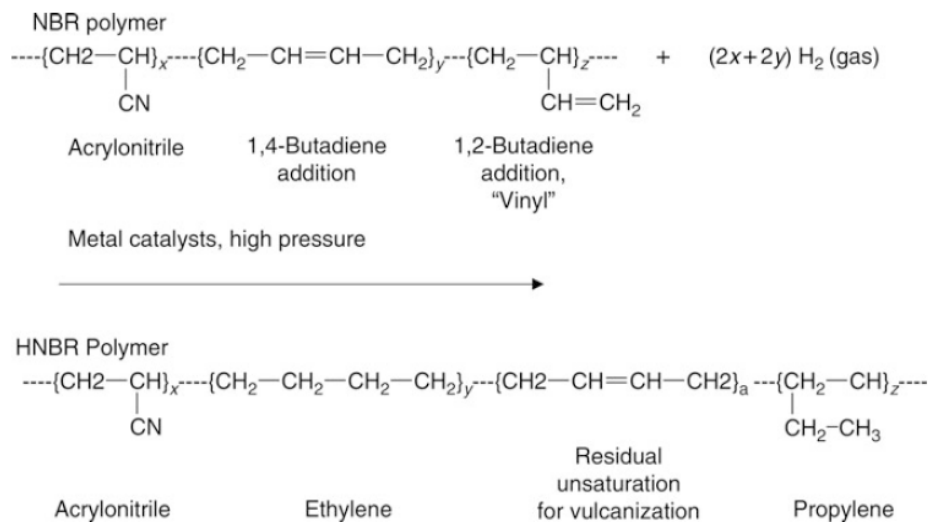


Figure 2.38 Catalytic hydrogenation of NBR to prepare HNBR and the polymer microstructure of HNBR

The reaction of hydrogenation is generally accomplished by catalysis in the existence of the great-pressure hydrogen as depicted in Figure 2.39. HNBR is able to be noted as a tetrapolymer that comprises by the acrylonitrile, ethylene produced via the hydrogenation of the 1,4-butadiene portion, propylene created by the hydrogenation of the 1,2-butadiene segments, and leftover butadiene units. HNBR keeps the properties of fuel and oil resistance and adaptability at smaller heats of NBR and acquires a temperature and oxidation resistance similar to EPDM rubber. A specific aspect correlation of feature between NBR and HNBR is demonstrated in Figure 2.39.

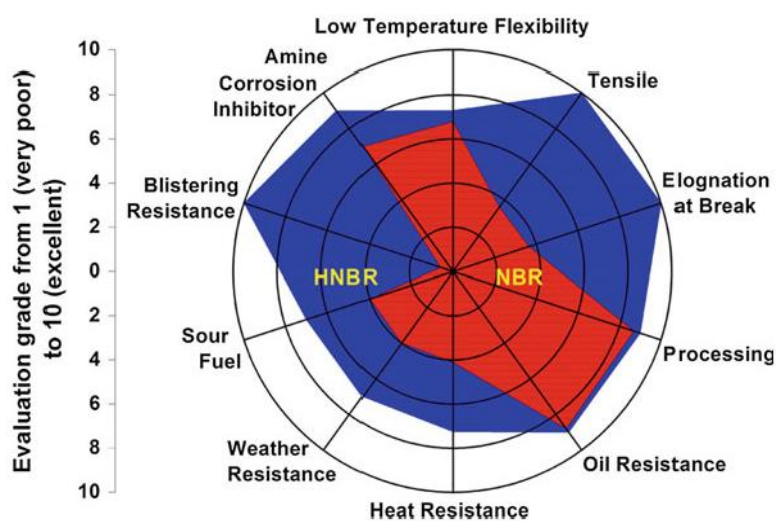


Figure 2.39 HNBR versus NBR property comparison

Resistant Ozone of HNBR present image of a crucial development above that of NBR. Nonetheless, the disadvantage of utilizing HNBR is the raised cold flow at the time of hydrogenation. Cold flow is the damage of a product at room temperature as an extrinsic stress (force) is put on regularly over long periods of time. In spite of the raising cold flow, HNBR consists of the broad operating temperature (-40 to 165 °C) with slightest deterioration over long time. HNBR is subject as well to the analogous impacts of the NBR in connection with the amount of the constitutional units. In addition, a larger concentration of acrylonitrile will bring about either an increment in resistance to temperature and petroleum-based lubricants and fuels or a degrade in the small heat operation whilst a smaller concentration of acrylonitrile will do the completely different. Owing to HNBR's greater strength, ozone and temperature resistance, developed fuel, and other properties, it is considered as a high-performance rubber and priceless in very harsh environments where NBR is not appropriate (Markovic, G. Visakh, 2017).

2.12.3 Carboxylated nitrile rubber (XNBR)

Carboxylated nitrile rubber (XNBR) is a terpolymer consisting of an unsaturated monomer consists of acrylic or methacrylic acids, acrylonitrile and butadiene (Laskowska et al., 2014). Lateral carboxyl functionalities $-\text{COOH}$ is able to

make more healing sites and assist the progress of utilizing of healing agents to respond with the groups of carboxyl with the objective of ionic bond structure. The generally known curing agents (healing agents) utilized to fabricate ionic cross-links are depended on salts and oxides of multivalent metal compounds for instance calcium oxide (CaO), zinc oxide (ZnO), and magnesium oxide (MnO). (Laskowska et al., 2014) XNBR is a substance whose molecules have opposite positive and negative poles. It is a highly reactive polymer which possesses outstanding compatibility with non-polar and polar resin elements (Mousa et al., 2012). XNBR has a particular quality of a great level of cooperation with fillers to improve the XNBR's properties. XNBR consists of greater strength and enhanced damping properties compared to NBR. All of these typical features make a high number of possibilities of XNBR like a matrix polymer. XNBR is usually reserved to applications which are likely to experience from ultimate force and wear (Seals, 2019).

2.12.4 Hydrogenated carboxylated nitrile rubber (HXNBR)

In a like manner to NBR, XNBR is also able to revise via a reaction of hydrogenation to improve the XNBR's mechanical and physical properties. The polymer microstructure of HXNBR is demonstrated in Figure 2.40. The hydrogenated XNBR is usually designated as HXNBR. Inserting a carboxylic acid sort linked to the strength of character of HNBR to produce HXNBR is usual to increase additionally HNBR's great abrasion resistance, mechanical strength, and adhesion properties. HXNBR is principally fabricated by LANXESS along with the trend mark namely Therban® XT (*Therban® xt*, 2019).

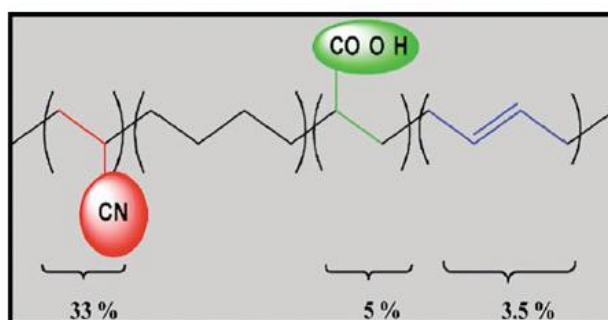


Figure 2.40 Polymer microstructure of HXNBR

Therban XT-based compositions show uncommonly great tear strength at high heats comparing to normal Therban HNBR which has brand name namely LANXESS HNBR and other synthetic elastomers. Moreover, Therban XT exhibits outstanding properties' adhesion to various materials such as synthetic fibers, plastics, and metals over a wide and higher heats ranging (Rempel & Wang, 2017). The HXNBR's physical properties is superior to high rank of durability and strength illustrated by HNBR. Therban XT, HXNBR versus normal Therban, HNBR properties comparison of few factor is demonstrated in Figure 2.41 below.

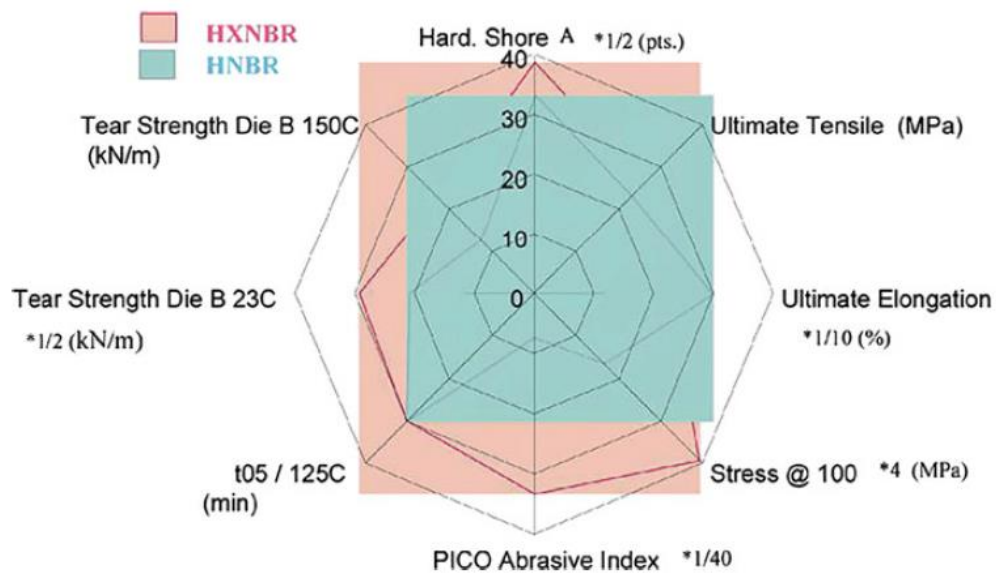


Figure 2.41 HXNBR versus HNBR properties comparison

In spite of the enhanced qualities of HXNBR, this rubber sort is generally restricted to very great scenarios, where severe operation is needed, according to the high price demanded to fabricate the rubber. This price is belonging to the additional steps and chemical like the expensive metal catalysts needed to make the HXNBR. HXNBR is prioritized above price and an optimal rubber for using in the very great strength and durability application and it is an effective method to reduce the price by mixing the Therban XT alongside other rubbers like normal Therban. At the same time the active groups' level (COOH) is reduced by the mixing process that is able to make better processability of HXNBR once blending with active constituent like zinc diacylate (Markovic, G. Visakh, 2017).

2.12.5 Styrene–butadiene rubber (SBR)

Styrene–butadiene rubber (SBR) is an alternative synthetic rubber to NBR and has analogous traits to NR. SBR is a mixture of butadiene and styrene and it can be gotten by resolution anionic polymerization (S-SBR) and like a free radical emulsion polymerization (E-SBR) processes (Rempel & Wang, 2017). The E-SBR is utilized more broadly in industrial manufacturing. SBR is usually compared to NR as a result of their analogous properties and is especially beneficial by reason of its good resistance to brake both water and fluids. Brake fluids' resistance causes SBR very beneficial in the motor vehicle industry and more particularly the industry of wheel. Nevertheless, SBR is not productive in cases of petroleum oil and weather resistance. Moreover, SBR is restricted by its weak tear strength without support of fillers like carbon black and small elasticity particularly at greater heats (Obrecht et al., 2011). SBR is able to work at lower heats with the temperature from -46 to 100 °C of operation. The number of styrene rubber utilized in a blending combination is usually diminished once a greater level of temperature resistance is demanded. SBR turns into harder as it becomes older according to the increment number of polymer form interlinking as a reason of oxidation. This aspect will be considered to avoid the long-term use of SBR in plenty of cases because of the low elasticity of aged SBR. SBR is the cheapest rubber in a group of almost all kinds of rubbers. This advantage allows SBR an outstanding material for blend process in term of reducing price (Markovic, G. Visakh, 2017).

2.12.6 Chloroprene rubber (CR)

Chloroprene rubber (CR) or neoprene is a group of synthetic rubbers which are fabricated via free radical polymerization of chloroprene. It is an adjustable and flexible rubber according to its great resilience, tensile strength, fire and oil resistance and deterioration by ozone and oxygen over a broad ranging of heat (Arshad et al., 2017). CR is moderate from its mediate water resistance and not effective in solvent surroundings. The price belonging to the production of Neoprene rubber limits its utilization to particular properties needed for exact applications. CR

consists of plenty of fascinating rubber characteristics and in this manner, it has been broadly utilized to arrange the blends with other rubbers (Markovic, G. Visakh, 2017).

2.12.7 Polyvinyl chloride (PVC)

Polyvinyl chloride (PVC) is a synthetic polymer created from the polymerization of vinyl chloride (the third-most broadly created synthetic plastic polymer). It is identified by rigid structure and featherweight. Nonetheless, it is able to be formed in a softer and more adaptable structure after being involved in a plasticizer like phthalate esters. Nearly all productions of PVC could be heated and combined with a plasticizer to maintain the plastic flexible at low heats at which point the desire for adaptability is over rigidity (Allsopp & Vianello, 2000). PVC possesses a broad design of applications varying from raincoats and bathing curtains to household plumbing and window frame (Markovic, G. Visakh, 2017).

2.13 Natural rubber (NR)

Natural rubber (NR) is the one and only kind of rubber which is able to be physically removed and purified from existent living things. NR latex could be seen in the *Hevea brasiliensis* tree as a white sap in the way that illustrated in Figure 2.42. The rubber tree's residence is at the Amazon rain forest. Nowadays, the large farm of *Hevea brasiliensis* are found as well in Southeast Asia; predominantly in Indonesia, Malaysia, and Thailand (Heinz-Hermann Greve, 2000). Then this latex is clotted to create the moisture less natural rubber utilized in products stretching over various industries.



Figure 2.42 *Hevea Brasiliensis*, the rubber tree

Presently, one among the outstanding utilizations of NR is to fabricate rubber gloves for medical works on account of two crucial properties of NR. Those properties are abrasion and chemical resistance. NR is usually recognized for its great physical properties containing tear resistance, large tensile strength, small compression set, and high abrasion (Heinz-Hermann Greve, 2000). This admits NR to possess much wider applications. NR has the great advantages apart from most other synthetic rubbers. First convenience is its superb vibration dampening characteristics. Secondly, its outstanding bonding capabilities to metal substrates. Lastly, its great surface friction properties. In contrast, NR has weak resistance to petroleum oils so it cannot use in the oil industry and has weak ozone and UV resistance therefore this kind of rubber is not appropriate for in the open air utilization. The NR's temperature operation range is from about -51 to 104 °C. This demonstrates that NR is able to perform of maintaining flexible at low temperatures (Markovic, G. Visakh, 2017).

2.14 Ethylene–propylene–diene rubber-based nanoblends

EPDM is a nonpolar and saturated rubber with very low —C=C content. The EPDM rubber's form is illustrated in Figure 2.43. Distinct qualities of EPDM are according to the ratios of diene, ethylene, and propylene. The choice of the specific quality of EPDM relies upon the traits of the final products. Distinct proportion of monomers allow distinct traits to EPDM. The wide-ranging of EPDM polymers are formed by differing the kind of diene termonomer, molecular weight, ethylene/propylene ration and level, and molecular weight distribution. The available elastomers consist of 50 percent to greater than 75 percent ethylene's weight. Containing smaller ethylene amount, the polymers are not difficult to process and amorphous. In addition, greater amount of ethylene offers the better physical properties of crystalline polymers yet it has more difficulty in processing (Marinović-Cincović et al., 2013). Having large ethylene amount makes EPDM becomes the best material for thermal insulator in space applications (Deuri et al., 1988). The impact of the propylene and ethylene amount on the crystallinity and the T_g of EPDM was checked into thoroughly by (Baldwin & Strate, 1972). They released that EPDM's T_g with different amount of the propylene and ethylene in a nonlinear way and usually

raised with the increasing of propylene amount. EPDM's crystallinity gains with the surge of ethylene amount and reduces with that of propylene number (Baldwin & Strate, 1972; Bhuvaneshwari et al., 2006). Great crystallinity is connected with great mechanical properties and this is the reason why great ethylene amount offers great green strength to EPDM (Kole et al., 1993). Otherwise, great propylene amount offers low hardness in EPDM together with more adaptable at low heat and more elasticity (Gamlin et al., 2003). (Allen, 1983) state that ethylene amount improves the cross-linking efficiency of the EPDM as well.

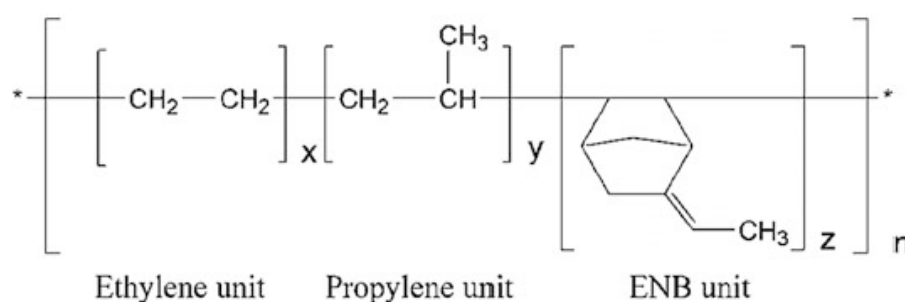


Figure 2.43 The structure of EPDM rubber macromolecules

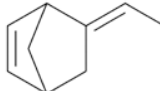
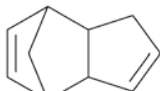

The first commercial EPDM rubbers are fabricated by the incidental copolymerization of ethylene and propylene in solution utilizing Ziegler–Natta catalysts. Because of these fully saturated composites, they were greatly resistant to polar liquids, temperature, oxidation, ozone, and weathering (Marinović-Cincović et al., 2013).

The third monomer in EPDM is integrated to do addition to unsaturation to the polymer. These are commonly non-combined dienes. Non-combined dienes are integrated for making unsaturation in EPDM are dicyclopentadiene (DCPD), 5-ethylidene-2-norbornene (ENB), and 1,4-hexadiene (HD). These combined dienes get the profit of one double bond in the period of copolymerization with both propylene and ethylene, whilst it reserves the other in the side structure of EPDM for sulfur vulcanization. In most cases, increment in diene number raises the vulcanization's rate. The additional content of diene is started from

0.5 to 12 wt% (Allen, 1983). Distinct sorts of dienes offer distinct properties to EPDM due to the distinct in structures. The most broadly used one is EPDM along ENB as diene monomer (Table 2.3).

EPDM demonstrates numerous properties containing water and aging resistance, temperature stability, and elasticity at very low heat. Thus, EPDM is broadly utilized to numerous rubber products for instance, in styrene– butadiene and butadiene rubbers and as a substitute for natural rubber. One great thing among most significant characteristics of EPDM is the competence to obtain great contents of enlarge lubricants, fillers, and other supplement without influence working ability with any important tolerance to the final properties (Gwailly et al., 1998).

Table 2.3 The basic properties of diene rubber components in the EPDM rubber

Diene component	Formula	Molecular mass	Physical state
(E)-5-ethylidenebicyclo[2.2.1]hept-2-ene (EN)		120	Fluid
3a,4,7,7a-tetrahydro-1H-4,7-methanoindene (DCPD)		132	Solid
(E)-hexa-1,4-diene (HD)		82	Solid

EPDM is a quickly growing synthetic rubber which is utilized in various applications in industry. EPDM is more constant than other common elastomers. Unluckily, the EPDM application is limited because of it consists of weak solvent resistance and adhesion properties. Their chemical and physical properties suggest them as engineering materials for aircraft material, insulators for electricity, automotive and chemical industry, and numerous other fields. The mixing of EPDM and NBR rubbers was operated to obtain the best properties from each constituent (Jovanović et al., 2013). Nonetheless, mixing EPDM with NBR (as demonstrated in Figure 2.44) could enhance the aforementioned conveniences of EPDM due to the polar NBR shows outstanding solvent resistance and adhesion properties. A few researches illustrating the use of mixing EPDM and NBR have been previously published (Grigoryeva & Karger-Kocsis, 2000; Sau et al., 1998; Wu et al., 2004). Moreover, the morphology of the mixture of polymer/polymer is determined by the

mixing ration, blending process, viscosity, and each element's surface property (Kang et al., 1999; Pukánszky et al., 1990). Researchers have searched the solubility properties of water in elastomers stood on RPDM/NBR for utilize as marine application's items, packing items, and biomedical tools (Aminabhavi et al., 1986). Additionally, NBR, EPDM, and halobutyl rubbers have been composited for a plenty of automotive applications (Vara, R, 1994). The vulcanizing system's impact on EPDM and NBR properties has also been researched (Maity & Chakraborty, 1994; Namboodiri & Tripathy, 1992).

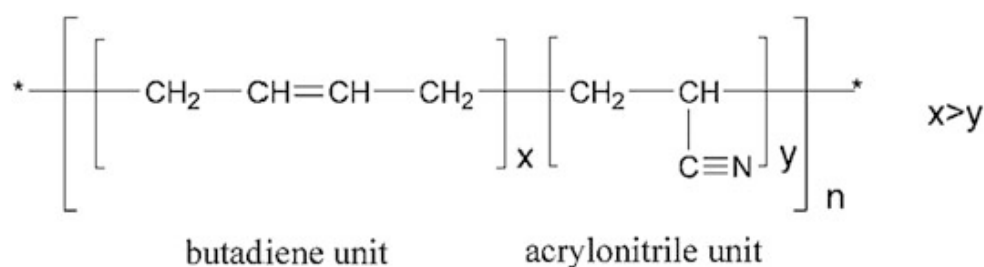


Figure 2.44 The structure of NBR rubber macromolecules

Elastomers do not have a filler composition are not crucial in practice in any applications. Thus, an elastomer is typically mixed with fillers to produce a combination (filler load is frequently about 30 to 50 percent) in practice application. In the last two decades, a modernized class of material, nanofiller has found out as a filler in polymer compounds. This modernized class of material has one measurement at worst in the nanorange (for instance 10–9 m). CB containing 10 to 30 nm and precipitated silica consisting 30 to 100 nm yet endure the conventional fillers for this reason. Unmistakably, the essential elements for strengthening by fillers are great distribution and improved cooperation with the rubber chains. There are three kinds of nanofillers according to their dimensions in polymer matrices. These dimensions of the particle could be in the arrangement of nanometers, isodimensional nanoparticles and thus come into sight as rounded particles. The nanoparticle fillers consist of carbon black, silicon carbide, titanium dioxide, silica, zinc oxide, and aluminum. Only two dimensions are in the scale of nanometer, and the third is bigger, producing an

elongated chain, as in nanofibers, nanotubes, or whiskers. The fillers create more powerful elastomers and they were of essential significance from a realistic point of view. Organic (carbon black) and inorganic (silica) fillers were usually supplemental to the elastomers. So far, the predominant well-known filler for rubber qualification is carbon black which covers all its variations such as acetylene blacks, furnace, thermal, and channel. Carbon black refers to elemental carbon (C) in the structure of rounded particles of colloidal size. Carbon black's particles are come together into collections and bunches as it is gotten by the explosion or thermal breakdown of hydrocarbons. The grades of CB distinct from one another concerning their collection shape and structure and particle size. About the glossary, agglomerates consist of a great amount of aggregates which are physically held together, as against to the endless graphitic chain that connects the piece inside the assemblage (Figure 2.45).

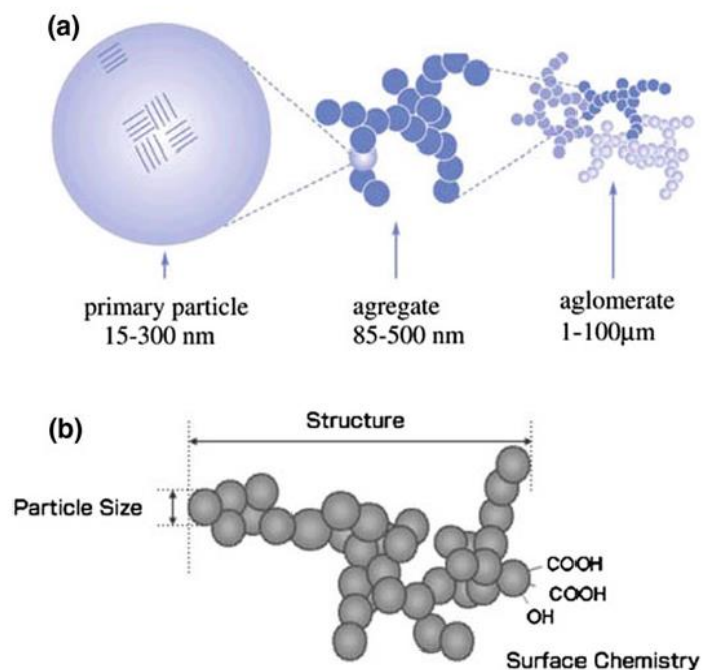


Figure 2.45 Dimension of carbon black primary particle size and dimension of aggregate and agglomerate which have been made in cross-linking reaction of elastomer and filler (a) and basic properties of carbon black (b)

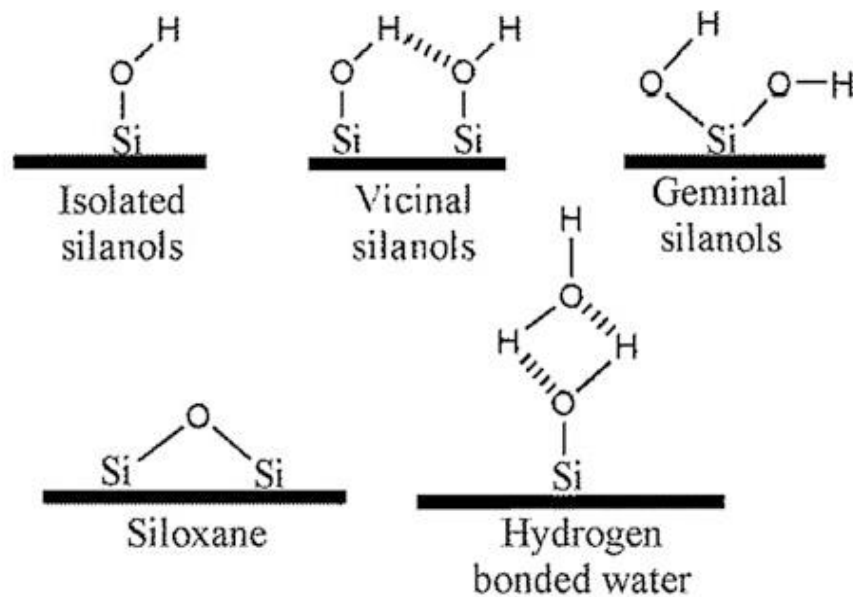


Figure 2.46 Types of silanol group in the surface particle of silica

Silica which is without definite shape or character exists of oxygen and silicon put in an order in a tetrahedral chain of a three-dimensional lattice. Silica does not have long-range crystal arrangement and has only short-range arranging domains. When silanol sorts (SiOH) presents on the surface of silica (Figure 2.46) produces powerful interaction of particle and particle. The trend for filler agglomeration increases by this thing. The concentration of surface silanol affects the level of surface hydration. High degree of hydration could unfavorably influence the physical properties of the final composition (Markovic, G. Visakh, 2017).

2.15 Carbon black (CB)

CB is a material fabricated by the in inadequate ignition of having great weigh petroleum goods and has high surface dimension to volume ratio of a structure of paracrystalline carbon. It is utilized for the most part as the strengthen filler in tires and other rubber goods. There are many types of carbon black which utilized in tire as illustrated in Table 2.5. generally, carbon black is utilized for the improvement of elastomers for aircraft vibration command parts and machine mounts in industry as well. Moreover, it upgrades the wear resistance and tensile strength of

NR. The CB production of 70 percent is utilized in automobile wheel. Similarly, it assists to upgrade the thermal conductivity in the rubber that utilized in wheel and drives the heat out from the belt and tread space. This assists to raise the wheel's life and decrease the thermal deterioration. The carbon black consists of chemisorbed oxygen compounds containing quinonic, lactonic, carboxylic, and phenolic sorts above their surfaces which provide to the volatile nature of the material. Many types of carbon black are categorized depend on its plenty of factors including porosity, particle size, structure, and surface area and activity. These factors consist of direct impact on the rubber composition's properties. In most cases, the tensile and modulus properties in mechanical properties gain alongside with reduction of particle size owing to the natural rubber nanocomposite (NRN) demonstrates high amounts of abrasion resistance, viscosity, and electrical conductivity. The carbon black material's particle size is equivalent straightforwardly to the properties of scorch resistance. For the most part, carbon black's Mooney viscosity and modulus base on the stowing and form of the CB in the matrix of NR. Fillers (the CB-based) strengthen the rubber blending and decrease the blending cost. The physicochemical interactions of NR matrix with carbon black reinforces upgrade the NRN. Current tendency in NRNs exhibits inquisitiveness to utilize CB-based hybrid fillers to upgrade the physicommechanical characteristics of the NRNs (Bhattacharya & Bhowmick, 2010; Thaptong et al., 2014).

Table 2.5 Types of carbon black used in tires

Name	Abbrev.	ASTM design	Particle size (nm)	Tensile strength (Mpa)	Relative laboratory abrasion	Relative road wear abrasion
Superabrasion furnace	SAF	N110	20-25	25.2	1.35	1.25
Intermediate SAF	ISAF	N220	24-33	23.1	1.25	1.15
High abrasion furnace	HAF	N330	28-36	22.4	1	1
Easy processing channel	EPC	N300	30-35	21.7	0.8	0.9
Fast extruding furnace	FEF	N550	39-55	18.2	0.64	0.72
High modulus furnace	HMF	N683	49-73	16.1	0.56	0.66
Semi-reinforcing furnace	SRF	N770	70-96	14.7	0.48	0.6
Fine thermal	FT	N880	180-200	12.6	0.22	-
Medium thermal	MT	N990	250-350	9.8	0.18	-

2.16 Vulcanization chemicals

The rubber merchandises are distinguished by great resilience following mechanical deformation. The original measure is recovered rapidly after the force is released. This rubber elasticity issues from a 3 dimensional chains of long-structure rubber particles that were connected to one another at cross-linking location. Vulcanization is the chemical mechanism of producing these cross-links between polymer networks. The sticky unprocessed rubber is transformed by inevitable Newtonian flow into the elastomer. Either sulfur or peroxides are utilized primarily as curing agents; particularly, to a low range, exceptional crosslinking agents might be occupied. Recovering load after damage is a work of the amount of chain-producing polymer network per unit volume. Expanding the amount of cross-links delivers tightness over more polymer network and therefore enlarging the recovering load (Engels et al., 2011).

2.17 Vulcanization accelerators

Sulfur is an agent which has a slow-moving cross-linking. With the absence of both activators and accelerators the reaction takes 5h at 140 °C to cross-link NR. Moreover, the ageing properties, inadequate crosslink densities, toughness are obtained event a sulfur amount utilized is 8%. Accelerating in vulcanization results from PbO, MgO, Ca(OH)₂, and Sb₂S₃ were identified shortly beyond the discovery of sulfur vulcanization. By reason of the initiation of organic accelerators, these inorganic nearly lose their significance. The improvement of accelerator in the past event is useful for accelerated sulfur cross-linking comprehension. Oenslager perceive the activating impact of organic physical foundation including aniline on sulfur cross-linking in 1906 in US. Both C₂H₄N₂S₄Zn and C₆H₁₂N₂S₃ were found around 1919-1920 during the thorough check on the dithiocarbamate derivatives, the control of Vulcanization kinetics, and especially the beginning of reaction in the test. Simultaneously, other efficient activators of accelerated sulfur cross-linking such as ZnO and SA were also discovered. The significance of organic vulcanization accelerators depends on their extremely growing rate of cross-linking reaction with sulfur that provides the short vulcanization time leads to economically well-founded

rank. The utilization of vulcanization accelerators enable vulcanization at low temperature as well and thus prevents high temperature wreck to the rubber and develops ageing resistance (Engels et al., 2011).

2.18 Classification of Organic Accelerators.

Nowadays, there are approximately 80 different substances of commercial and accessible accelerators for sulfur cross-linking systems and the amount of compounds which are able to perform the acceleration is even greater. The group of the greatest significant accelerators in line with their international abbreviations and chemical constitution is provided in Table 2.6.

Table 2.7 Typical sulfur cross-linking systems for carbon black filled rubbers

Component	NR	SBR	NBR	IIR	EPDM
Sulfur, phr	2.5	2	1.5	2	1.5
Zinc oxide, phr	5	5	5	3	5
Stearic acid, phr	2	2	1	2	1
CBS, phr	0.6	1			
MBTS, phr			15	0.5	
MBT, phr					1.5
TMTD, phr				1	0.5
ZDBC, phr					1.5

With competent selection of an accelerator or a mixture of accelerators, most entire desired processing, cross-linking typical features, and vulcanized properties can be acquired. Table 2.7 demonstrates some of ordinary sulfur cross-linking systems for CB-filled rubbers as EPDM, NBR, NR, IIR, and SBR. These CV systems distinct in their amount of S and in the nature and dose of the accelerator, subject to the substrate. Begin from the fundamental formulations, particular necessities can be complied by the changing of the S-accelerator proportion and by mixture of dissimilar accelerators (Engels et al., 2011).

Table 2.6 The most important accelerators groups

Group	International abbreviation	Chemical name
Sulfenamides	CBS	<i>N-cyclohexyl-2-benzothiazylsulfenamide</i>
	TBBS	<i>N-tert-butyl-2-benzothiazylsulfenamide</i>
	MBS	2-morpholinothiobenzothiazole
	DCBS	<i>N,N</i> -dicyclo-2-benzothiazylsulfenamide
	OTOS	<i>N</i> -oxydiethylenethiocarbamyl- <i>N'</i> -oxydiethylenesulfenamide
Thiazoles	MTB	2-mercaptobenzothiazole
	MBTS	dibenzothiazyl disulfide
	ZMBT	zinc 2-mercaptobenzothiazole
Thiurams	TMTD	tetramethylthiuram disulfide
	TMTM	tetramethylthiuram monosulfide
	TETD	tetraethylthiuram disulfide
	DPTT	dipentamethylene thiuram tetrasulfide
	TBzTD	tetrabenzylthiuram disulfide
Dithiocarbamates	ZDMC	zinc dimethyldithiocarbamate
	ZDEC	zinc diethyldithiocarbamate
	ZDBC	zinc dibutyldithiocarbamate
	ZEPC	zinc ethylphenyldithiocarbamate
	Z5MC	zinc pentamethylene dithiocarbamate
	ZBEC	zinc dibenzoyldithiocarbamate
Guanidines	DPG	<i>N,N'</i> -diphenylguanidine
	DOTG	<i>N,N'</i> -di- <i>o</i> -tolylguanidine
	OTBG	<i>o</i> -tolylbiguanide
Thioureas	ETU	ethylthiourea
	DETU	diethylenethiourea
	DPTU	<i>N,N'</i> -diphenylthiourea
Other accelerators		aldehyde – amine condensation products
		amines
		dithiophosphates
		xanthates
		triazines

2.19 Accelerator activators

The mixture of inorganic and organic activators must be utilized to improve the complete action of organic vulcanization accelerators. Adding ZnO to rubber blends involving S and accelerators noticeably improves cross-link quantity. For common-function rubbers NR and SBR, using more ZnO up to 5phr induces great tensile strength and stress rates. Greater utilization no longer influent on these properties.

The impact of cadmium and bismuth oxides are related to those of ZnO. Nevertheless. They are not utilized through financial and environmental logic. Either magnesium or calcium oxides are less satisfactory due to their inferior crosslink densities production. The lead PbO and Pb₃O₄ are utilized as activators when vulcanize with exceptionally little swelling in water are needed. The accelerator, rubber, ZnO, and S are activated more by fatty acids. Zinc stearate or SA is usually utilized. Apart from activation, fatty acids and their salts develop two significant vulcanized properties such as filler dispersion and process ability. The utilization of particular zinc salts instead of ZnO can lead to an increment density of crosslink and a development in inversion manner. Zinc diamminediisocyanate has been brought in for EPDM cross-linking (Engels et al., 2011).

2.20 Typical properties and types of fillers

2.20.1 Action of fillers

The characteristics of industrial rubber blends and their vulcanization are found out by many factors such as the nature and amount of the fillers applied — the nature and number of the polymers utilized — the anti-degradants — the crosslinking system — the plasticizers. SBR and BR which are non-self-reinforcing rubber provide insufficiency and have barely vulcanizations with the absence of reinforcing fillers such as CB or silica.

Fillers are rank with reference to their chemistry — first into CB and white filler — natural rubber and synthetic rubber. The differentiation is built technologically in two ways — between having movement or strengthen fillers — between inactive or extender fillers. The former is utilized to obtain special

vulcanization characteristics; the latter, to create the inexpensive blends (to extend it). Deviating reinforcing impacts of fillers improve plenty of vulcanization characteristics including hardness, stress, compound viscosity, tear resistance, and toughness. Meanwhile, other features including elongation at break and impact resilience are defective (Engels et al., 2011).

2.21 Sulfur vulcanization

2.21.1 Vulcanization reagents

Plenty of reagents that are correlated with the sulfur vulcanization of polydienes, for instance NR, have been improved. Reagents are categorized into prevulcanization preventor, accelerators, retarders, vulcanization agents, and activators. Vulcanization agents contain elemental S (including insoluble S and colloidal S) or an organic S donor as following: tetramethylthiuram disulfide (TMTD) or 4,4'-dithiobismorpholine (DTDM). The most significant categories of accelerators are those depended on dithiocarbamic acid, sulfonamides, guanadines, and benzothiazoles. These categories of these accelerators following by their speed of vulcanization and chemical structure are demonstrated in Table 2.8.

Table 2.8. Classification of accelerator groups and their relative curing speeds

Type	Abbreviations	Relative curing speed
Guanidines	DPG	Slow
Dithiocarbamates	ZDBC	Very fast
Thiurams	TMTD, TMTM, DPTTS	Very fast
Thioureas	ETU	Fast
Thiophosphates	DIPDIS	Semi-fast
Thiazoles	MBT, MBTS, ZMBT	Moderate
Sulfenamides	CBS, MBS	Fast

The activators which usually called the runner-up accelerators might be utilized to potentiate accelerators. Beneficial runner-up accelerators involve nitrogen-containing bases, metal oxides (generally ZnO), and fatty acids. To get long time processing by avoiding premature vulcanization (scorch), the pre-vulcanization

preventers and retarders are included. Retarders involve acidic combinations (benzoic acids — phthalic anhydride — salicylic) and nitroso combination (N nitrosodiphenylamine). The most universally utilized pre-vulcanization preventers is N-cyclohexylthiophthalimide (CTP) (Akiba & Hashim, 1997).

2.21.2 Accelerated vulcanization

It spends 4 to 5 hours and is not the commercial significance anymore to vulcanize rubber by S without accelerators. With the presence of accelerators, best curing can be achieved rapidly in 2 to 5 min. Sped up sulfur vulcanization is appropriate for either NR and synthetic counterpart (IR) or for EPDM, NBR, BR, SBR, butyl rubber (IIR). Common fundamental recipe for accelerated sulfur vulcanization involves S and/or a S donor of 0.5 to 4 phr, SA of 1 to 4 phr, an accelerator or a combination of accelerators, and ZnO of 2 to 10 phr. The primary factors by sort and rank considering are the S donors and accelerators. Vulcanization systems have 3 categories (Table 2.9) depended on the amount of S and the proportion of accelerator to S — conventional — semi-efficient (semi-EV) — efficient (EV). EV category utilize less or nearly nil (along with a S donor) ranks of S and a relatively great ranks of particles accelerators. Table 2.10 shows the well resultant vulcanized uses S to build chains in which the crosslinks are principally monosulfidic and which display a small amount of main-chain modifications. The utilization of EV category in NR decreases or removes inversion exclude at too great curing heats. Therefore, the result of vulcanization demonstrates a great resistance to thermal and oxidative ageing.

Table 2.9. Compositions of conventional, semi-EV and EV vulcanization systems

Type	Sulfur (S, phr)	Accelerator (A, phr)	A/S ration
Conventional	2.0-3.5	1.2-0.4	0.1-0.6
Semi-EV	1.0-1.7	2.5-1.2	0.7-2.5
EV	0.4-0.8	5.0-2.0	2.5-12

Table 2.10. Vulcanizate structure and properties of three different sulfur-curing systems

	Conventional	Semi-EV	EV
Poly- and disulfidic crosslinks (%)	95	50	20
Monosulfidic crosslinks (%)	5	50	80
Cyclic sulfide concentration	high	medium	low
Low-temperature crystallization resistance	high	medium	low
Heat-ageing resistance	low	medium	high
Reversion resistance	low	medium	high
Compression set, 22 h at 70 °C (%)	30	20	10

Fatty acids are usually viewed as essential activators together with ZnO. Fatty-acid activators (include SA) have a work to solubilize the ZnO and a secondary impact to raise the content of zinc sulfide produced. The zinc salts of fatty acids (the kind of surfactant) dissolved impenetrable accelerators to create the real catalyst. A usual system of an accelerated S vulcanization that depicts the function of ZnO together with fatty acids and amine activators as demonstrated in Figure 2.47. Amines or zinc carboxylates has the function of facilitating the commencement of the constituent sulfur ring to create polysulfide ions [step (2), Scheme 1] that raises the vulcanization amount but consists of little impact on the efficiency of vulcanization. The second function of reactors is to raise the concentration of dissolved zinc-accelerator-mercaptide structures that are in charge for either the sulfurization of the rubber [step (3), Scheme 1] or for the dusulfuration of polysulfide crosslinks to create di- and monosulfide crosslinks [steps (4) and (5), Scheme 1], with rising the effectiveness of vulcanization (Akiba & Hashim, 1997).

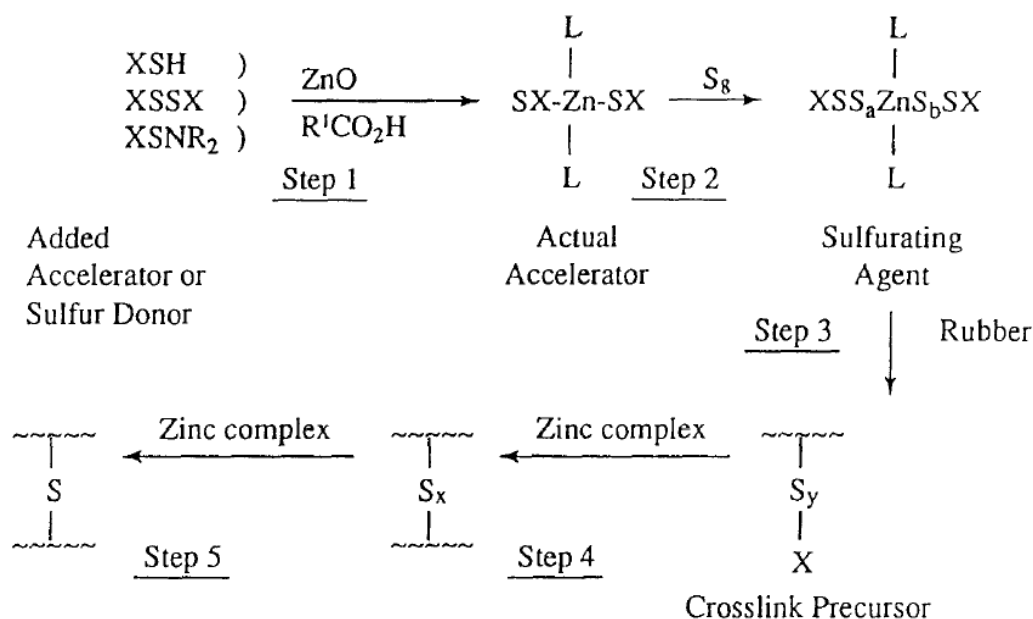


Figure 2.47 The role ZnO, fatty acid and activator in accelerated sulfur vulcanization.

X- accelerator residue, L – ligand (basic nitrogen or zinc carboxylate)

2.22 Peroxide crosslinking

2.22.1 General features of peroxide crosslinking

A broadly type of peroxides is able to be utilized to crosslink nearly all sort of elastomers. The significance of peroxides is their capability to crosslink soaked elastomers. Those capabilities are ethylene-propylene rubber (EPR), low-density polyethylene (LDPE), and silicones that are not able to be crosslinked with other sorts of vulcanizing agents. An index of accessible peroxides in the commerce and their ten hour haft-life temperatures is demonstrated in Table 2.11. Principally, the diacyl peroxides are benefitful for the crosslinking of silicone elastomers. Meanwhile, both ketal and diakyl peroxides are utilized mainly for either diene or ethylene-propylene elastomers. Come up to S vulcanization, crosslinking by peroxides is an uncomplicated procedure. The convenience and drawback of peroxide crosslinking are sum up in Table 2.12 (Akiba & Hashim, 1997).

Table 2.11. Peroxides for curing of elastomers

Peroxide type	Examples	10 h Half-life (°C)*
Diacyl peroxide		20-75
	Dibenzoyl peroxide	73
	Di(2,4-dichlorobenzoyl) peroxide	54
<i>t</i> -Alkyl peroxyesters		49-107
	<i>t</i> -Butyl perbenzoate	105
Di-(<i>t</i> -alkyl peroxy) ketals		92-115
	1,1-Di- <i>t</i> -butyl peroxy-3,3,5-trimethylcyclohexane	96
Di- <i>t</i> -alkyl peroxides		
	Di- <i>t</i> -butyl peroxide	128
	Di-cumyl peroxide	115
	2,5-Dimethyl-2,5-di-(<i>t</i> -butyl peroxy) hexane	119

*The temperature at which the peroxide has a half-life of 10 h.

Table 2.12. Advantages and disadvantages of peroxide crosslinking

Advantages	Disadvantages
Short crosslinking time	Expensive crosslinking agent
Simple compounding	Low mechanical strength (TB, flex resistance)
Good heat-aging resistance	Crosslinking inhibited for kind of compounding ingredient
Less tension set and strain	Difficult hot-air cure
No mold contamination	Need secondary, cure of high temperature long time
Transparent rubbers possible	

2.23 Previous studies of fillers

Fillers are supplemental to the TPE materials in order to get the fancy change in their properties of and to achieve best properties. Supplementary of fillers to plastic or rubber polymer is a well-known and an attractive method to increase several physical properties. When adding the small particles, it can tremendously increase both the mechanical and transport properties of elastomer and polymer (Katz, HS. Milewski, 1981). The reinforcement by filler in filled blends depends on

complexity of filler particles and their aggregation, physicochemical properties of the constituents, polymer filler interactions, distribution and dispersion of filler in each phase of the blend, and the large range of particle dimensions. Nonetheless, the dealing with the reinforcement of PTE by particulate fillers is found in the literature of several research works. Strengthening TPE with fillers usually increases in tensile strength, modulus, and hardness as detected in PP/NR/RR composites (Ismail & Suryadiansyah, 2004), NR/PP blends (Sangwichien et al., 2008), and NBR/EVA TPVs (Varghese et al., 1999). Fillers content of carbon black and silica can increase tensile strength, Young's modulus, and hardness. Furthermore, the surface of the filler (i.e., silica and nanoclay) may act as a nucleating agent for semi-crystalline polymers and altered the amount or type of crystallinity, as observed in EPDM/PP TPVs (Bazgir et al., 2004; Naderi et al., 2007).

(Jha et al., 1999) studied the impact of CB and silica on key performance of nylon 6/ACM compounds. It was found that lower amount of carbon black (i.e., 10-20 phr) improved the expansion at break of the compounds without any noticeable alteration in tensile strength. At higher CB amount (i.e., 30 phr), Young's modulus, tensile strength and elongation at break decreased in the comparison with that of the unfilled blend. Moreover, it is attractive to mark that the 30 phr silica-filled blend demonstrates the greatest extensibility and tensile strength. This is due to greater polymer-filler cooperation. However, hardness of the filled blends for all types of fillers used increase with the addition of fillers, while the tension set decreased. The improvement of tensile strength and elongation at break by using low concentration of silica, carbon black and clay was also observed in SBR/HDPE blends (Jayasree & Predeep, 2008) and silica-filled EPDM/PP blends (Bazgir et al., 2004). These inspection regarding the impact of fillers in thermoplastic elastomer based on rubber-plastic compounds are not accurately conforming the results stated by others. For example, (Coran & Patel, 1980) investigated that the extra of CB or clay in PP/EPDM and nylon 6/NBR compounds reducing in expansion of the compounds with an increment of tension set features. It was postulated that the filler stays in the rubber phase and consists the impact of either reinforcing the rubber or raising its volume portion. The distinctness in the performance of filled PP/EPDM, nylon

6/NBR and nylon 6/ACM TPEs was explained on the basis of the reactive nature of the later types compound scheme (Jha et al., 1999). In term of PP/EPDM and nylon 6/NBR, that are non-interactive in nature, the fillers might move to the area of interfacial location of connection among the rubber and elastic stage during the melt blending process. Therefore, lowering the affinity among the 2 components is a consequence.

The extra of fillers can have disadvantageous effect to many crucial properties of rubber-plastic compound; but, its utilization in thermoplastic elastomeric rubber-plastic compound it limited, as testified to the articles (Coran & Patel, 1980; De & Bhowmick, 1990). As the hard-plastic phase hands over the reinforcement to the compounds, adding of strengthening fillers is frequently not significant. It was inspected by (De & Bhowmick, 1990) that CB fillers could not hand over the reinforcement in PP/EPDM TPEs, in contrary traditionally cured EPDM rubber formulations. (Coran & Patel, 1980) stated that adding of low content of clay in nylon 6/NBR TPEs had little impact on firmness, inflexibility, or power but decreased in extensibility was observed. In addition to, impact of fillers on thermoplasticity is uncompromising; and, in order to acquire the adequate profit of filler utilization, plasticizers are utilized to get back either thermoplasticity or extensibility. (George et al., 2006) found that tensile strength decreased with increasing cork storing. This might be attributed to the inadequate soaking of the filler by the rubber and might be attributed to the huge particle size of the filler.

2.24 Previous study of O-ring seal testing

(Morrell et al., 2003) studied about the Poly(acrylonitrile-butadiene) rubber (NBR) O-rings which accelerated in the air below 12.5% of compressive strength at the heat up to 110 °C. They have determined the compressing setting characteristics along with oxygen by using the O-ring below the practiced load conditions and examined and determined utilizing time-heat superposition and Arrhenius kinetics. It was found that the compressing setting offers a single deterioration operation with an activating power of 81.03 kJmol⁻¹. It is match well with the activation power gotten from oxygen utilization of 74.3 kJmol⁻¹. As a result

of solvent swell and oxygen uptake experiments, the predominant impact on thermal ageing of rubber is oxidative cross-linking, promoting to the element becoming solid and breakable. Compression set can predict the life of the tire.

(Nabil et al., 2013) researched on the compound of NR and virgin EPDM rubber and compared with natural rubber and recycled EPDM rubber by using a mixture on a two-roller tire grinder. By giving the carbon black filler at 30 phr by studying 3 different thermals such as thermo-oxidative ageing, thermogravimetric analysis, and dynamic mechanical determination. It was found that either thermal ageing or thermogravimetric determination of the compounds involving great heaviness proportion of original or recycled EPDM offered greater thermal stability and recycled EPDM made up of crosslinking precursor, higher crosslink amount was inspected while recycled EPDM amount was raised.

(Yamabe et al., 2013) presented the impact of hydrogen pressure and temperature on the fracture behaviour of O-rings made from EPDM rubber using peroxide as a link and using white fillers under the high-pressure. Circuit of hydrogen gas using a developed durability tester operated at hydrogen pressure from 10-70 MPa and temperatures from 30-100 °C found that increasing hydrogen pressure will cause the cracks to expand more and at a pressure of 10 Mpa, the tire will cause swelling and the crack circuit in the O-ring has more serious damage. By increasing the pressure of hydrogen gas and temperature, it has the serious fracture below high temperature due to the degradation of the mechanical properties of EPDM rubber.

(Kundera & Bochnia, 2014) utilizes PolyJet-Matrix electronic and a worldwide testing machine to study the relaxation characteristics of O-ring seals under 3 parameters loading including time, loading and dislocation. The relaxation manners gotten are explained in detail with predefined statistical works by utilizing a Prony series. It was found that utilization of PolyJet-Matrix electronic provided a productive way to design models of elastomeric materials together with the instances being the O-rings produced and operated corresponding to their relaxation manner. Although viscoelastic characteristics of elements effects to the amount of loading and time of its equalization, yet, still it has other factor that also do including the shape

(geometry) of the O-rings, stress state and friction power on the surfaces in contact with the housing materials.

(Lee et al., 2012) studied the tribological manner of FKM fluorocarbon elastomer by investigation with the purpose of developing suitable accelerated wear experimental aspect for this sort of enclosed element. Their reference for wear pattern of the sample is the ordinary testing aspect (condition) with exceed 1000 h of operating time. The results of ordinary testing aspect are utilized to compare with accelerated operating aspect. The results obtained are as following: the alumina pieces of w1 mm alongside with oil effect to the mixing by increasing a factor of 58 of FKM sample's wear. The wear of ordinary testing is maintaining. Their research finding is helpful in the life prediction of FKM elastomeric seals.

(Lingerkar & Khonsari, 2010) conducted an experimental research to observe the impact of various pressure and sliding speed across an O-ring seal and the effect of temperatures, power loss and friction torque at the contact between the rotating shaft and O-ring. The circular cross-section test sample, Nitrile butadiene rubber with the hardness of 70 Shore A is selected for this experiment. At the same time as testing, the O-ring power loss and heats were calculated at 0.61 mm gap from the O-ring. It was found that the sliding speed enlarges the O-ring power loss in a relatively linear fashion. Additionally, the result shows that when applying high different pressures across an O-ring raise the friction power. On the other hand, the friction torque is also increased at high different pressure but it decreases when high speed shaft is applied. Furthermore, the increment in sliding velocity and different test pressure effect and raise the interfacial temperatures.

(Marlier, 2010) conducts a pilot study to test for leak tightness between the EPDM O-rings and the flanges in order to avoid the sticking between them under heat aging tests. The test was done by measuring the seal life at a given temperature and used in TN International security examined documents to maintain the leak compactness of EPDM O-rings after the usual and occurrence aspect of conveying. It was found out that the method incorporates much conservatism and yet contribute a better comprehension of the wreck inhibit of EPDM O-rings that permit TN International to develop its packages' production and safety justifications.

(Zeng et al., 2016) used HNBR O-ring to test the corrosion in simulated wellbore status by utilizing self-designed compressing simulator and autoclave at 140 °C and 35 MPa that consisting 0.5 MPa of CO₂ for 168 h. The mechanical characteristics were tested and Energy-dispersive X-ray spectroscopy were scanned for crack morphology evaluation. The result shows that the test under the compression mood provides more severe corrosion than the test under the free mood. Additionally, in the free mood, liquid corrosion is more severe. The mechanical characteristics reduce as a result of infiltration of corrosive media and

chemical process that altered the form of rubber networks which make the poor reinforcement work of CB.

(Xiao Kun, Gu Xiaohui, 2014) simulated the study to evaluate the dependability of the O-ring for a safety device. 32 O-rings is used to test for degradation at four different heat (50 °C, 60 °C, 70 °C and 80 °C) according to the aging process of rubber elements and the fixed stress accelerated degradation experiment. It was found that the ageing method of the O-ring increases the manner and is possible for the O-ring to manage accelerated deterioration experiment.

(Moore et al., 1989) observes many deteriorations of O-ring seals by conducting the analyses and subscale experiments. The test of deteriorations and failure of O-ring were identified by different conditions such as heat, pressure, oil, extrusion gap, seal fracture, seal infection and O-ring location. It was found that the pressure at which full seal completeness is set up can be chosen for a particular O-ring seal arrangement. Cut O-ring seals can be as a result of both heal and fail according to the adjustment of the cut and the orientation of the pressure, contributing an early sealing connection is built. The result of healing or leakage might or might not be able to be reproduced based on the related location of the mark to the sealing surface. O-ring oil is able to cover seal leakage based on the grease components, amount, area to flow, heat and experimental pressure. Nevertheless, seal completeness can be authenticated constantly by providing adequate duration and pressure. The increment of pressure affect and increase seal deterioration or seal contaminations.

They also recommend some ways to maintain the quality of O-ring as the following: O-ring seal with extra safety factor shall be tested to performing pressure. slightest oil could be utilized according to the seal assembly. Oil must be compatible with the seal elements and supposed seal performing conditions. Seal shall be operated with the a-ring seals directed as they should be with the performing pressure. Irregular seals have to be changed and a seal which heals is not trustworthy seal and might be unsuccessful under usage. Seal failing would contain checkup of the seal, oil and sealing surface. Principally, O-ring seals would not be tied together excluding emergency circumstances. For great completeness of seals, the contamination with free lubricants only that can be utilized. The surface of seal must be free of deterioration after the convenient surface accomplishment.

(Stolarski & Tucker, 1996) conduct a study on the frictional performance of an O-ring seal at the commencement of linear motion. Their objective is to observe the relation between O-ring's friction and measure pressure at the initiation of linear motion of a shaft. The amounts of distinct O-ring elements are conducted and a PTFE-enclosed silicone seal provides the smallest friction under dry conditions. As the results of operating O-ring seals over a series of pressures up till 10 MPa across to strong steel surfaces at a fixed coarseness of 0.2 mm demonstrate that

the frictional power stands on the variate pressure over the seal, the form of the seal and connection state. The result show that the frictional power reaches very great amount at great pressures. Additionally, constant numbers for the frictional power were hard to receive through a great error on seal squeeze that as a consequence of differentiation in O-rings' cross-section dimension. It would have a troubles in realistic applications where an accurate rank of friction is needed if there is an absence of frictional power constancy from seal to seal. The impact of oil of the O-ring/shaft interface is the declination in friction. Nevertheless, the distinctness between a lubricant and grease in the efficiency of lowering friction is not important.

2.25 Fuel cell

Fuel Cell is a tool which electrochemically produces electricity continuously as a gaseous fuel is burnt in a continuous manner by a chemical reaction. Fuel cells represent a next-generation energy conversion device in future conveying and immobile energy manufacturing (Song et al., 2017). It is a direct power conversion tool that consists a power source including an oxidant such as air or oxygen and natural gas, hydrogen, ethanol, methanol, formic acid, or phosphoric acid. This tool directly transforms the chemical energy of the fuel oxidation into electrical power (Lin et al., 2017).

A fuel cell consists of three major components: two electrodes such as cathode and anode and one electrolyte. One electrolyte formed of non-conductive elements to allow charges to pass over between catalytic electrodes. Two electrodes, one positive called cathode and another negative called anode. The reaction that generates voltage occurs at the electrodes (Sutharssan et al., 2017). It also has a catalyst to boost the reaction at the electrodes. Presently, to defeat the sluggish kinetics of the oxygen reduction reaction, fuel cells utilize the expensive catalyst, namely platinum. Due to the use of expensive platinum; therefore, the decision has changed to use the low price and possible choice (precious metal catalysts). Those low-cost catalysts shall consist of great oxygen reduction reaction catalytic reaction and generate low-level H_2O_2 when setting up in a fuel cell scheme. There are a number of work that have reported the elements that chemically doped C elements

with heteroatoms and could generate a huge concentration of active locations with great operation for ORR. Those elements are N, B, P, S, and F (Song et al., 2017).

Although fuel cells are now offset by the cost of platinum (Ratso et al., 2017) they are still interesting due to their highly efficient, very low emission of pollution, many size scale use, and very little pollution by forming a harmless byproduct, namely water (Mumtaz et al., 2017).

Scientists and inventors have researched and designed numerous types of fuel cells to find out the greater efficiency one. The choices of electrodes play a significant role to fabricate the great efficient electrolyte. For instance, the selection of electrodes and the equipment used to create them depend on the electrolyte. (Xueye Chen et al., 2017; Sammes et al., 2012) indicated the five major fuel types in Table 2.13 such as Alkaline fuel cell (AFC), Phosphoric acid fuel cell (PAFC), and Proton exchange membrane fuel cell (PEMFC) which are operated at low temperature and SOFC and Molten carbonate fuel cell (MCFC) which are tested at high heat.

Table 2.13 Kind of electrolytes and their efficiency, temperature, and output

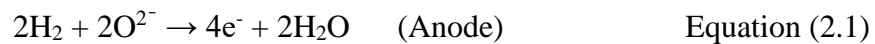
Types of Fuel Cell	PEMFCs	AFCs	PAFCs	MCFCs	SOFCs
Efficiency (%)	40 -50	About 70	40 – 80	60 – 80	About 60
Temperature (°C)	About 80	150 – 200	150 – 200	About 650	1000
Output (kW)	50 - 250	0.3 - 5	Up to 200	Up to 2000	Up to 100

2.25.1 Solid Oxide Fuel Cell (SOFC)

SOFC are efficient energy generation (more than 50% efficiency), clean and efficient conversion, and potential power sources on a huge scale with a clean output (Garcia-Garcia et al., 2017; Xu et al., 2017). It uses a number of fuels such as hydrogen, hydrocarbons, syngas, ammonia, and solid carbon (Zhang et al., 2017). SOFC operates at extreme high temperatures from 600 °C to 850 °C and as high as 900 °C (J. H. Kim et al., 2017). The scheme of SOFC is illustrated in Figure 2.48.

This type of fuel cells uses hard-ceramic materials as the electrodes and electrolyte. The high-temperature operation allows SOFC to reform fuels internally too. The internal reforming at this high temperature enables the various use of fuels such as hydrogen, natural gas, biogas, liquid hydrocarbons, and shale gas. The flexibility of fuel use is one of the great advantages of SOFC (Hou et al., 2017). Due to their high-temperature operation, it made SOFC be able to have a fast-kinetic process which is no need the expensive noble metal catalysts. another advantage of this fuels cell is they have no problem of leakage or corrosion as it uses all-solid-state structure (Zhang et al., 2017) and has low impact to the environment pollution (Cheng & He, 2017; Meng et al., 2017). The high-temperature operation also has disadvantages resulting in quick degradation and shorter lifetime (Arshad et al., 2017).

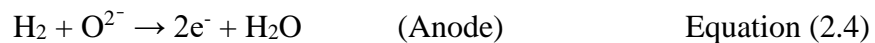
The electrochemical reactions associated with hydrogen fuel and carbon monoxide are:



The overall cell reaction in SOFC is:



The electrochemical reactions associated with hydrogen only are:



The overall cell reaction is:

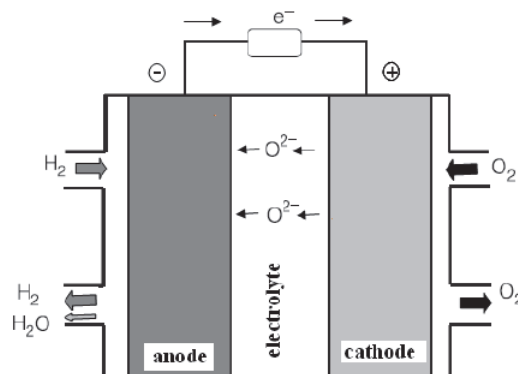


Figure 2.48 Schematic of a solid oxide fuel cell (SOFC)

CHAPTER 3

MATERIALS AND METHODS

3.1 Materials

Natural rubber, Standard Thai Rubber 5L Grade (STR 5L) produced by Chana Namyang Company Limited, Thailand and Ethylene propylene diene monomer (EPDM) ENB, Keltan[®] 6950C DE, Ethylene content 44 ± 2.1 wt%, ENB 9.0 ± 0.8 wt%, Mooney viscosity 65 ± 4 MU, volatile matter 0.5 wt%, density 0.86 g/cm³ purchased from the company Lanes Limited, Thailand were chosen as the major composites for blend formulations. Precipitated silica with a cetyl trimethylammonium bromide (CTAB) definitive surface area (O. Stenzel, H.-D. Luginsland, S. Uhrlandt, A. Wehmeier (to Degussa AG). U.S. Patent 7608234, Oct. 27, 2009) of 171 m²/g (Ultrasil 7005, Evonik GmbH, Germany), bis-(triethoxysilylpropyl) tetrasulfide (TESPT) with S amount of about 22 wt% (Zhenjiang Wholemark Fine Chemicals, China). The Carbon black N330 Grade produced by Thai Carbon Black Co., Ltd and purchased from Optical Boss Partnership was also selected as vulcanization filler to enhance efficiency. Other accelerators such as N-tert-Butyl-2-benzothiazolesulfenamide (TBBS) with chemical formula C₁₁H₁₄N₂S₂ produced by Henan Yuanye Industry Co., Ltd., China were used as a catalyst for vulcanization in sulfur systems, Zinc oxide (ZnO) and Sulphur (S) produced by West Chemical Company Limited, Thailand were used as a stimulant to make the catalyst work more efficiently and vulcanized substance causing the bonding of rubber, Steric acid (SA) produced by Imperial Chemical Company Limited was selected as an activator couple with ZnO, and additive compatibility, Homogenisator 501 grade produced by Dog Deutsche Oelfabrik Co., Ltd., Germany was chosen as a substance to increase the compatibility between natural rubber and EPDM rubber. Another antioxidance, Butylated reaction product of p-cresol and dicyclopentadiene (Wingstay[®] L) was produced by Goodyears Co., Ltd.

3.2 Compound preparation

The compound formulation used for this study is demonstrated in Table 3.14. In all formulations, all elements have the same amount excluding the

hybrid filler's content of silica and CB. The various amount of silica and CB were prepared to make the distinctness of filler proportion. Nevertheless, the number of hybrid filler was fixed at 60 phr. So, the number of silica and CB was classify from 10 to 50 phr. The compounds were labelled as S0, S10, S20, S30, S40, S50 and S60. The figure takes the place after the letter "S" demonstrates the quantity of silica in the samples. For instance, S50 contains 50 phr of silica and 10 phr of CB.

The numbers of TESPT used in this formulation were standed on the CTAB definitive surface area of the silica as stated in the Equation (3.1) as offered by (Guy et al., 2009).

$$\text{Number of TESPT (phr)} = 0.00053 \times Q \times \text{CTAB} \quad \text{Equation (3.1)}$$

Where Q is the silica amount (phr) and CTAB is definitive surface area of the silica utilized (m^2/g).

Table 3.14. Blend formulations

Ingredients	Amount (phr)						
	S60	S50	S40	S30	S20	S10	S0
STR 5L	30	30	30	30	30	30	30
EPDM	70	70	70	70	70	70	70
N330	0	10	20	30	40	50	60
Silica	60	50	40	30	20	10	0
TESPT	5.25	4.37	3.50	2.62	1.75	0.87	0
TBBS	1.2	1.2	1.2	1.2	1.2	1.2	1.2
ZnO	3.0	3.0	3.0	3.0	3.0	3.0	3.0
SA	1.0	1.0	1.0	1.0	1.0	1.0	1.0
Wingstay L	1.0	1.0	1.0	1.0	1.0	1.0	1.0
S	1.8	1.8	1.8	1.8	1.8	1.8	1.8
Homogenisator 501	5.0	5.0	5.0	5.0	5.0	5.0	5.0

Mixing was operated using an internal mixer with a mixing chamber of 480 cm^3 (Chareon Tut Co., LTD., Thailand) (Figure 3.49). The mixer was performed at a safety factor (fill factor) of 85 % and a rotor velocity of 60 rpm with the mixing

temperature of 60 °C. All ingredients, except the curatives (Accelerator, TBBS and Vulcanizing agent, S) were combined with rubber in a laboratory-size internal mixer (Dispersion mixer, model MX500-D75L90). 8 mn of mixing in the internal mixer was used. Subsequently, the blend was combined more on a two roll-mill machine (Figure 3.50) and then the curatives were added and mixed. Finally, 6 end-roll passes and 4 bending passes were made before sheeting off and preserved one day prior to incorporation of TBBS and Sulfur on a luke-warm two-roll mill.



Figure 3.49 Internal mixer



Figure 3.50 Two-roll mill machine

3.3 Cure characteristics

The cure characteristics were figured out using a Moving Die Rheometer, MDR 2000 (Model, Country) (Figure 3.51). The increment in torque (S') at a heat of 160 °C, a frequency of 8.33 percent Hz and 2.79 percent strain was calculated for haft hour. The ultimate vulcanization time ($t_{c,90}$) was measured and utilized for press-curing of the specimen.



Figure 3.51 Moving Die Rheometer, MDR 2000

3.4 Vulcanization and measurement of mechanical properties

The blends were press vulcanized at 160 °C to $t_{c,90} \pm 2$ min. The vulcanized sheets consisting a measurement of approximately 2 mm were die-cut to dumbbell shaped samples for tensile determination including modulus 100, 200, and 300 percent and elongation at break. The tests were performed at a crosshead speed of 500 mm/mins owing to ASTM D412 by utilizing a Tensile Testing Machine, Zwick Roell Germany (Z010) (Figure 3.52). The specimens having 6 mm thickness were used to measure the hardness according to ASTM D2240, using Shore Instruments Durometer set, Instron model (Figure 3.53). The median values of tensile taken from five specimens are reported.



Figure 3.52 Tensile Testing Machine, Zwick Roell Germany (Z010)



Figure 3.53 Shore Instruments Durometer set, Instron model

3.5 Thermo-oxidative aging

The dumbbell-shaped samples were located in a stove that has the air circulating at 100 °C for 2 days following ISO 188 method A to determine thermal aging properties. The aged samples were then measured for mechanical properties. The changes in mechanical properties such as hardness, modulus, tensile strength, and elongation at break after thermal aging were used to find out the thermal aging resistance. The retention of these mechanical characteristics was computed according to Equation (3.2) as mentioned by (Nabil et al., 2013).

$$\text{Retention (\%)} = \frac{\text{Value after ageing}}{\text{Value before ageing}} \times 100 \quad \text{Equation (3.2)}$$

3.6 O-ring molding

The O-rings were formed in the O-ring mold housing (Figure 3.54) with the temperature of 160 °C and pressure of 1400 psi (100 kg/cm²) by using the compression machine, PR1D-W280L300 PM (Figure 3.55).

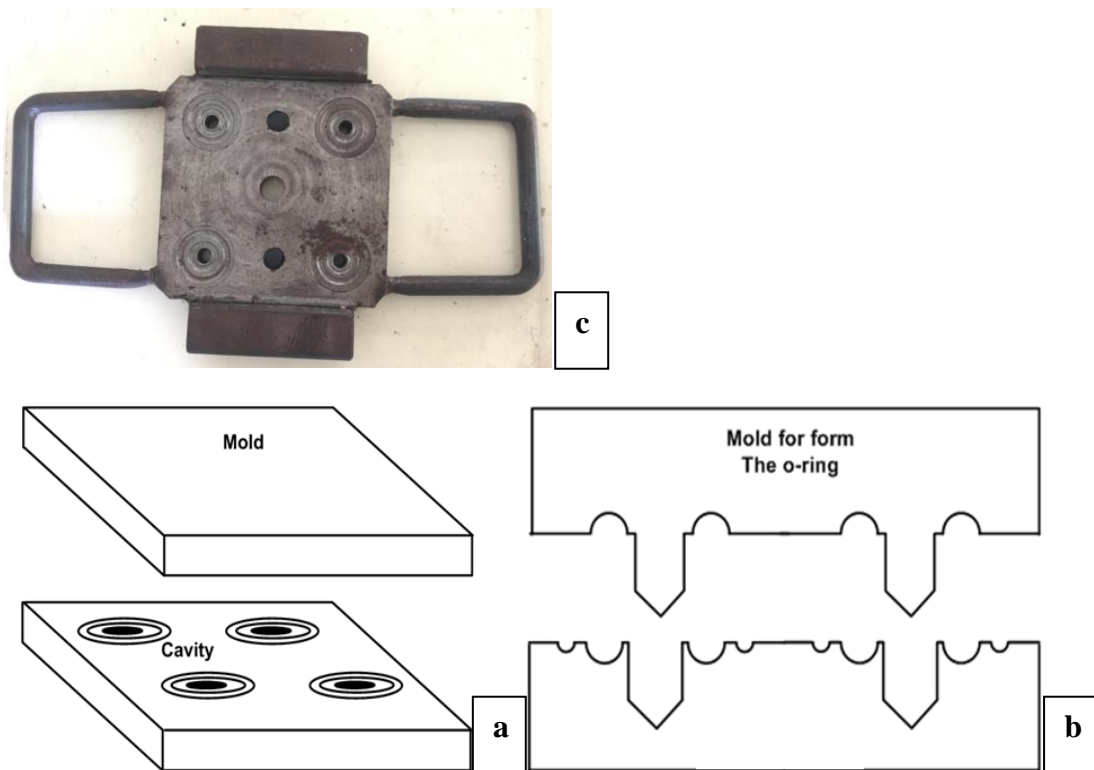


Figure 3.54. (a) Top view of mold housing, (b) Cross-section view of Mold housing, (c) O-rings mold with four housing.



Figure 3.55 Compression machine, PR1D-W280L300 PM

3.7 O-rings used in SOFC testing system

The O-rings were tested at the mating surface (a) and (b) in the solid oxide fuel cell system (Figure 3.56) and (Figure 3.57) that requires the furnace to operate at 800 °C with the gas flow rate of 0.5 L/minute, temperature of about 27 to 31°C at inlet gas flow (b), and temperature of approximately 53 to 58°C at the outflow gas (a). The fuel cell testing system was tested for 1 hour to get the stability of gas flow rate. When the system is able to operate, the O-rings were installed and tested at the mating surface for 1 hour, 6 hours, 12 hours, and 24 hours. The installation of O-ring rubber in the mating surface pipes/valves in SOFC testing system is illustrated in Figure 3.58.

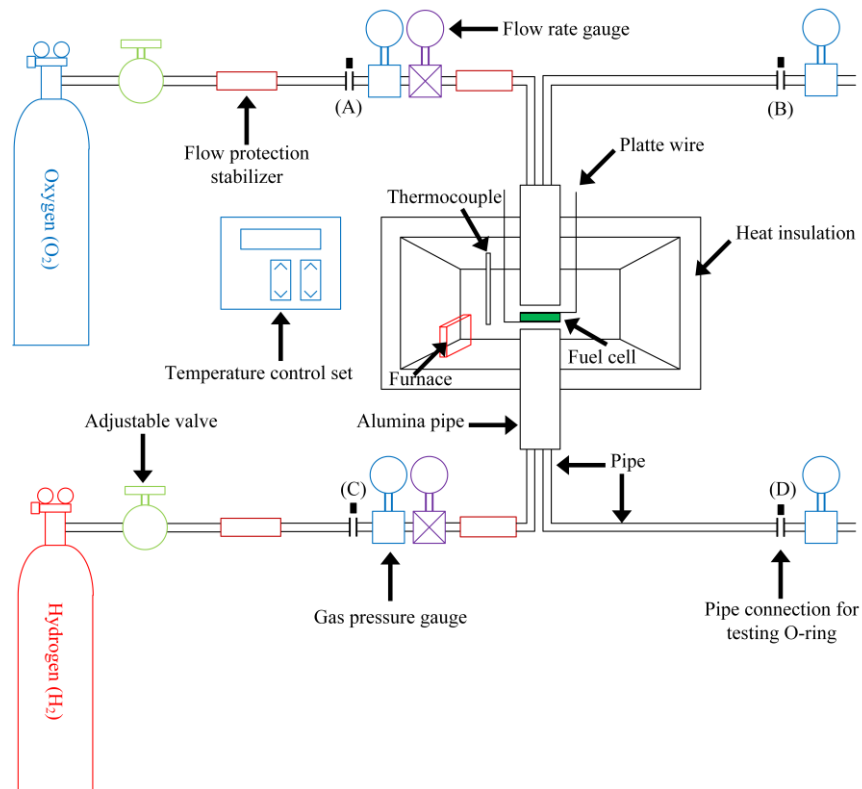


Figure 3.56. Schematic of solid oxide fuel cell testing system.

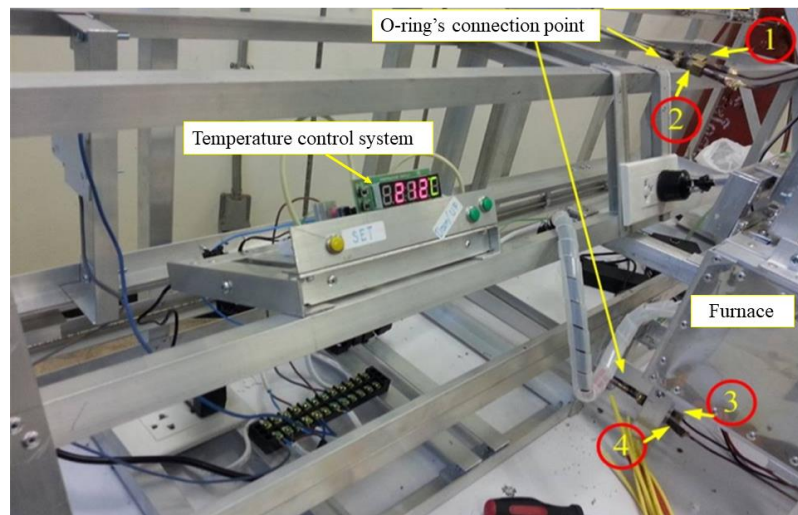


Figure 3.57. Solid oxide fuel cell testing system; (1) inlet of oxygen gas, (2) outflow of hydrogen gas.



Figure 3.58. Installation of O-rings in the mating surface pipes/valves in Solid oxide fuel cell testing system.

3.8 Observations of crack morphology and fracture surface

After testing for 1 hour, 6 hours, 12 hours, and 24 hours in SOFC testing system, all the O-rings were used to check and observe their surface and cross-section characteristics through Scanning Electron Microscope (SEM) (Figure 3.59) to see the effect of gas and temperature on the O-rings rubbers. The O-rings with blend at 40/20 of silica/CB-filled NR/EPDM compounds was selected for the study of crack morphology and fracture surface.



Figure 3.59 Scanning Electron Microscope

3.9 Data analysis

Mechanical properties including tensile strength, modulus, elongation at break and hardness before ageing and after ageing of the prepared O-ring were compared with the standard O-ring.

Non parameter test with two related samples test was used to find out the difference of four factors of mechanical properties (tensile strength, modulus, elongation at break and hardness) between the prepared O-ring and standard O-ring. For all tests, a P -value < 0.05 were considered to represent significant differences.

Wilcoxon Signed Ranks Test was applied to test and compare the mean of difference of prepared O-ring's factors to the standard O-ring's factors. All data analysis was carried out by using IBM SPSS Statistics version 23 (Leonid & Lyamshev, 2004).

CHAPTER 4

RESULTS AND DISCUSSIONS

4.1 Cure characteristics

4.1.1 Scorch time (min)

The scorch time of NR/EPDM compounds filled with silica/CB hybrid filler is depicted in Figure 4.60. The results show that the scorch time (t_{s2}) strongly reduces with increasing silica content. This shorter t_{s2} may be associated with the impact of the moisture-treated silanol sorts on the surfaces of silica including the hydrolysis of the nitrogen-sulfur chain of TBBS, leading to the rapid onset of crosslinking (Butler & Freakley, 1992; Ignatz-Hoover, 1999; K. J. Kim & Vanderkooi, 2005).

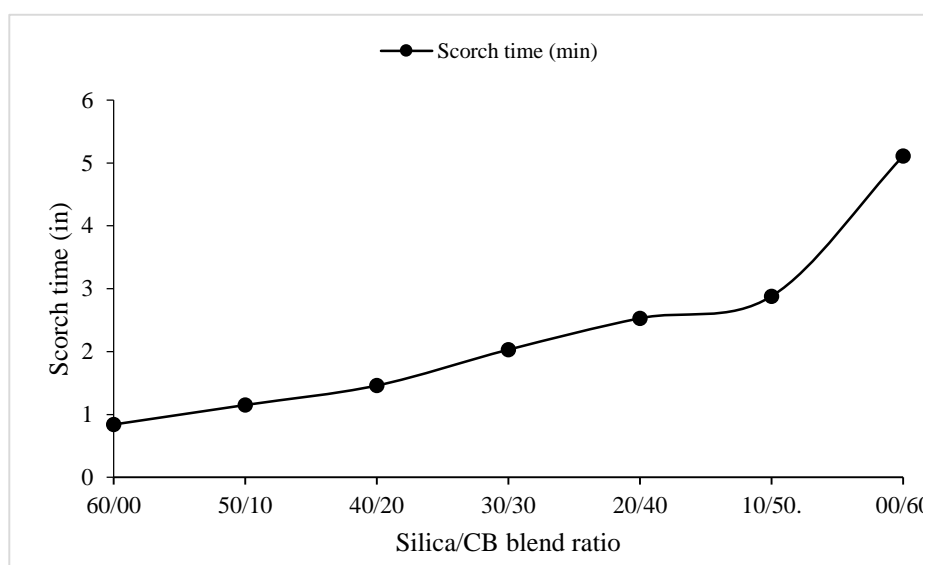


Figure 4.60 Scorch time

4.1.2 Cure time (min)

In Figure 4.61, the cure time (t_{s90}) increases with the increasing amount of silica until 50 phr. Later it goes down when the further amount of silica is added. The decrease when more than 50 phr of silica amount is added can be by the reason of these compounds have experienced higher thermal history while mixing because of their greater compound viscosities. It is obvious that during mixing, the shear heating

is larger when the amount of silica is added due to the increment of compound viscosity. This justification is subsidized by the rheometer cure curves as illustrated in Figure 4.61. That compounds that have a larger amount of silica provide greater minimum torque, demonstrating greater viscosities compared to others Figure 4.62.

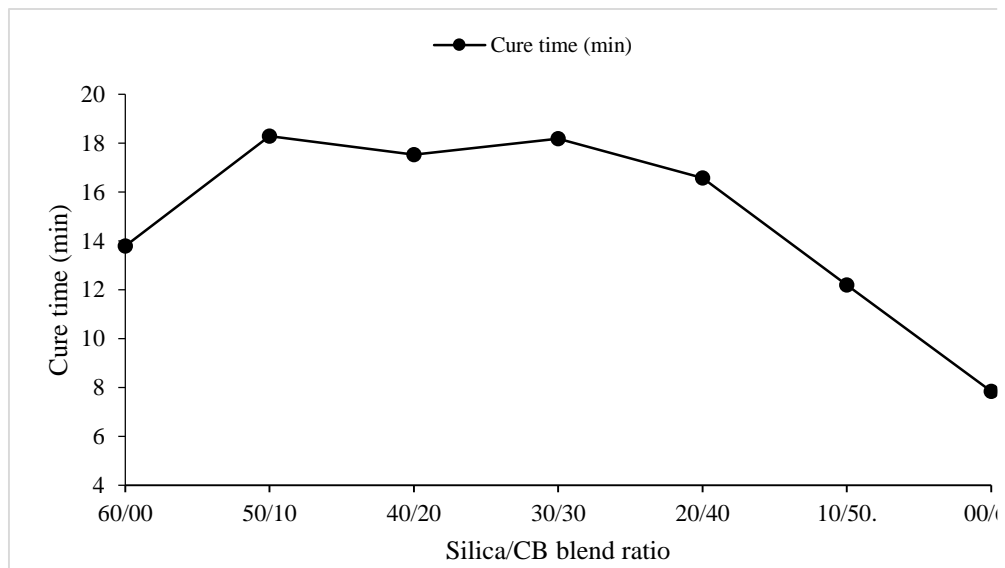


Figure 4.61 Cure time

4.1.3 Minimum torque (N.m)

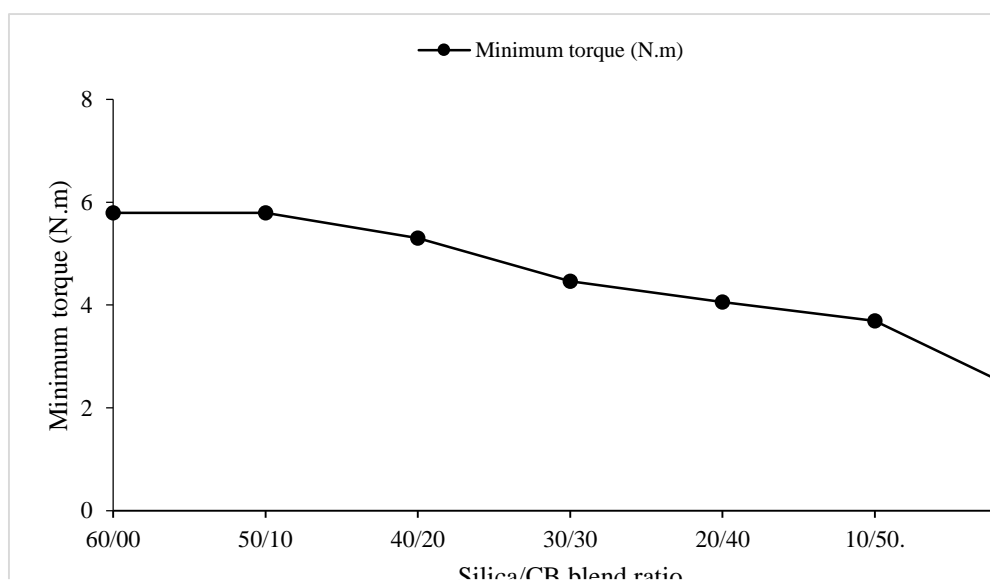


Figure 4.62 Minimum torque

4.2 Mechanical properties

The mechanical properties of each proportion were tested including tensile strength, modulus at 100%, 200%, and 300%, elongation, and hardness. These mechanical properties are illustrated in Table 4.15 and Table 4.16.

Table 4.15. Mechanical properties of vulcanized blended rubber before aging

Silica/CB	Tensile strength (Mpa)	Modulus 100%	Modulus 200%	Modulus 300%	Elongation at break (%)	Hardness (Shore A)
60/00	6.90	3.50	5.20	6.50	324	72.53
50/10	8.00	3.60	5.60	7.20	394	69.30
40/20	11.30	3.60	5.80	8.10	447	69.16
30/30	7.90	3.10	5.00	6.90	414	68.23
20/40	9.60	3.20	5.40	7.40	439	67.23
10/50	6.00	3.40	6.00	-	225	68.20
00/60	16.30	4.00	7.70	11.40	461	66.86

Table 4.16. Mechanical properties of vulcanized blended rubber after aging

Silica/CB	Tensile strength (Mpa)	Modulus 100%	Modulus 200%	Modulus 300%	Elongation at break (%)	Hardness (Shore A)
60/00	6.60	4.00	5.60	-	293	74.13
50/10	8.20	4.00	6.20	7.90	364	71.53
40/20	11.20	4.50	7.30	9.60	405	70.93
30/30	8.60	3.80	6.00	7.90	382	70.83
20/40	11.40	4.10	6.80	9.10	429	69.67
10/50	7.30	4.50	-	-	187	70.76
00/60	19.90	5.30	10.60	15.70	393	70.10

Table 4.17. Mechanical properties of standard O-ring based on Thai Industry Standard

Properties of standard O-ring based on TSI		Water	Lubricant	Gasoline
Hardness	IRHD (CM)	65-75	65-75	65-75
Tensile strength	Mpa	9	7.8	7.8
Elongation at break	%	200	200	160
Modulus	MPa	2.7	2.7	2.7

4.2.1 Tensile strength (MPa)

Figure 4.63 shows the tensile strength of all rubber compounds. Using the same amount of natural rubber to EPDM rubber at the ratio of 30/70 of all proportions with the various ratio of silica:CB hybrid from 00:60, 10:50, 20:40, 30:30, 40:20, 50:10, and 60:00, it was found that the tensile strength of controlled filler CB (00:60) was very high than the silica's and other formula. Regardless the control formula of CB filler, the tensile strength of all blending likely to raise with increment of silica number up to 20 phr. Then it went down when the silica amount reaches 30 phr. This result is also found in (Prasertsri & Rattanasom, 2012). Then the tensile strength increases in 40 phr of silica loading and goes down again in 50 phr of silica content.

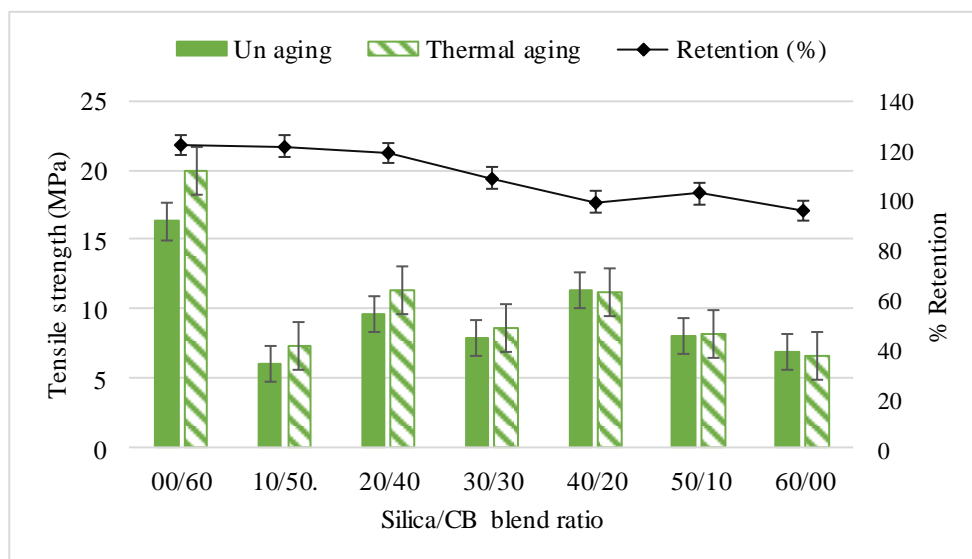


Figure 4.63. Tensile strength at different blend ratios of un-aged and aged carbon black filled NR/EPDM.

4.2.2 Modulus

The 100% modulus of both thermal aging and un aging of rubber blends is illustrated in Figure 4.64. The modulus of silica control formula was higher than the CB's. The modulus likely to reduce gradually when the silica content lower than 40 phr and then it starts to increase from 40, 50, and 60 phr of silica loading. The

100% modulus of unaging samples have higher modulus than before aging. This is probably due to the good crosslinking of EPDM rubber during it was heated.

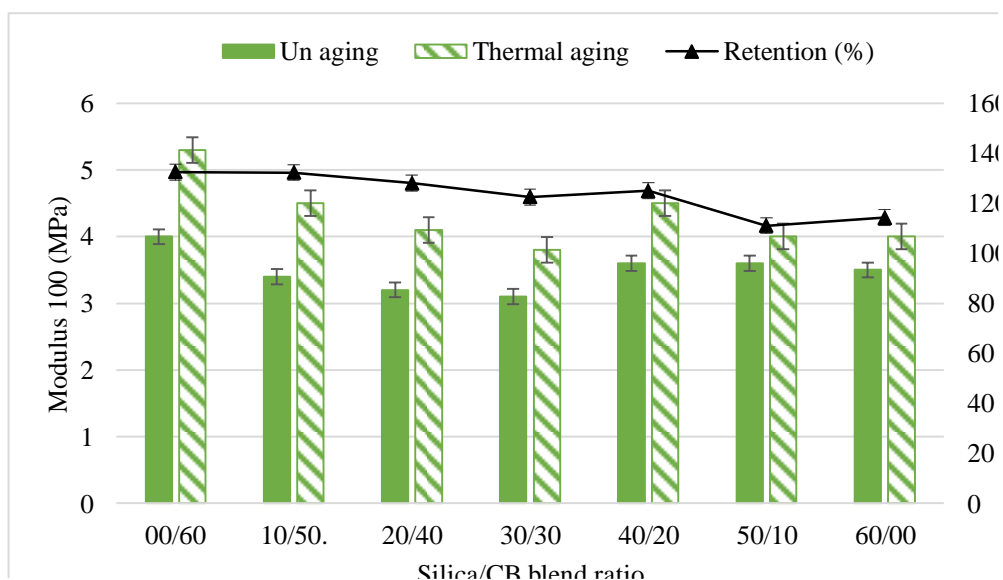


Figure 4.64. The 100% modulus at different blend ratio of un-aged and aged carbon black filled NR/EPDM.

4.2.3 Elongation

Figure 4.65 demonstrates that the elongation at the break of the CB control formula is higher than the silica. The elongations at break of all silica/CB hybrid fillers are not so different except the sample of 10/50 proportion. The elongation at break lightly goes down by increasing the amount of silica and it decreases just after silane is supplemental (Prasertsri & Rattanasom, 2012). On the other hand, the aged sample has lower values of elongation at break than the unaged specimens. This result demonstrates the increasing of crosslink structure by cause of post-curing during ageing treatment and leads to the reduction of the mobility of the rubber networks.

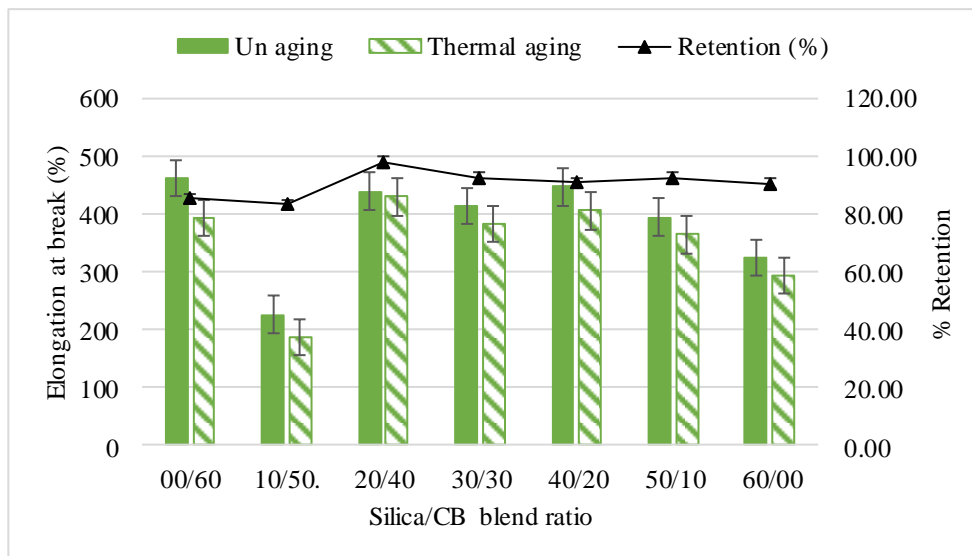


Figure 4.65. Elongation at break at different blend ratio of un-aged and aged carbon black filled NR/EPDM.

4.2.4 Hardness

Figure 4.66 shows the hardness of the vulcanized rubber blends before aging and aging are gradually increased due to the increment of silica loading. It was found that the control formula of silica (60:00) provides the highest hardness than the control formula of CB. The proportions which content the silica up to 40 – 50 phr gives the high hardness after the control formula of silica. This result indicates that the silica filler affects the hardness of the rubber blends. The more amount of silica rises, the more content of silane added into the compound so the addition of silane also provides stiffer composite corresponding well with its higher crosslinking density (Prasertsri & Rattanasom, 2012). Moreover, the hardness after aging increased with more amount of EPDM rubber because when it got heated it will have a link between the chain rather than a cut in chain. An increase in hardness can be attributed to crosslinking reactions (Kömmling et al., 2016).

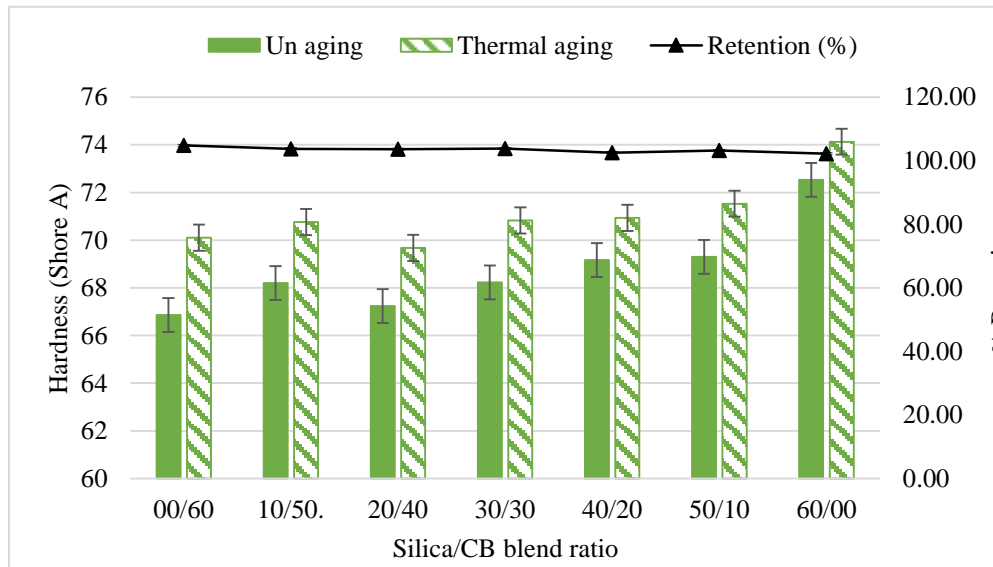


Figure 4.66. Hardness properties at different blend ratio of un-aged and aged carbon black filled NR/EPDM.

4.3 Comparison of mechanical properties between the prepared O-ring and standard O-ring based on Thai Industry Standard

Statistic test for mechanical properties (F1: tensile strength, F2: modulus, F3: elongation at break and F4: hardness) used Wilcoxon Signed Ranks Test to test the mean of difference of each factor of mechanical properties of prepared O-ring with standard O-ring. The results show that the mechanical properties of prepared O-ring are not different to the standard's (P -value of standard with 60/00 = 0.273, 50/10 = 0.273, 40/20 = 0.144, 30/30 = 0.465, 20/40 = 0.465, 10/50 = 1.000 and 00/60 = 0.273 > significant level 0.05).

Table 4.18 Wilcoxon Signed Ranks Test Statistics

Wilcoxon=(Paired)	Z	P-value
Standard with 60/00	-1.095	0.273
Standard with 50/10	-1.095	0.273
Standard with 40/20	-1.461	0.144
Standard with 30/30	-0.730	0.465
Standard with 20/40	-0.730	0.465
Standard with 10/50	0.000	1.000
Standard with 00/60	-1.095	0.273

Table 4.19 Mechanical properties of standard and prepared O-rings

Mechanical properties	Standard	60/00	50/10	40/20	30/30	20/40	10/50	00/60
Tensile strength (Mpa)	7.8	6.9	8	11.3	7.9	9.6	6	16.3
Modulus (Mpa)	2.7	3.5	3.6	3.6	3.1	3.2	3.4	4
Elongation at break (%)	160	324	394	447	414	439	225	461
Hardness (Shore A)	70	72.53	69.3	69.16	68.23	67.23	68.2	66.86

4.4 Price of prepared O-ring and standard O-ring

Since the mechanical properties of prepared O-ring and standard O-ring are not different, the price per prepared O-ring was calculated in Thai baht to compare with the price per standard O-ring in the market. The prices of prepared and standard O-ring are demonstrated in Table 4.20 and Table 4.21. The results illustrated that the price of prepared O-ring is cheaper than the standard O-ring due to the very low price of NR used in the formulation of prepared O-ring.

Table 4.20 Price of prepared O-ring in Thai baht

Materials (silica/CB:40/20)	phr	S.G	Volume	Weight (g)	Price in Thai Baht	Price per 1 Kg in Baht
STR 5L	30	0.92	27.6	49.43	2.27	46
EPDM	70	1.1	77	115.34	16.15	140
Silica	40	1.9	76	65.91	4.28	65
Carbon black, N330	20	1.7	34	32.95	5.17	156.83
TBBS	1.2	1.28	1.54	1.98	0.40	200
ZnO	3	5.57	16.71	4.94	0.59	120
SA	1	0.85	0.85	1.65	0.16	100
S	1.8	2.07	3.73	2.97	0.36	120
TESPT	3.50	1.03	3.60	5.76	0.78	135.72
Wingstay L	1	1.1	1.1	1.65	0.01	5.8
Homogenisator 501	5	1.1	5.5	8.24	1.65	200
Total price in one formulation				31.82		Baht
Total prepared O-rings				350		O-rings
Price per prepared O-ring				0.09		Baht

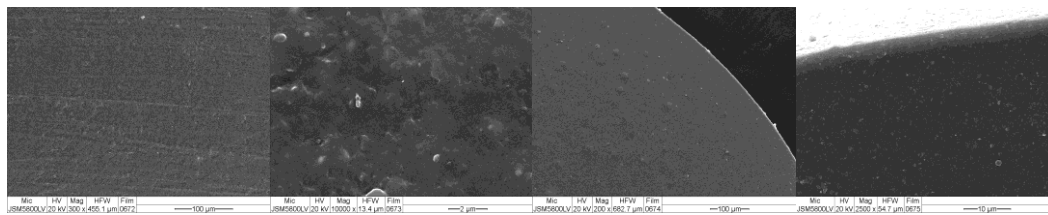
Table 4.21 Price of standard O-ring in Thai baht

Standard O-ring price in Baht	
Price in 225 pieces	128 Baht
Price per standard O-ring	0.57 Baht

4.5 Appearances of standard O-ring and O-ring rubber

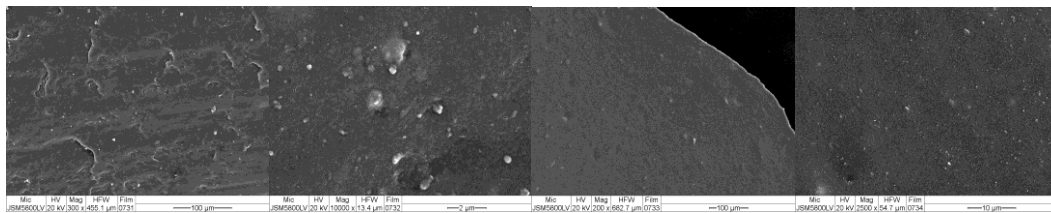
The surface of HP standard O-ring before test in SOFC looks smooth whereas the surface of the NR/EPDM filled silica/CB O-ring rubber is not smooth and have a clustering of white silica particles which indicates that the forming and mixing rubber with filler involving silica do not have a good dispersion within the rubber matrix due to the poor compatibility between highly polar silica and non-polar common intention rubbers and silica pieces have a great surface power because of a great concentration of silanol sorts on their surface and likely to self-associate via hydrogen bonding, promoting to the formation of a strong filler-filler network (Kaewsakul et al., 2014).

The characteristics of the HP standard O-ring and the NR/EPDM filled silica/CB O-ring rubber’s surface and cross-section before testing are shown in Figure 4.67 and Figure 4.68. The O-ring rubber products are illustrated in Figure 4.69.



(s'-1) Surface (s'-2) Surface (s'-3) Cross-section (s'-4) Cross-section

Figure 4.67. The surfaces’ characteristics and cross-sections of the standard O-rings.



(s-1) Surface (s-2) Surface (s-3) Cross-section (s-4) Cross-section

Figure 4.68. The surfaces’ characteristics and cross-sections of the NR/EPDM filled silica/CB O-rings with silica and CB ratio of 40/20.

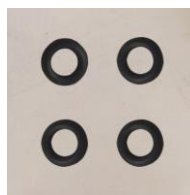
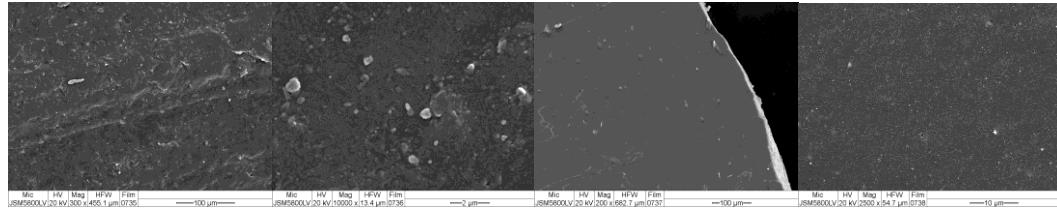


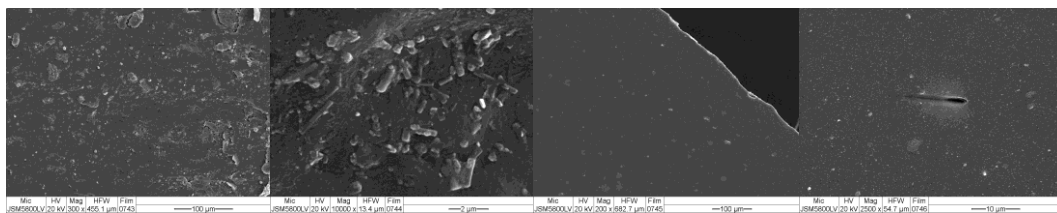
Figure 4.69. The NR/EPDM filled silica/CB O-ring rubber production.

4.6 Crack initiation and growth behavior in O-rings



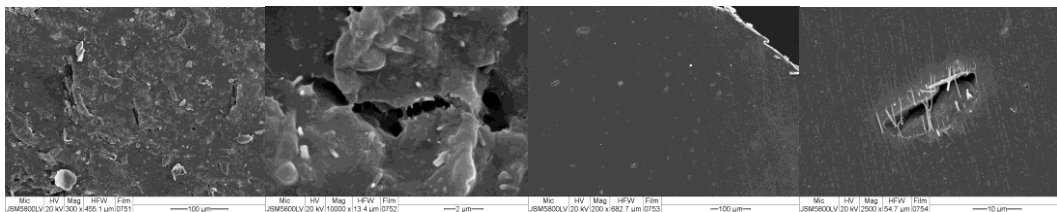
(a-1) Surface (a-2) Surface (a-3) Cross-section (a-4) Cross-section

(a) parts that are exposed to inlet gas for 1 hours



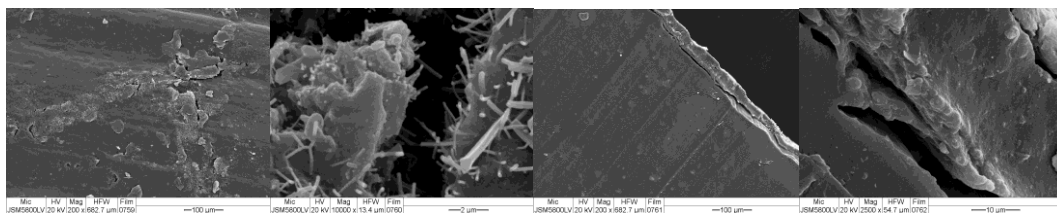
(b-1) Surface (b-2) Surface (b-3) Cross-section (b-4) Cross-section

(b) parts that are exposed to inlet gas for 6 hours



(c-1) Surface (c-2) Surface (c-3) Cross-section (c-4) Cross-section

(c) parts that are exposed to inlet gas for 12 hours



(d-1) Surface (d-2) Surface (d-3) Cross-section (d-4) Cross-section

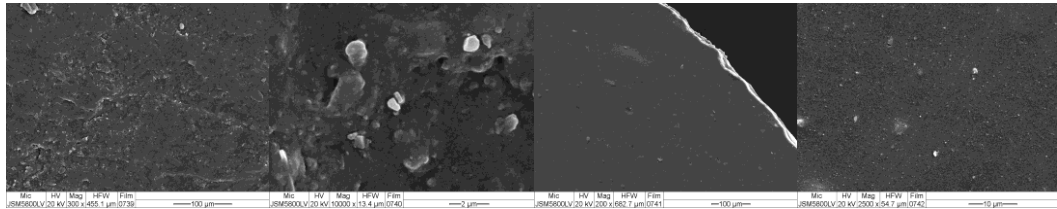
(d) parts that are exposed to inlet gas flow for 24 hours

Figure 4.70. The surfaces' characteristics and cross-section of the NR/EPDM filled silica/CB O-rings exposed to 1 hour, 6 hours, 12 hours, and 24 hours of oxygen gas in SOFC testing system at the inlet gas flow rate of 0.5 L/mn and temperature of 27 to 31°C.

When taken through the 0.5 L/min of oxygen gas at the inlet gas flow and the temperature of 27 to 31°C for 1 hour the surface and cross-section of the NR/EPDM filled silica/CB O-ring has no cracks Figure 4.70 (part a) similar to the one that exposed to the outlet gas flow and the temperature of 53 to 58°C in Figure 4.71 (part e). after 6 hours exposed to the inlet gas flow, the slight inner crack was initiated and the surface showed the separate of clustering Figure 4.70 (part b-4). The inner crack was also initiated at the part that exposed 6 hours to the outlet gas flow Figure 4.71 (part f-4). For 12 hours testing, the inner crack on the cross-section is more spacious than the one exposed to 6 hours (part c-4) and the traverse crack were found on the surface (part c-2). The traverse cracks were found at the edge of O-ring's cross-section (part d-3 and d-4) and the blistering (part d-2) were found after 24 hours exposed to the inlet gas flow.

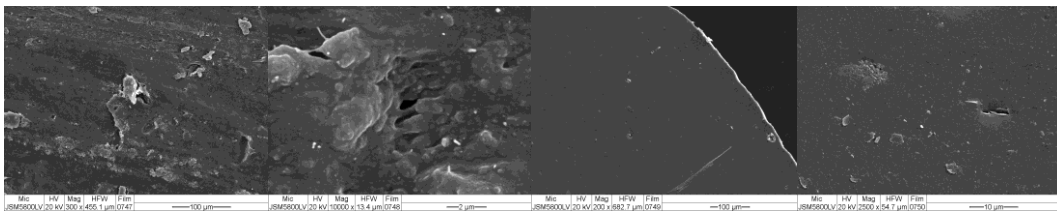
Figure 4.71 demonstrates the NR/EPDM filled silica/CB O-rings exposed to 1 hour, 6 hours, 12 hours, and 24 hours of oxygen gas in SOFC testing system at the outlet gas flow rate of 0.5 L/mn and temperature of 53 to 58°C. There were no cracks on the cross-section (part e-4) but the clustering seems separate on the surface (part e-2) after testing 1 hour. After 6 hours testing, the inner cracks were initiated and found (part f-4) and the surface has a shallow holes and nearly break (part f-2). The part that are exposed to outlet gas flow for 12 hours show the inner crack on the cross-section (part g-4) and have the traverse crack on the surface (part g-1 and g-2). The inner crack is more increasing in the cross-section (part h-4) and also cracks and blistering are severely on the surface (part h-1 and h-2) after 24 hours exposed to the outlet gas flow. The surfaces' characteristics and cross-section of the HP standard O-rings exposed to 1 hour, 6 hours, 12 hours, and 24 hours of oxygen gas in SOFC testing system at inlet flow rate of 0.5 L/mn and temperature of 53 to 58°C are illustrated in Figure 4.72. The inner cracks were not found on the O-ring after exposed to 1 hour of the inlet oxygen gas flow in SOFC (part a'). After 6 hours testing, the inner cracks were found on the cross-section (part b'-4) and minor cracks is also taken place on the surface (part b'-1 and b'-2). The inner crack like a hole was found in the cross-section (part c'-4) and slight and shallow traverse are found on the surface (part c'1 and c'2) following 12 hours exposed to the inlet oxygen gas in

SOFC. 24 hours later of testing, the many inner cracks were found in the cross-section (part d'-3 and d'-4) and the deep cracks were found on the surface of the O-ring (part d'-1 and d'-2).



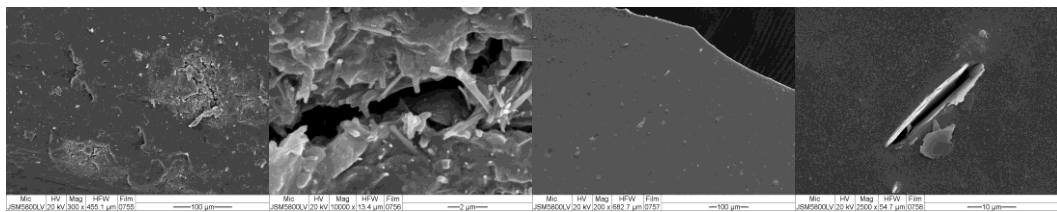
(e-1) Surface (e-2) Surface (e-3) Cross-section (e-4) Cross-section

(e) parts that are exposed to outlet gas for 1 hours



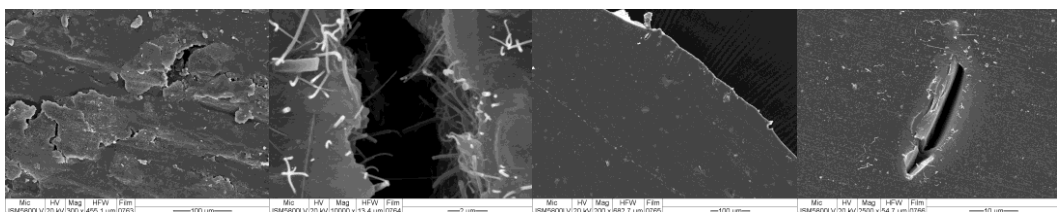
(f-1) Surface (f-2) Surface (f-3) Cross-section (f-4) Cross-section

(f) parts that are exposed to outlet gas for 6 hours



(g-1) Surface (g-2) Surface (g-3) Cross-section (g-4) Cross-section

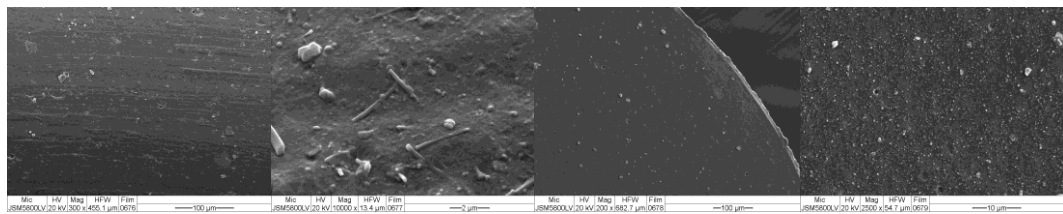
(g) parts that are exposed to outlet gas for 12 hours



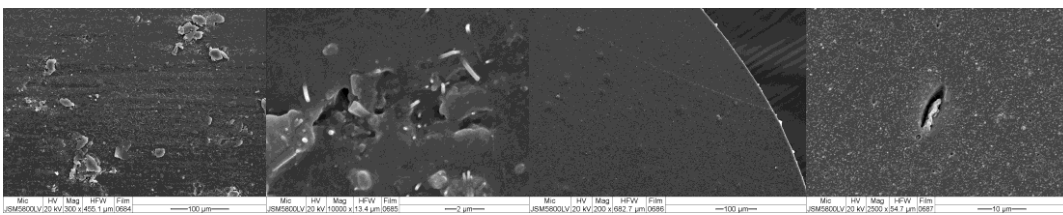
(h-1) Surface (h-2) Surface (h-3) Cross-section (h-4) Cross-section

(h) parts that are exposed to outlet gas flow for 24 hours

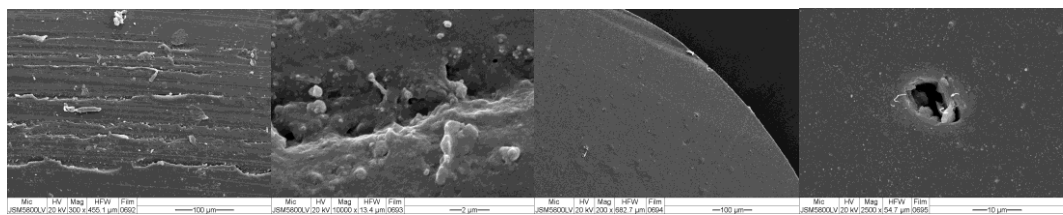
Figure 4.71. The surfaces' characteristics and cross-section of the NR/EPDM filled silica/CB O-rings exposed to 1 hour, 6 hours, 12 hours, and 24 hours of oxygen gas in SOFC testing system at the outlet gas flow rate of 0.5 L/mn and temperature of 53 to 58°C.



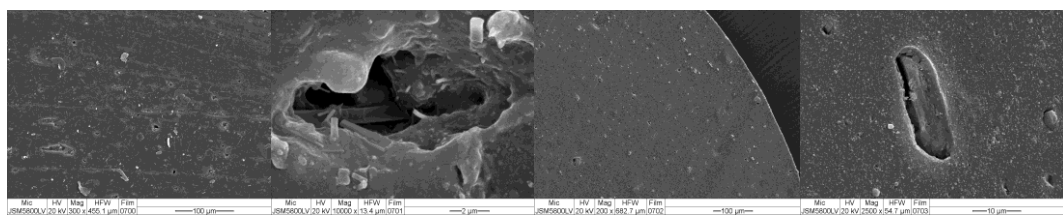
(a'-1) Surface (a'-2) Surface (a'-3) Cross-section (a'-4) Cross-section
(a') parts that are exposed to inlet gas for 1 hours



(b'-1) Surface (b'-2) Surface (b'-3) Cross-section (b'-4) Cross-section
(b') parts that are exposed to inlet gas for 6 hours



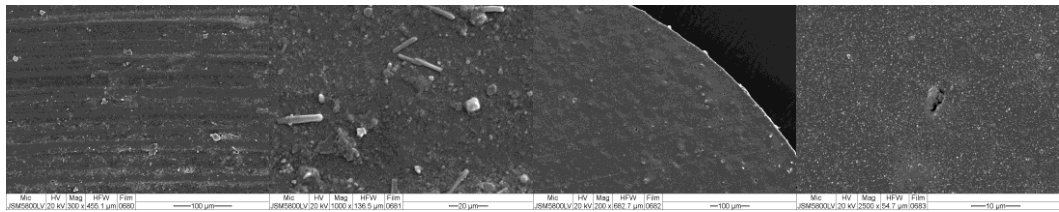
(c'-1) Surface (c'-2) Surface (c'-3) Cross-section (c'-4) Cross-section
(c') parts that are exposed to inlet gas for 12 hours



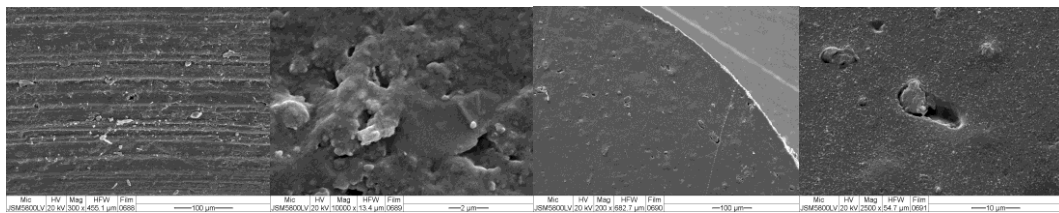
(d'-1) Surface (d'-2) Surface (d'-3) Cross-section (d'-4) Cross-section
(d') parts that are exposed to inlet gas for 24 hours

Figure 4.72. The surfaces' characteristics and cross-section of the standard O-rings exposed to 1 hour, 6 hours, 12 hours, and 24 hours of oxygen gas in SOFC testing system at inlet flow rate of 0.5 L/mn and temperature of 53 to 58°C.

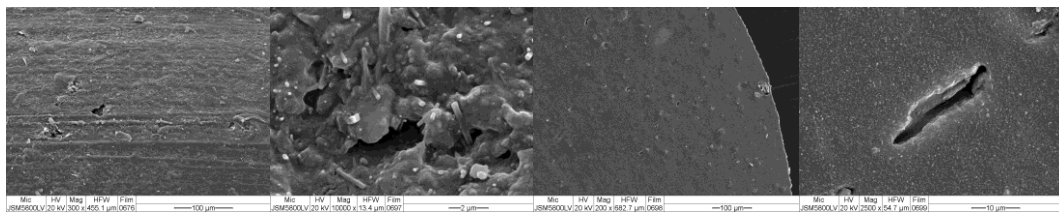
Figure 4.73 depicts the surfaces' characteristics and cross-section of the commercial/standard O-rings exposed to 1 hour, 6 hours, 12 hours, and 24 hours of oxygen gas in SOFC testing system at the outlet gas flow rate of 0.5 L/mn and



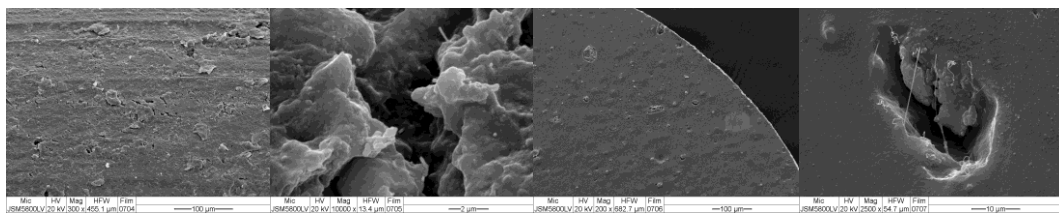
(e'-1) Surface (e'-2) Surface (e'-3) Cross-section (e'-4) Cross-section
(e') parts that are exposed to outlet gas for 1 hours



(f'-1) Surface (f'-2) Surface (f'-3) Cross-section (f'-4) Cross-section
(f') parts that are exposed to outlet gas for 6 hours



(g'-1) Surface (g'-2) Surface (g'-3) Cross-section (g'-4) Cross-section
(g') parts that are exposed to outlet gas for 12 hours



(h'-1) Surface (h'-2) Surface (h'-3) Cross-section (h'-4) Cross-section
(h') parts that are exposed to outlet gas flow for 24 hours

Figure 4.73. The surfaces' characteristics and cross-section of the standard O-rings exposed to 1 hour, 6 hours, 12 hours, and 24 hours of oxygen gas in SOFC testing system at the outlet gas flow rate of 0.5 L/mn and temperature of 53 to 58°C.

temperature of 53 to 58°C. Cracks were initiated at early 1 hours testing (part e'-4) but were not found on the surface (part e'-1). After 6 hours testing, the inner cracks were found bigger than 1-hour testing (part f'-4) and surface has slightly crack and

has the swelling (part f'-2). After 12 hours, the inner cracks were found bigger on the cross-section (part g'-4) and the swelling on surface started to have a slight traverse (part g'-2). The inner cracks are found and spacious in the cross-section (part h'-4) and the traverse cracks are found too on the surface (part h'-1 and h'-2) when exposed to the outlet oxygen gas flow for 24 hours.

Indeed, inner cracks of both the NR/EPDM filled silica/CB and HP standard O-rings were initiated during the 6 hours exposing to both inlet and outlet oxygen gas flow except the standard O-ring that are exposed to the outlet oxygen gas has the inner cracks initiated at 1 hour. The NR/EPDM filled silica/CB O-ring were found having and inner cracks then the traverse cracks and blistering without swelling at both inlet and outlet oxygen gas flow. Meanwhile the standard O-ring also has no swelling at the inlet gas flow and has swelling before having the traverse cracks at the outlet gas flow which has higher temperature than at the inlet gas flow. This is due to the high amount of EPDM rubber in the formulation which it has high thermal resistance. Even though there are the presence of initial inner crack after 1 hour and 6 hours, slight fracture after 6 and 12 hours and shallow and deep traverse after 24 hours testing inside the O-rings, still the prepared and standard O-rings can be used at the mating surface and continue to test in the SOFC.

CHAPTER 5

CONCLUSION

The O-rings were produced by using the EPDM and NR as the major composites. Blends of NR/EPDM filled silica/CB were prepared in the internal mixing and on a two-roll mill. The mechanical properties NR/EPDM filled silica/CB before and after aging were carried out. The best compound of NR/EPDM filled silica/CB were selected to make O-rings. The surface and cross-section morphology of the NR/EPDM filled silica/CB were also investigated and compared with the HP standard O-ring after testing and exposed to oxygen gas diffusion at the mating surfaces with the flow rate of 0.5 L/minute and the temperature ranging from 27 to 31 °C (inlet) and 53 to 58 °C (outflow) in the SOFC testing system for 1 hour, 6 hours, 12 hours, and 24 hours. As a result, the compound with the ratio of the silica/CB of 40:20 provides the best mechanical properties and pass the standard O-ring (TIS 2728-2559) (*P*-value of standard with prepared O-rings: 60/00 = 0.273, 50/10 = 0.273, 40/20 = 0.144, 30/30 = 0.465, 20/40 = 0.465, 10/50 = 1.000 and 00/60 = 0.273 > significant level 0.05) and the price of prepared O-ring is cheaper than the standard O-ring due to the very low price of NR used in the formulation of prepared O-ring. After testing in SOFC, still the prepared and standard O-rings can be used to test in SOFC although there are some inner cracks after 1 hour and 6 hours, slight fracture after 12 hours and shallow and deep traverse inside the O-ring after 24 hours testing.

SUGGESTIONS

For future work, it is recommended to find the conditions for preparing the silica in order to match the NR and EPDM rubber. Another suggestion is to find the ways to increase the life of the O-ring from the compound rubber for a long time, which may change the type of rubber or chemicals in the preparation formula.

REFERENCES

- Akiba, M., & Hashim, A. S. (1997). *M. Akiba and A. S. Hashim, Vulcanization and crosslinking in elastomers, Prog. Polym. Sci., vol. 22, no. 3, pp. 475–521, 1997.* 22(96). https://doi.org/10.1007/978-3-642-42054-2_7
- Akulichev, A. G., Echtermeyer, A. T., & Persson, B. N. J. (2018). Interfacial leakage of elastomer seals at low temperatures. *International Journal of Pressure Vessels and Piping, 160*, 14–23. <https://doi.org/10.1016/j.ijpvp.2017.11.014>
- Allen, R. D. (1983). Fundamentals of Compounding Epdm for Cost/Performance. *Journal of Elastomers and Plastics, 15*(1), 19–32.
- Allsopp, M., & Vianello, G. (2000). *Poly (Vinyl Chloride). Ullmann's encyclopedia of industrial chemistry.*
- Aminabhavi, T. M., Manjeshwar, L. S., & Cassidy, P. E. (1986). Water permeation through elastomer laminates. IV. NBR/EPDM. *Journal of Applied Polymer Science, 32*(2), 3719–3723. <https://doi.org/10.1002/app.1986.070320227>
- Arshad, M. S., Mushtaq, N., Ahmad, M. A., Naseem, S., Atiq, S., Ahmed, Z., Ali, R., Abbas, G., & Raza, R. (2017). Nickel foam anode-supported solid oxide fuel cells with composite electrolytes. *International Journal of Hydrogen Energy.* <https://doi.org/10.1016/j.ijhydene.2017.06.036>
- Atkinson, S. (2002). Decompression modelling of elastomer seals promises to eliminate downtime. *Sealing Technology, 2002*(12), 8–11.
- Baldwin, F. P., & Strate, G. Ver. (1972). Polyolefin Elastomers Based on Ethylene and Propylene. *Rubber Chemistry and Technology, 45*(3), 709–881. <https://doi.org/10.5254/1.3544730>
- Bazgir, S., Katbab, A. A., & Nazockdast, H. (2004). Silica-reinforced dynamically vulcanized ethylene-propylene-diene monomer/polypropylene thermoplastic elastomers: Morphology, rheology, and dynamic mechanical properties. *Journal of Applied Polymer Science, 92*(3), 2000–2007.
- Bhattacharya, M., & Bhowmick, A. K. (2010). Synergy in carbon black-filled Natural rubber nanocomposites. Part I: Mechanical, dynamic mechanical properties, and morphology. *Journal of Materials Science, 45*(22), 6126–6138. <https://doi.org/10.1007/s10853-010-4699-6>

- Bhuvaneswari, C. M., Sureshkumar, M. S., Kakade, S. D., & Gupta, M. (2006). Ethylene-propylene diene rubber as a futuristic elastomer for insulation of solid rocket motors. *Defence Science Journal*, *56*(3), 309–320.
- Briscoe, B. J., & Liatsis, D. (1992). Internal crack symmetry phenomena during gas-induced rupture of elastomers. In *Rubber Chemistry and Technology* (Vol. 65, Issue 2, pp. 350–373). <https://doi.org/10.5254/1.3538617>
- Briscoe, B. J., Savvas, T., & Kelly, C. T. (1994). “Explosive decompression failure” of rubbers: a review of the origins of pneumatic stress induced rupture in elastomers. *Rubber Chemistry and Technology*, *67*(3), 384–416. <https://doi.org/10.5254/1.3538683>
- Butler, J., & Freakley, P. K. (1992). Effect of humidity and water content on the cure behavior of a natural-rubber accelerated sulfur compound. In *Rubber Chemistry and Technology* (Vol. 65, Issue 2, pp. 374–384).
- Chen, Xueye, Li, T., Shen, J., & Hu, Z. (2017). From structures, packaging to application: A system-level review for micro direct methanol fuel cell. In *Renewable and Sustainable Energy Reviews* (Vol. 80, pp. 669–678). <https://doi.org/10.1016/j.rser.2017.05.272>
- Chen, Xuming, Bartos, J., Salem, H., & Zonoz, R. (2016). Elastomers for high pressure low temperature hplt sealing. *Proceedings of the Annual Offshore Technology Conference*, *5*, 3828–3842. <https://www.onepetro.org/conference-paper/OTC-27227-MS>
- Cheng, J., & He, J. (2017). Electrical properties of scheelite structure ceramic electrolytes for solid oxide fuel cells. *Materials Letters*, *209*, 525–527. <https://doi.org/10.1016/j.matlet.2017.08.094>
- Coran, A. Y., & Patel, R. (1980). Rubber-thermoplastic compositions - 2. NBR-Nylon thermoplastic elastomeric compositions. *Rubber Chemistry and Technology*, *53*(4), 781–794.
- Cui, T., Chao, Y. J., & Van Zee, J. W. (2013). Thermal stress development of liquid silicone rubber seal under temperature cycling. *Polymer Testing*, *32*(7), 1202–1208. <https://doi.org/10.1016/j.polymertesting.2013.07.009>
- De, S. K., & Bhowmick, A. K. (1990). *Thermoplastic elastomers from rubber-plastic*

blends.

- Derham, C. J. (1997). Transient effects influencing sealing force in elastomeric O ring seals. *Plastics, Rubber and Composites Processing and Applications*, 26(3), 129–136.
- Deuri, A. S., De, P. P., Bhowmick, A. K., & De, S. K. (1988). Studies on the ageing of EPDM based rocket insulator compound by stress relaxation and the effect of propellant binder. *Polymer Degradation and Stability*, 20(2), 135–148. [https://doi.org/10.1016/0141-3910\(88\)90082-1](https://doi.org/10.1016/0141-3910(88)90082-1)
- Embury, P. (2004). High-pressure gas testing of elastomer seals and a practical approach to designing for explosive decompression service. *Sealing Technology*, 2004(6), 6–11. [https://doi.org/10.1016/S1350-4789\(04\)00231-4](https://doi.org/10.1016/S1350-4789(04)00231-4)
- Ender, D. H. (1986). Elastomeric seals. *Chemtech*, 16(1), 52–56. <https://ci.nii.ac.jp/naid/80002760473/>
- Engels, H.-W., Weidenhaupt, H.-J., Pjeroth, M., Hofmann, W., Menting, K.-H., Mergenhagen, T., Schmoll, R., & Uhrlandt, S. (2011). Rubber, 9. Chemicals and Additives. *Ullmann's Encyclopedia of Industrial Chemistry*.
- Epstein, P. S., & Plesset, M. S. (1950). On the stability of gas bubbles in liquid-gas solutions. *The Journal of Chemical Physics*, 18(11), 1505–1509.
- Gamlin, C. D., Dutta, N. K., & Choudhury, N. R. (2003). Mechanism and kinetics of the isothermal thermodegradation of ethylene-propylene-diene (EPDM) elastomers. *Polymer Degradation and Stability*, 80(3), 525–531. <https://www.sciencedirect.com/science/article/pii/S0141391003000363>
- Garcia-Garcia, F. J., Beltrán, A. M., Yubero, F., González-Elipé, A. R., & Lambert, R. M. (2017). High performance novel gadolinium doped ceria/yttria stabilized zirconia/nickel layered and hybrid thin film anodes for application in solid oxide fuel cells. *Journal of Power Sources*, 363, 251–259.
- Gent, A. N., & Lindley, P. B. (1961). Internal Rupture of Bonded Rubber Cylinders in Tension. *Rubber Chemistry and Technology*, 34(3), 925–936. <https://royalsocietypublishing.org/doi/abs/10.1098/rspa.1959.0016>
- Gent, A. N., & Tompkins, D. A. (1969). Nucleation and growth of gas bubbles in elastomers. *Journal of Applied Physics*, 40(6), 2520–2525.

<https://doi.org/10.1063/1.1658026>

- George, J., Neelakantan, N. R., Varughese, K. T., & Thomas, S. (2006). Failure properties of thermoplastic elastomers from polyethylene/nitrile rubber blends: Effect of blend ratio, dynamic vulcanization, and filler incorporation. *Journal of Applied Polymer Science*, *100*(4), 2912–2929. <https://doi.org/10.1002/app.21381>
- Gillen, K. T., Bernstein, R., & Wilson, M. H. (2005). Predicting and confirming the lifetime of o-rings. *Polymer Degradation and Stability*, *87*(2), 257–270. <https://doi.org/10.1016/j.polymdegradstab.2004.07.019>
- Gillen, Kenneth T., Clough, R. L., & Wise, J. (1996). Prediction of elastomer lifetimes from accelerated thermal-aging experiments. *Advances in Chemistry Series*, *249*, 553–554. <https://www.osti.gov/biblio/522769>
- Grigoryeva, O. P., & Karger-Kocsis, J. (2000). Melt grafting of maleic anhydride onto an ethylene-propylene-diene terpolymer (EPDM). *European Polymer Journal*, *36*(7), 1419–1429. [https://doi.org/10.1016/S0014-3057\(99\)00205-0](https://doi.org/10.1016/S0014-3057(99)00205-0)
- Guy, L., Daudey, S., Cochet, P., & Bomal, Y. (2009). New insights in the dynamic properties of precipitated silica filled rubber using a new high surface silica. *KGK Kautschuk Gummi Kunststoffe*, *62*(7–8), 383–391.
- Gwaily, S. E., Abdel-Aziz, M. M., & Madani, M. (1998). Thermal and Electrical Studies on Irradiated Silica-Ethylene-Propylene Diene Monomer (SiO₂/EPDM) Composites. *Polymer Testing*, *17*(4), 265–287. [https://doi.org/10.1016/S0142-9418\(97\)00048-2](https://doi.org/10.1016/S0142-9418(97)00048-2)
- Heinz-Hermann Greve. (2000). Rubber, 2. natural. *Ullmann's Encyclopedia of Industrial Chemistry*.
- Hou, N., Li, P., Lv, T., Yao, T., Yao, X., Gan, T., Fan, L., Mao, P., Zhao, Y., & Li, Y. (2017). Sm_{0.5}Ba_{0.5}MnO₃- Δ anode for solid oxide fuel cells with hydrogen and methanol as fuels. *Catalysis Today*, *298*, 33–39.
- Ignatz-Hoover, F. (1999). Review of vulcanization chemistry. *Rubber World*, *220*(5), 24,26-30,101-102.
- Ismail, H., & Suryadiansyah. (2004). Effects of Filler Loading on Properties of Polypropylene-Natural Rubber-Recycle Rubber Powder (PP-NR-RRP) Composites. *Journal of Reinforced Plastics and Composites*, *23*(6), 639–650.

<https://doi.org/10.1177/0731684404032869>

- Jayasree, T. K., & Predeep, P. (2008). Effect of fillers on mechanical properties of dynamically crosslinked styrene butadiene rubber/high density polyethylene blends. *Journal of Elastomers and Plastics*, 40(2), 127–146. <https://doi.org/10.1177/0095244307083865>
- Jha, A., Dutta, B., & Bhowmick, A. K. (1999). Effect of fillers and plasticizers on the performance of novel heat and oil-resistant thermoplastic elastomers from nylon-6 and acrylate rubber blends. *Journal of Applied Polymer Science*, 74(6), 1490–1501. [https://doi.org/10.1002/\(SICI\)1097-4628\(19991107\)74:6<1490::AID-APP22>3.0.CO;2-U](https://doi.org/10.1002/(SICI)1097-4628(19991107)74:6<1490::AID-APP22>3.0.CO;2-U)
- Jovanović, V., Samaržija-Jovanović, S., Budinski-Simendić, J., Marković, G., & Marinović-Cincović, M. (2013). Composites based on carbon black reinforced NBR/EPDM rubber blends. *Composites Part B: Engineering*, 45(1), 333–340. <https://doi.org/10.1016/j.compositesb.2012.05.020>
- Kaewsakul, W., Sahakaro, K., Dierkes, W. K., & Noordermeer, J. W. M. (2014). Flocculation Kinetics and Filler-Rubber Interaction in Silica-Reinforced NR Compounds. *186th Technical Meeting of Rubber Division*, 1–20.
- Kang, T. K., Kim, Y., Lee, W. K., Park, H. D., Cho, W. J., & Ha, C. S. (1999). Properties of uncompatibilized and compatibilized poly(butylene terephthalate)-LLDPE blends. *Journal of Applied Polymer Science*, 72(8), 989–997.
- Katz, H. S., Milewski, J. (1981). Handbook of Fillers for Plastics. *Filler for Polymer Composite*.
- Kim, J. H., Shin, S. S., Noh, H. S., Son, J. W., Choi, M., & Kim, H. (2017). Tailoring ceramic membrane structures of solid oxide fuel cells via polymer-assisted electrospray deposition. *Journal of Membrane Science*, 544, 234–242. <https://doi.org/10.1016/j.memsci.2017.09.027>
- Kim, K. J., & Vanderkooi, J. (2005). Temperature effects of silane coupling on moisture treated silica surface. *Journal of Applied Polymer Science*, 95(3), 623–633. <https://doi.org/10.1002/app.21373>
- Koga, A., Uchida, K., Yamabe, J., & Nishimura, S. (2011). Evaluation on High-Pressure Hydrogen Decompression Failure of Rubber O-ring Using Design of

- Experiments. *International Journal of Automotive Engineering*, 2(4), 123–129. https://doi.org/10.20485/jsaeijae.2.4_123
- Kole, S., Chaki, T. K., Bhowmick, A. K., & Tripathy, D. K. (1993). Effect of compatibiliser, curing sequence and ageing on the thermal stability of silicone rubber, EPDM rubber and their blends. *Polymer Degradation and Stability*, 41(1), 109–116. [https://doi.org/10.1016/0141-3910\(93\)90069-U](https://doi.org/10.1016/0141-3910(93)90069-U)
- Kömmling, A., Jaunich, M., & Wolff, D. (2016). Effects of heterogeneous aging in compressed HNBR and EPDM O-ring seals. *Polymer Degradation and Stability*, 126, 39–46. <https://doi.org/10.1016/j.polymdegradstab.2016.01.012>
- Kundera, C., & Bochnia, J. (2014). Investigating the stress relaxation of photopolymer O-ring seal models. *Rapid Prototyping Journal*, 20(6), 533–540. <https://doi.org/10.1108/RPJ-04-2013-0043>
- Lach, C. L. (1993). *Effect of Temperature and O-Ring Gland Finish on Sealing Ability of Viton V747-75*. November.
- Laskowska, A., Zaborski, M., Boiteux, G., Gain, O., Marzec, A., & Maniukiewicz, W. (2014). Ionic elastomers based on carboxylated nitrile rubber (XNBR) and magnesium aluminum layered double hydroxide (hydrotalcite). *Express Polymer Letters*, 8(6), 374–386. <https://doi.org/10.3144/expresspolymlett.2014.42>
- Lee, S. H., Yoo, S. S., Kim, D. E., Kang, B. S., & Kim, H. E. (2012). Accelerated wear test of FKM elastomer for life prediction of seals. *Polymer Testing*, 31(8), 993–1000. <https://doi.org/10.1016/j.polymertesting.2012.07.017>
- Leonid, M., & Lyamshev, L. M. (2004). Library of Congress Cataloging-in-Publication Data Visit the CRC Press Web site at www.crcpress.com. In *America*.
- Lin, J. S., Kumar, S. R., Ma, W. T., Shih, C. M., Teng, L. W., Yang, C. C., & Lue, S. J. (2017). Gradiently distributed iron oxide@graphene oxide nanofillers in quaternized polyvinyl alcohol composite to enhance alkaline fuel cell power density. *Journal of Membrane Science*, 543, 28–39.
- Lingerkar, K., & Khonsari, M. M. (2010). On the effects of sliding velocity and operating pressure differential in rotary O-ring seals. *Proceedings of the Institution of Mechanical Engineers, Part J: Journal of Engineering Tribology*,

- 224(7), 649–657. <https://doi.org/10.1243/13506501JET755>
- Maity, S. K., & Chakraborty, K. K. (1994). Studies on curing characteristics of natural rubber-, nitrile rubber-, and silicone rubber-based filled compounds in the presence of boron compounds. *Die Angewandte Makromolekulare Chemie*, 221(1), 11–31. <https://doi.org/10.1002/apmc.1994.052210102>
- Marinović-Cincović, M., Janković, B., Jovanović, V., Samaržija-Jovanović, S., & Marković, G. (2013). The kinetic and thermodynamic analyses of non-isothermal degradation process of acrylonitrile-butadiene and ethylene-propylene-diene rubbers. *Composites Part B: Engineering*, 45(1), 321–332. <https://www.sciencedirect.com/science/article/pii/S1359836812005124>
- Markovic, G. Visakh, P. (2017). Polymer blends: state of art. *Recent Developments in Polymer Macro, Micro and Nano Blends*, 1–15.
- Marlier, R. (2010). First tests results for determination of seal life of EPDM O-rings at high temperature (determined by unique method). *Packaging, Transport, Storage & Security of Radioactive Material*, 21(1), 37–40.
- Meng, X., Wang, S., Lü, S., Yu, W. W., Sui, Y., Yang, L., Wei, M., Cao, J., & Yang, J. (2017). Structural, thermal and electrochemical properties of SrCo_{0.8}Fe_{0.1}Ga_{0.1}O_{3-δ} cathode material for intermediate-temperature solid oxide fuel cells. *Journal of Alloys and Compounds*, 727, 27–33.
- Moore, N. B., Hellums, J., Chang, R. T. S., & Engineering, C. O. (1989). *O-Ring Seal Failure Mechanisms*. 83–94.
- Morrell, P. R., Patel, M., & Skinner, A. R. (2003). Accelerated thermal ageing studies on nitrile rubber O-rings. *Polymer Testing*, 22(6), 651–656. [https://doi.org/10.1016/S0142-9418\(02\)00171-X](https://doi.org/10.1016/S0142-9418(02)00171-X)
- Mousa, A., Heinrich, G., Simon, F., Wagenknecht, U., Stöckelhuber, K. W., & Dweiri, R. (2012). Carboxylated nitrile butadiene rubber/hybrid filler composites. *Materials Research*, 15(4), 671–678. <https://doi.org/10.1590/S1516-14392012005000086>
- Mumtaz, S., Ahmad, M. A., Raza, R., Arshad, M. S., Ahmed, B., Ashiq, M. N., & Abbas, G. (2017). Nano grained Sr and Zr co-doped BaCeO₃ electrolytes for intermediate temperature solid oxide fuel cells. *Ceramics International*, 43(16),

- 14354–14360. <https://doi.org/10.1016/j.ceramint.2017.07.192>
- Nabil, H., Ismail, H., & Azura, A. R. (2013). Comparison of thermo-oxidative ageing and thermal analysis of carbon black-filled NR/Virgin EPDM and NR/Recycled EPDM blends. *Polymer Testing*, *32*(4), 631–639.
- Naderi, G., Lafleur, P. G., & Dubois, C. (2007). Microstructure-properties correlations in dynamically vulcanized nanocomposite thermoplastic elastomers based on PP/EPDM. *Polymer Engineering and Science*, *47*(3), 207–217. <https://doi.org/10.1002/pen.20673>
- Namboodiri, C. S. S., & Tripathy, D. K. (1992). Strain-dependent isothermal damping behaviour of filled EPDM rubber. Effect of vulcanizing system. *Plastics, Rubber and Composites Processing and Applications*, *17*(3), 171–178.
- O-Ring Design Guide*. (1990). http://www.hitechseals.com/includes/pdf/o-ring_brochure.pdf
- Obrecht, W., Lambert, J.-P., Happ, M., Oppenheimer-Stix, C., Dunn, J., & Krüger, R. (2011). Rubber, 4. Emulsion Rubbers. In *Ullmann's Encyclopedia of Industrial Chemistry*. Wiley-VCH Verlag GmbH & Co. KGaA.
- Ono, H., Fujiwara, H., & Nishimura, S. (2018). Penetrated hydrogen content and volume inflation in unfilled NBR exposed to high-pressure hydrogen—What are the characteristics of unfilled-NBR dominating them? *International Journal of Hydrogen Energy*, *43*(39), 18392–18402.
- ParkerHannifinCorporation. (2018). O-Ring Guide. *Parker Hannifin - O-Ring Guide - Catalog*, 1–94.
- Plc, D. (2007). *O-rings*. <https://www.m-seals.co.uk/seal-supplier/>
- Prasertsri, S., & Rattanasom, N. (2012). Fumed and precipitated silica reinforced natural rubber composites prepared from latex system: Mechanical and dynamic properties. *Polymer Testing*, *31*(5), 593–605.
- Pukánszky, B., Tüdös, F., Kolařík, J., & Lednický, F. (1990). Ternary composites of polypropylene, elastomer, and filler: Analysis of phase structure formation. *Polymer Composites*, *11*(2), 98–104. <https://doi.org/10.1002/pc.750110205>
- Ratso, S., Kruusenberg, I., Käärík, M., Kook, M., Saar, R., Kanninen, P., Kallio, T., Leis, J., & Tammeveski, K. (2017). Transition metal-nitrogen co-doped carbide-

- derived carbon catalysts for oxygen reduction reaction in alkaline direct methanol fuel cell. *Applied Catalysis B: Environmental*, 219, 276–286. <https://doi.org/10.1016/j.apcatb.2017.07.036>
- Rempel, G. L., & Wang, H. (2017). *Nitrile Rubber Latex Blends: Preparation, Characterization and Applications* (pp. 67–88). https://doi.org/10.1007/978-3-319-48720-5_3
- Sammes, N. M., Galloway, K., Serincan, M. F., Suzuki, T., Yamaguchi, T., Awano, M., & Colella, W. (2012). Solid oxide fuel cells. In *Handbook of Climate Change Mitigation* (Vol. 4, pp. 1703–1727). https://doi.org/10.1007/978-1-4419-7991-9_44
- Sangwichien, C., Sumanatrakool, P., & Patarapaiboolchai, O. (2008). Effect of filler loading on curing characteristics and mechanical properties of thermoplastic vulcanizate. *Chiang Mai Journal of Science*, 35(1), 141–149. http://www.academia.edu/download/43340601/10-11-10-47d1e_1_.pdf
- Sau, K. P., Chaki, T. K., & Khastgir, D. (1998). Carbon fibre filled conductive composites based on nitrile rubber (NBR), ethylene propylene diene rubber (EPDM) and their blend. *Polymer*, 39(25), 6461–6471.
- Schulze, M., Knöri, T., Schneider, A., & Gülzow, E. (2004). Degradation of sealings for PEFC test cells during fuel cell operation. *Journal of Power Sources*, 127(1–2), 222–229. <https://doi.org/10.1016/j.jpowsour.2003.09.017>
- Seals, E. (2019). *KRYNAC*®. 1–2.
- Sinhal, S. C. and Kendall, K. (2003). *High Temperature Solid Oxide Fuel Cells*, Netherlands. *Elsevier*.
- Solutions, T. S. (2016). *O-Rings and Back-up Rings*. https://www.tss-static.com/remotemedia/media/globalformastercontent/downloadsautomaticlycreatedbyscript/catalogs/o_ring_gb_en.pdf
- Song, P., Barkholtz, H. M., Wang, Y., Xu, W., Liu, D., & Zhuang, L. (2017). High-performance oxygen reduction catalysts in both alkaline and acidic fuel cells based on pre-treating carbon material and iron precursor. *Science Bulletin*, 62(23), 1602–1608. <https://doi.org/10.1016/j.scib.2017.10.020>
- Stevenson, A., & Morgan, G. (1995). Fracture of Elastomers by Gas Decompression.

- In *Rubber Chemistry and Technology* (Vol. 68, Issue 2, pp. 197–211).
<https://doi.org/10.5254/1.3538735>
- Stolarski, T. A., & Tucker, M. (1996). Frictional performance of an O-ring type seal at the commencement of linear motion. *Tribology Letters*, 2(4), 405–416.
<https://doi.org/10.1007/BF00156912>
- Sutharssan, T., Montalvao, D., Chen, Y. K., Wang, W. C., Pisac, C., & Elemara, H. (2017). A review on prognostics and health monitoring of proton exchange membrane fuel cell. In *Renewable and Sustainable Energy Reviews* (Vol. 75, pp. 440–450). <https://doi.org/10.1016/j.rser.2016.11.009>
- Tan, J., Chao, Y. J., Yang, M., Lee, W. K., & Van Zee, J. W. (2011). Chemical and mechanical stability of a Silicone gasket material exposed to PEM fuel cell environment. *International Journal of Hydrogen Energy*, 36(2), 1846–1852.
<https://doi.org/10.1016/j.ijhydene.2009.12.048>
- Thaptong, P., Sirisinha, C., Thepsuwan, U., & Sae-Oui, P. (2014). Properties of Natural Rubber Reinforced by Carbon Black-based Hybrid Fillers. *Polymer - Plastics Technology and Engineering*, 53(8), 818–823.
- The Definitive O-Ring Design Guide O-Ring Design Guide Content*. (2019).
 Therban® xt. (2019). 2019.
- Troufflard, J., Laurent, H., Rio, G., Omnès, B., & Javanaud, S. (2018). Temperature-dependent modelling of a HNBR O-ring seal above and below the glass transition temperature. *Materials and Design*, 156, 1–15.
- Vara, R. J. D. (1994). Developments in fuel hoses to meet changing environmental needs. *Rubber World*, 209(6), 24–31.
- Varghese, H., Bhagawan, S. S., & Thomas, S. (1999). Effects of blend ratio, crosslinking systems and fillers on the morphology, curing behavior, mechanical properties, and failure mode of acrylonitrile butadiene rubber and poly(ethylene-co-vinyl acetate) blends. *Journal of Applied Polymer Science*, 71(14), 2335–2364. [https://doi.org/10.1002/\(SICI\)1097-4628\(19990404\)71:14<2335::AID-APP7>3.0.CO;2-5](https://doi.org/10.1002/(SICI)1097-4628(19990404)71:14<2335::AID-APP7>3.0.CO;2-5)
- Williams, D. (2009). Proceedings of the 9th International Conference on Greenhouse Gas Control Technologies, GHGT-9. In *Energy Procedia* (Vol. 1, Issue 1).

- Wu, D., Wang, X., & Jin, R. (2004). Toughening of poly(2,6-dimethyl-1,4-phenylene oxide)/nylon 6 alloys with functionalized elastomers via reactive compatibilization: Morphology, mechanical properties, and rheology. *European Polymer Journal*, 40(6), 1223–1232.
- Xiao Kun, Gu Xiaohui, P. C. (2014). Reliability Evaluation of the O-type Rubber Sealing Ring for Fuse Based on Constant Stress Accelerated Degradation Testing. *Mechanical Engineering*, 50(16).
- Xu, H., Chen, B., Zhang, H., Sun, Q., Yang, G., & Ni, M. (2017). Modeling of direct carbon solid oxide fuel cells with H₂O and CO₂ as gasification agents. *International Journal of Hydrogen Energy*, 42(23), 15641–15651. <https://doi.org/10.1016/j.ijhydene.2017.05.075>
- Yamabe, J., Koga, A., & Nishimura, S. (2013). Failure behavior of rubber O-ring under cyclic exposure to high-pressure hydrogen gas. *Engineering Failure Analysis*, 35, 193–205. <https://doi.org/10.1016/j.engfailanal.2013.01.034>
- Zeng, D., He, Q., Li, T., Hu, J., Shi, T., Zhang, Z., Yu, Z., & Liu, R. (2016). Corrosion mechanism of hydrogenated nitrile butadiene rubber O-ring under simulated wellbore conditions. *Corrosion Science*, 107, 145–154. <https://doi.org/10.1016/j.corsci.2016.02.028>
- Zhang, Y., Yu, F., Wang, X., Zhou, Q., Liu, J., & Liu, M. (2017). Direct operation of Ag-based anode solid oxide fuel cells on propane. *Journal of Power Sources*, 366, 56–64. <https://doi.org/10.1016/j.jpowsour.2017.08.111>
- Zhou, C., Zheng, J., Gu, C., Zhao, Y., & Liu, P. (2017). Sealing performance analysis of rubber O-ring in high-pressure gaseous hydrogen based on finite element method. *International Journal of Hydrogen Energy*, 42(16), 11996–12004. <https://doi.org/10.1016/j.ijhydene.2017.03.039>

VITAE

Name Mr. Chea Sophos

Student ID 5910920052

Educational Attainment

Degree	Name of Institution	Year of Graduation
Engineer's degree (Water Resources Engineering and Rural Infrastructure)	Institute of Technology of Cambodia	2016

Scholarship Awards during Enrolment

Asian Development Bank, Ministry of Water Resources and Meteorology, and Institute of Technology of Cambodia Scholarship.

Scholarship Awards for Master Studies Thailand's Education Hub for Southern Region of ASEAN Countries (TEH-AC 098/2017).

List of Publication and Proceeding

Chea S, Oeurng C (2017) Flow simulation in an ungauged catchment of Tonle Sap Lake Basin in Cambodia: Application of the HEC-HMS model. The European Water Resources Association (EWRA). Water Utility Journal 17: 3-17.

Chea S, Luengchavanon M, Ananchaenwong E, Techato K, Jutidamrongphan W, Chaiprapat S, Niyomwas S, Marthosa S (2019) Development of O-ring from the NR/EPDM filled silica/CB hybrid filler for use in solid oxide fuel cell testing system. Polymer testing. (In process).